

**SYNTHESIS, CHARACTERIZATION, AND BIOLOGICAL STUDIES OF NOVEL  
ORGANOANTIMONY(V) CYANOXIMATES**

A Master's Thesis

Presented to

The Graduate College of

Missouri State University

In Partial Fulfillment

Of the Requirements for the Degree

Master of Science, Chemistry

By

Kevin Anthony Pinks

August 2020

Copyright 2020 by Kevin Anthony Pinks

# SYNTHESIS, CHARACTERIZATION, AND BIOLOGICAL STUDIES OF NOVEL ORGANOANTIMONY(V) CYANOXIMATES

Chemistry

Missouri State University, August 2020

Master of Science

Kevin Anthony Pinks

## ABSTRACT

The requirement of new antimicrobial treatments has become an urgent field in the last two decades. Multi-drug resistant (MDR) bacteria are now resistant to common antibiotics such as penicillin, cephalosporin, and carbapenems. To antagonize such bacteria 8 novel organoantimony(V) cyanoximates were synthesized with the purpose to be characterized and submitted for biological activity studies. The eight organoantimony(V) cyanoximates were characterized by elemental analysis, thermal analysis, IR-,  $^{13}\text{C}\{^1\text{H}\}$  NMR, some with UV-visible spectroscopy, and single crystal X-ray analysis. Eight new crystal structures were determined. All organoantimony(V) cyanoximates demonstrated a pentavalent coordinated distorted trigonal bipyramid polyhedron of the Sb(V) atom. Cyanoxime anionic ligands of each determined structure were bound to Sb(V) in a monodentate fashion. Antimicrobial Disk studies indicated that  $\text{Sb}(\text{Ph})_4(\text{ACO})$ ,  $\text{Sb}(\text{Ph})_4(\text{ECO})$ , had significant antimicrobial effect against all three strains: two gram-negative a) *Escherichia coli* strain S17 and b) *Pseudomonas aeruginosa* strain PAO1, alongside a single gram-positive Methicillin-resistant *Staphylococcus aureus* strain NRS70.  $\text{Sb}(\text{Ph})_4(\text{TCO})$  and  $\text{Sb}(\text{Ph})_4(\text{TDCO})$  had significant effects on the gram- positive Methicillin-resistant *Staphylococcus aureus* strain NRS70, but essentially no antimicrobial activity for gram-negative strains used. Antimicrobial broth dilution MIC assays were completed against the same strains as antimicrobial disk studies but changed the compounds tested. Using  $\text{Sb}(\text{Ph})_4(\text{MCO})$  as the only Sb(V) cyanoximate along with the free cyanoximes  $\text{H}(\text{MCO})$ ,  $\text{H}(\text{ECO})$ , and  $\text{Na}[\text{H}(\text{ACO})_2]$ . Results indicated that free cyanoximes have no antimicrobial effect as the DMSO solvent used in these assays contributed to the inhibition factor to the MIC of the cell cultures. Antifungal disk assays concluded that  $\text{Sb}(\text{Ph})_4(\text{ECO})$  was effective against *Cryptococcus neoformans* and *Candida albicans* in a positive trend.  $\text{Sb}(\text{Ph})_4(\text{TCO})$  followed in antifungal activity against both strains.  $\text{Sb}(\text{Ph})_4(\text{ACO})$  and  $\text{Sb}(\text{Ph})_4(\text{TDCO})$  were only effective at inhibition of *Cryptococcus neoformans*. Antifungal MIC assays were conducted and concluded that the free cyanoximes had zero effect on antifungal activity against both fungi. On the other hand,  $\text{Sb}(\text{Ph})_4(\text{MCO})$  had shown MIC levels ranging from 10 - 50  $\mu\text{g}/\text{mL}$ .

**KEYWORDS:** cyanoximes, organoantimony(V), antimicrobial, antifungal, antibiotic-resistance, X-ray single crystal analysis

**SYNTHESIS, CHARACTERIZATION, AND BIOLOGICAL STUDIES OF NOVEL  
ORGANOANTIMONY(V) CYANOXIMATES**

By

Kevin Anthony Pinks

A Master's Thesis  
Submitted to the Graduate College  
Of Missouri State University  
In Partial Fulfillment of the Requirements  
For the Degree of Master of Science, Chemistry

August 2020

Approved:

Nikolay Gerasimchuk, Ph.D., Thesis Committee Chair

Richard Biagioni, Ph.D., Committee Member

Reza Sedaghat-Herati, Ph.D., Committee Member

Marianna Patrauchan, Ph.D., Committee Member

Julie Masterson, Ph.D., Dean of the Graduate College

In the interest of academic freedom and the principle of free speech, approval of this thesis indicates the format is acceptable and meets the academic criteria for the discipline as determined by the faculty that constitute the thesis committee. The content and views expressed in this thesis are those of the student-scholar and are not endorsed by Missouri State University, its Graduate College, or its employees.

## ACKNOWLEDGEMENTS

I would first acknowledge my teacher, research advisor, and committee chair, Dr. Nikolay Gerasimchuk. He has been relentless to help me understand the concepts of inorganic, bioinorganic, and organometallic chemistry, every time we discussed I learned something important. Without his guidance, expertise, and patience this project would have not been close to completing, thank you. Next, I thank all my committee members, Dr. Biagioni, Dr. Herati, and Dr. Patrauchan for their guidance, edits, and remarks over my thesis. Dr. Biagioni has also been a great advisor and has helped me whenever I needed help with an instrument. I would also like to thank all of the Gerasimchuk research group members that I met along my journey through these last three years, as I have learned a lot from every one of you. I would like to thank my friends: Alex, Arkanil, Justin, and Luckio for joining me in our journeys through graduate school. Each of you have given me so much support and fun experiences in the past two years, the times I was with you guys were one of the best times of my life, thanks B's. Next I would like to thank everyone in the Chemistry department and graduate college for all of their support. Finally, I would like to thank my parents Kevin G. and Sharon L. Pinks for their loving support throughout my entire academic career.

Therefore, I dedicate this thesis to my parents Kevin and Sharon.

## TABLE OF CONTENTS

I. Introduction	Page 1
I.1. Antibiotic Resistance	Page 1
I.2. Mechanisms Of Antibiotic Resistance	Page 2
I.2.1. Modifications of the antibiotic molecule	Page 2
I.2.2. Decrease of drug uptake by increase of efflux	Page 3
I.2.3. Changes in target sites	Page 4
I.2.4. Resistance due to global cell adaptations	Page 4
I.3. Further complications with antibiotic resistance	Page 4
I.4. Drug discovery and the search for new antimicrobial agents	Page 5
II. Literature Review	Page 7
II.1. Introduction Of Bioinorganic Chemistry	Page 7
II.2. Antimony: Chemistry And Applications	Page 7
II.1.1. Applications of antimony	Page 9
II.1.2. Medicinal applications of antimony	Page 10
II.3. Coordination Compounds: An Introduction	Page 13
II.4. Cyanoximes: Ligands For Coordination Compounds	Page 16
III. Research Goals	Page 22
IV. Experimental	Page 23
IV.1. Experimental And Characterization Methods	Page 23
IV.1.1. Reagents and general considerations	Page 23
IV.1.2. Vibrational spectroscopy	Page 24
IV.1.3. UV-visible spectra	Page 24
IV.1.4. NMR spectra	Page 24
IV.1.5. X-ray crystallography	Page 24
IV.1.6. Thermal stability studies	Page 25
IV.2. Synthesis of H(MCO): Synthesis Of 3-Morpholin-4-yl-3-oxopropionitrile, The H(MCO) Cyanoxime Precursor, Pre-MCO	Page 26
IV.3. Synthesis Of H(MCO): From Its Precursor (pre-MCO)	Page 27
IV.4. Synthesis Of Ag(I)L Salts From HL Acids	Page 27
IV.5. Synthesis Of Sb(Ph) <sub>4</sub> L, The Metathesis Reaction	Page 29
IV.6. Synthesis Of Thioamide Sb(Ph) <sub>4</sub> L', From TIL' Salts	Page 31
IV.7. Antimicrobial Studies: Kirby-Bauer Single Disk Test	Page 33
IV.8. Antimicrobial Broth Dilution Minimal Inhibition Concentration (MIC) Assays	Page 34

IV.9. Antifungal Studies: Kirby-Bauer Single Disk Test And MIC Assays	Page 35
V. Results and Discussion	Page 37
V.1. X-Ray Single Crystal Analysis	Page 37
V.1.1. Trends found in Sb(Ph) <sub>4</sub> cyanoximates crystal structure	Page 37
V.1.2. Crystal structure of Sb(Ph) <sub>4</sub> (ACO).	Page 38
V.1.3. Crystal structure of Sb(Ph) <sub>4</sub> (2PCO).	Page 42
V.1.4. Crystal structure of Sb(Ph) <sub>4</sub> (3PCO).	Page 45
V.1.5. Crystal structure of Sb(Ph) <sub>4</sub> (4PCO).	Page 49
V.1.6. An unexpected result: crystal structure of Sb(Ph) <sub>3</sub> (ECO) μ-oxo-dimer.	Page 52
V.1.7. Crystal structure of the monomeric Sb(Ph) <sub>4</sub> (ECO).	Page 56
V.1.8. Crystal structure of Sb(Ph) <sub>4</sub> (MCO).	Page 61
V.1.9. Crystal structure of Sb(Ph) <sub>4</sub> (TCO), two polymorphs.	Page 65
V.2. Differential Scanning Calorimetry – Thermal Gravimetry Analysis (DSC/TGA)	Page 74
V.3. Vibrational Spectroscopy: Infrared Spectroscopy	Page 75
V.4. NMR Spectroscopy – <sup>13</sup> C{ <sup>1</sup> H} Results.	Page 75
V.5. UV-Visible Spectroscopy.	Page 81
V.6. Antimicrobial Studies	Page 84
V.6.1. First set of inhibition measurements on solid media.	Page 85
V.6.2. Second set of inhibition measurements.	Page 86
V.6.3. Initial broth dilution MIC tests.	Page 87
V.7. Antifungal Studies	Page 88
V.7.1. Kirby-Bauer disk assays.	Page 88
V.7.2. MIC antifungal activity assay.	Page 89
VI. Conclusions and Summary	Page 95
VII. Future Work	Page 97
VIII. Literature Cited	Page 98
Appendices	Page 108

Appendix A. Instrumentation of TG/DSC Analysis	Page 108
Appendix A-1. A – general view of the thermal analyzer showing blow torch used for crucible cleaning and tools; B – cleaning of alumina crucible with flame; C – opened furnace view showing two beams with aluminacrucibles for differential analysis.	Page 108
Appendix B. Traces of TG/DSC analyses.	Page 109
Appendix B-1. TG/DSC traces for a sample of Sb(Ph) <sub>4</sub> (2PCO) showing compounds melting with rapidly following decomposition.	Page 109
Appendix B-2. TG/DSC traces for a sample of Sb(Ph) <sub>4</sub> (4PCO) showing compounds melting with rapidly following decomposition.	Page 109
Appendix B-3. TG/DSC traces for a sample of Sb(Ph) <sub>4</sub> (ACO) showing compounds melting with rapidly following decomposition.	Page 110
Appendix B-4. TG/DSC traces for a sample of Sb(Ph) <sub>4</sub> (TCO) showing compounds melting with rapidly following decomposition.	Page 110
Appendix B-5. TG/DSC traces for a sample of Sb(Ph) <sub>4</sub> (MCO) (in usable range) showing compounds melting followed by decomposition.	Page 111
Appendix B-6. TG/DSC traces for a sample of Sb(Ph) <sub>4</sub> (TDCO) (in usable range) showing compounds melting followed by decomposition.	Page 111
Appendix C. Crystal checkCIF Reports for Studied Complexes	Page 112
Appendix C-1. checkCIF-reports for Sb(Ph) <sub>4</sub> (ACO).	Page 112
Appendix C-2. checkCIF-reports for Sb(Ph) <sub>4</sub> (2PCO).	Page 114
Appendix C-3. checkCIF-reports for Sb(Ph) <sub>4</sub> (3PCO).	Page 117
Appendix C-4. checkCIF-reports for Sb(Ph) <sub>4</sub> (4CO).	Page 120
Appendix C-5. checkCIF-reports for the Sb(Ph) <sub>3</sub> (ECO) $\mu$ oxo-dimer.	Page 123
Appendix C-6. checkCIF-reports for Sb(Ph) <sub>4</sub> (ECO) monomer.	Page 126
Appendix C-7. checkCIF-reports for Sb(Ph) <sub>4</sub> (MCO).	Page 129
Appendix C-8. checkCIF-reports for Sb(Ph) <sub>4</sub> (TCO) polymorph 1.	Page 132
Appendix C-9. checkCIF-reports for Sb(Ph) <sub>4</sub> (TCO) polymorph 2.	Page 135



Appendix D. Biological Activity Studies Data.	Page 140
Appendix D-1. Raw data and statistical analysis of Sb(Ph) <sub>4</sub> (ACO) in the first round of inhibition zone measurements.	Page 1
Appendix D-2. Raw data and statistical analysis of Sb(Ph) <sub>4</sub> (ECO) in the first round of inhibition zone measurements.	Page 1
Appendix D-3. Raw data and statistical analysis of Sb(Ph) <sub>4</sub> (TCO) in the first round of inhibition zone measurements.	Page 142
Appendix D-4. Statistical analysis of the second round of Inhibition zone measurements for antimicrobial testing.	Page 143
Appendix D-5. Effect of DMSO concentration on MIC of studied selected strains.	Page 144

## LIST OF TABLES

Table 1. Elements and weight percentages found in the human body.	Page 8
Table 2. Bond energies between Sb and halogens chalcogens and N - typical ligands in organoantimony compounds	Page 11
Table 3. Color, yield, and elemental analysis of synthesized organoantimony(V) cyanoximates and their precursors.	Page 36
Table 4. Crystal data and structure refinement of $\text{Sb(Ph)}_4(\text{ACO})$ .	Page 40
Table 5. Selected bond lengths ( $\text{\AA}$ ) and angles ( $^\circ$ ) of the cyanoximes and metal complex center in $\text{Sb(Ph)}_4(\text{ACO})$ .	Page 41
Table 6. Crystal data and structure refinement of $\text{Sb(Ph)}_4(2\text{PCO})$ .	Page 43
Table 7. Selected bond lengths ( $\text{\AA}$ ) and angles ( $^\circ$ ) of the cyanoxime and metal complex center in $\text{Sb(Ph)}_4(2\text{PCO})$ .	Page 44
Table 8. Crystal data and structure refinement of $\text{Sb(Ph)}_4(3\text{PCO})$ .	Page 47
Table 9. Selected bond lengths ( $\text{\AA}$ ) and angles ( $^\circ$ ) of the cyanoxime and metal complex center in $\text{Sb(Ph)}_4(3\text{PCO})$ .	Page 48
Table 10. Crystal data and structure refinement of $\text{Sb(Ph)}_4(4\text{PCO})$ .	Page 51
Table 11. Selected bond lengths ( $\text{\AA}$ ) and angles ( $^\circ$ ) of the cyanoximes and metal complex center in $\text{Sb(Ph)}_4(4\text{PCO})$ .	Page 52
Table 12. Crystal data and structure refinement of the $\text{Sb(Ph)}_3(\text{ECO})$ $\mu$ -oxo-dimer.	Page 55
Table 13. Selected bond lengths ( $\text{\AA}$ ) and angles ( $^\circ$ ) of the cyanoxime and metal complex center in $\text{Sb(Ph)}_3(\text{ECO})$ $\mu$ -oxo-dimer. BR denotes the bridge oxygen connecting the dimer.	Page 56

Table 14. Crystal data and structure refinement of monomeric Sb(Ph) <sub>4</sub> (ECO).	Page 58
Table 15. Selected bond lengths (Å) and angles (°) of the cyanoxime and metal complex center in Sb(Ph) <sub>4</sub> (ECO) molecule <b>A</b> .	Page 59
Table 16. Selected bond lengths (Å) and angles (°) of the cyanoximes and metal complex center in Sb(Ph) <sub>4</sub> (ECO) molecule <b>B</b> .	Page 59
Table 17. Crystal and refinement data for the crystal Sb(Ph) <sub>4</sub> (MCO).	Page 62
Table 18. Selected bond lengths (Å) and angles (°) of the cyanoximes and metal complex center in the first independent molecule <b>A</b> , in the ASU of Sb(Ph) <sub>4</sub> (MCO).	Page 63
Table 19. Selected bond lengths (Å) and angles (°) of the cyanoxime and metal complex center in the second independent molecule <b>B</b> , in the ASU of Sb(Ph) <sub>4</sub> (MCO).	Page 64
Table 20. Crystal and refinement data for the crystal Sb(Ph) <sub>4</sub> (TCO), polymorph <b>1</b> .	Page 67
Table 21. Selected bond lengths (Å) and angles (°) of the cyanoxime and metal complex center in the co-crystallized diastereomers of Sb(Ph) <sub>4</sub> (TCO) polymorph <b>1</b> , <i>trans-anti</i> (top) and <i>trans-syn</i> (bottom).	Page 68
Table 22. Crystal and refinement data for another polymorph of crystalline Sb(Ph) <sub>4</sub> (TCO) polymorph <b>2</b> .	Page 72
Table 23. Selected bond lengths (Å) and angles (°) of the cyanoxime and metal complex center in Sb(Ph) <sub>4</sub> (TCO) polymorph <b>2</b> of the 8 <sup>th</sup> independent molecule in the ASU, labeled as <b>Q</b> .	Page 73
Table 24. Analysis of bond lengths, bond and dihedral angles of the eight independent molecules of the Sb(Ph) <sub>4</sub> (TCO) polymorph <b>2</b> ASU.	Page 73

Table 25. Results of thermal analysis studies of organoantimony(V) cyanoximates.	Page 76
Table 26. Assignment of important vibrational frequencies ( $\text{cm}^{-1}$ ) for synthesized organoantimony(V) cyanoximates.	Page 77
Table 27. Tabulated chemical shifts of $^{13}\text{C}\{^1\text{H}\}$ NMR spectroscopy for the $\text{Sb}(\text{Ph})_4\text{Br}$ and organoantimony(V) cyanoximates' equivalent phenyl rings.	Page 78
Table 28. Tabulated values of chemical shifts of organoantimony(V) cyanoximates in the $^{13}\text{C}\{^1\text{H}\}$ NMR spectra.	Page 79-80

## LIST OF FIGURES

- Figure 1. An example of a dose-response curve. Page 8
- Figure 2. Representation of the concentration dependence of toxic and beneficial effects of metal ions on cell growth. Page 9
- Figure 3. Schematic representation of how chemical compounds enter the cell. Page 13
- Figure 4. Model of pentavalent antimonials as prodrugs. Page 14
- Figure 5. Types of bonding found in coordination and organometallic compounds. example of a dose-response curve. Page 15
- Figure 6. Currently known types of cyanoximes and their precursors. Page 15
- Figure 7. Structure of newly developed oxime-bearing compounds with antiviral properties. Page 17
- Figure 8. Examples of ampolydentate binding of the  $\text{ACO}^-$  anion. Page 17
- Figure 9. Geometrical isomers of cyanoximes. Page 18
- Figure 10. Deprotonation of cyanoximes with metal carbonates, hydroxides, and oxides in aqueous and polar organic solvents. Page 19
- Figure 11. Charge delocalization in yellow cyanoxime anion involving several resonance forms Page 19
- Figure 12. List of known cyanoximes ligands. Asterisks indicate compounds for which crystal structures were determined. Page 20
- Figure 13. Chemical structures of selected cyanoxime ligands and their commonly used abbreviations. Page 21

- Figure 14. A, Synthesis of the H(MCO) from its precursor obtained in two different ways. B, nistrosation of pre-MCO amide compound into protonated cyanoxime ligand. Page 27
- Figure 15. General synthesis of silver(I) salts of cyanoxime ligands from their protonated precursor. R represents the different cyanoximes. Page 28
- Figure 16. General synthesis of organoantimony(V) cyanoximates using the metathesis reaction with silver(I) salts. L represents the variety of ligands chosen for study. Page 30
- Figure 17. Instrumentation and accessories used for isolation of organoantimony(V) cyanoximates from Ag(I)Br. A Thermo Scientific centrifuge (left) with filtered nylon Eppendorf tubes (right). Page 30
- Figure 18. Progression of filtration using centrifugation a homogenous mixture of Sb(Ph)<sub>4</sub>(MCO) and AgBr in CH<sub>3</sub>CN (left), transferred into an Eppendorf tube (middle), and after centrifugation (right). Page 31
- Figure 19. Microscopic image of the Tl(TCO) salt. Page 32
- Figure 20. Microscopic image of desired crystalline organoantimony(V) cyanoximate, Sb(Ph)<sub>4</sub>(TCO). Page 32
- Figure 21. General synthesis of organoantimony(V) cyanoximates using the metathesis reaction with thallium(I) salts. L' represents the thioamide containing ligands. Page 33
- Figure 22. Microscopic image of desired crystalline organoantimony(V) cyanoximate, Sb(Ph)<sub>4</sub>(TDCO). Page 33
- Figure 23. Molecular structure and numbering scheme of principal atoms in the crystal structure of Sb(Ph)<sub>4</sub>(ACO). An ORTEP representation at 50% thermal ellipsoid probability. H-atoms omitted for clarity. Page 39
- Figure 24. Two least obstructed views of Sb(Ph)<sub>4</sub>(ACO) showing structure stabilization through intramolecular H-bonding of H1a and N1, A, along with the space filling model, B. Page 39

- Figure 25. **A**, analysis of the angles of the coordination polyhedron of Sb(V) in Sb(Ph)<sub>4</sub>(ACO). **B**, analysis of planarity between Sb(V) core and equatorial *ipso* carbons of the phenyl rings. Page 41
- Figure 26. Video microscope image of the crystal of Sb(Ph)<sub>4</sub>(2PCO) with indexed faces. Page 42
- Figure 27. An ORTEP drawing at 50% thermal ellipsoids probability level for the ASU Sb(Ph)<sub>4</sub>(2PCO) showing the numbering of principal atoms. H-atoms are omitted for clarity. Page 44
- Figure 28. Structure of intramolecular stabilization through electrostatic contact of equatorial phenyl ring  $\pi$ -system and pyridyl hydrogen of Sb(Ph)<sub>4</sub>(2PCO). Involved atoms are expressed in a space-filling mode. Page 45
- Figure 29. An ORTEP drawing at 50% thermal ellipsoids probability level for the ASU Sb(Ph)<sub>4</sub>(3PCO) showing the numbering of principal atoms. H-atom labels are omitted for clarity. Page 46
- Figure 30. The least obstructed view of the ASU of Sb(Ph)<sub>4</sub>(3PCO) showing intramolecular electrostatic contact of the pyridyl hydrogen (H7) with the nitrogen (N1) of the cyanoximes moiety. Page 46
- Figure 31. Geometry of the pentavalent antimony complex Sb(Ph)<sub>4</sub>(3PCO), showing a distorted trigonal bipyramid polyhedron coordination. Important bond lengths (A) and angles (B) of coordination are shown. Page 48
- Figure 32. View of the off-plane distance in the distorted trigonal-bipyramid coordination polyhedron of Sb(Ph)<sub>4</sub>(3PCO). Page 49
- Figure 33. An ORTEP drawing at 50% thermal ellipsoids probability level for the ASU Sb(Ph)<sub>4</sub>(4PCO) showing the numbering of principal atoms. H-atoms are omitted for clarity. Page 50
- Figure 34. Packing of two structures of Sb(Ph)<sub>4</sub>(4PCO) showing stabilization short electrostatic contact between the centers of the 4-pyridyl centroid and phenyl rings with phenyl hydrogens. Page 50

- Figure 35. An ORTEP drawing at 50% thermal ellipsoids probability level for the ASU in the structure of  $\text{Sb}(\text{Ph})_3(\text{ECO})$   $\mu$ -oxo-dimer showing the numbering of principal atoms. H-atoms are omitted for clarity. Page 53
- Figure 36. Scheme of suggested path for the dimerization of organoantimony(V) in moist conditions. Page 54
- Figure 37. An ORTEP drawing at 50% thermal ellipsoids probability level for the two crystallographically independent molecules in the ASU of  $\text{Sb}(\text{Ph})_4(\text{ECO})$  monomer showing the numbering of principal atoms. H-atoms are omitted for clarity. Page 57
- Figure 38. Two different views of the crystal packing in the unit cell in the structure  $\text{Sb}(\text{Ph})_4(\text{ECO})$  molecule **A** (red) and molecule **B** (purple). Page 60
- Figure 39. Two views of the crystal packing in the unit cell Sb atom on a special position gliding plane. Independent molecules **A** and **B** are labeled for clarity. Page 60
- Figure 40. Two independent molecules in the ASU of the structure of  $\text{Sb}(\text{Ph})_4(\text{MCO})$ ; and ORTEP drawing at 50% thermal ellipsoids probability level. Principal atoms are labeled, with H atoms are omitted for clarity. Page 63
- Figure 41. Molecular structure and labeling of principal atoms in the structure of  $\text{Sb}(\text{Ph})_4(\text{MCO})$  molecule **A** on the left, and some selected important bond lengths on the right. Page 64
- Figure 42. Video microscope image of the crystal of  $\text{Sb}(\text{Ph})_4(\text{TCO})$ , polymorph **1**, with indexed faces. Page 66
- Figure 43. Two co-crystallized diastereomers, trans-syn and trans-anti, of the structure of  $\text{Sb}(\text{Ph})_4(\text{TCO})$ ; an ORTEP drawing at 50% thermal ellipsoids probability level. Principal atoms are labeled, with H atom labels are omitted for clarity. Page 69



- Figure 44. Two least obstructed views of the two diastereomers of  $\text{Sb}(\text{Ph})_4(\text{TCO})$  in the ASU representing H bonding stability between the amide hydrogen (N-H3a) and O1a. Ratios of diastereomers are shown. Page 69
- Figure 45. Geometry of the pentavalent antimony complex  $\text{Sb}(\text{Ph})_4(\text{TCO})$  diastereomers, showing a distorted trigonal bipyramid polyhedron coordination. Important bond lengths and angles of coordination are shown. Page 70
- Figure 46. Molecular structure and numbering scheme for principal atoms in the one of the eight individual molecules in the ASU for the structure  $\text{Sb}(\text{Ph})_4(\text{TCO})$  polymorph 2. An adoption of the trans-syn configuration by the cyanoxime moiety is shown. Page 71
- Figure 47. Structure of the Q (or 8th) different polymorph shown of  $\text{Sb}(\text{Ph})_4(\text{TCO})$  with representation of H-bonding between the amide and phenyl hydrogen's with the oxygen from the oxime moiety. Page 74
- Figure 48. Traces of weight loss (green) and heat flow (blue for the  $\text{Sb}(\text{Ph})_4(\text{ECO})$  monomer showing the melting point of the compound at 144°C followed by its decomposition. Page 75
- Figure 49. General Structure representing the substitution patterns for the phenyl ring of organoantimony(V) cyanoximates. L = ligands and Br, in the case of  $\text{Sb}(\text{Ph})_4\text{Br}$ . Page 78
- Figure 50. Observed correlations between acidity of the free cyanoxime HL and chemical shift of the *ipso* carbon in NMR spectra of organoantimony(V) cyanoximates. Page 81
- Figure 51. Representation of the color gain of solutions of organoantimony(V) cyanoximates in the case of the compounds covalent integrity breaking down. Page 82
- Figure 52. An overlay of fragments of the UV-visible spectra of  $\text{Sb}(\text{Ph})_4(2\text{PCO})$  in DMSO at different temperatures, representing reversible equilibrium of covalent to ionic bonding of Sb(V) complex. Page 83

Figure 53. An overlay of fragments of the UV-visible spectra of $\text{Sb}(\text{Ph})_4(4\text{PCO})$ in propionitrile at different temperatures, representing reversible equilibrium of covalent to ionic bonding of $\text{Sb}(\text{V})$ complex.	Page 84
Figure 54. Round 1 of Inhibition zone measurements of $\text{Sb}(\text{Ph})_4(\text{ACO})$ against microbes.	Page 85
Figure 55. Round 1 of Inhibition zone measurements of $\text{Sb}(\text{Ph})_4(\text{ECO})$ against microbes.	Page 86
Figure 56. Round 1 of inhibition zone measurements of $\text{Sb}(\text{Ph})_4(\text{TCO})$ against microbes.	Page 86
Figure 57. Round 2 of inhibition zone measurements of $\text{Sb}(\text{Ph})_4\text{Br}$ , $\text{Sb}(\text{Ph})_4(\text{ECO})$ , $\text{Sb}(\text{Ph})_4(\text{TCO})$ , and $\text{Sb}(\text{Ph})_4(\text{TDCO})$ against microbes.	Page 90
Figure 58. Antimicrobial MIC determination after six hours of inoculation with antimicrobial tests.	Page 91
Figure 59. Results of initial antimicrobial MIC determination after 24 hours of inoculation with antimicrobial test.	Page 92
Figure 60. Results of initial disk assays for antifungal activity studies.	Page 93
Figure 61. Results of initial MIC assays for antifungal activity studies.	Page 93
Figure 62. Second round of MIC assays for antifungal activity studies.	Page 94

## I. INTRODUCTION

Conducted work is dedicated to the synthesis and characterization of a series of novel organoantimony(V) compounds with oximes, and their biological activity evaluation as potential antimicrobial and antifungal treatments.

### I.1. Antibiotic Resistance

During a fifteen-year period in the 1930's, the first clinical use of antibiotics, such as penicillin and sulfonamide, directly decreased the mortality rate from infections in the US by 75%.<sup>1</sup> Today, antibiotics are still the safety net between humans and harmful infections. The Centers for Disease Control and Prevention estimates that at least 23,000 people in the U.S. die annually by infections from antibiotic-resistance organisms.<sup>2</sup> Gram-positive bacterial strains like methicillin-resistant *Staphylococcus aureus* (MRSA) and vancomycin-resistant Enterococci (VRE) are gaining leverage over antibiotic treatment.<sup>3</sup> Gram negative MDR bacteria pose a greater potential of resistance due to their multi-membrane structure, making them harder to treat.<sup>4</sup> This resistance poses a great enough threat, that the World Health Organization (WHO) named antibiotic resistance as one of the three most important public health threats of the century.<sup>5</sup>

To be able to describe the mechanisms of antibiotic resistance, it is important to understand how antibiotics work. Antibiotics are synthesized in cells as a defense mechanism to compete against other cells for critical nutrients and other requirements needed for survival.<sup>6</sup> Antibiotic effects on cells can be divided into two types, bacteriostatic and bactericidal. The former stops growth and cell division, while the latter kills the cell completely. In either case,

antibiotics require a sufficient concentration to perform any antibiotic applications.<sup>6</sup> In addition, antimicrobial resistance is ancient and is the result of various interactions between organisms and their environment. Most antimicrobial compounds are naturally produced molecules; therefore, bacteria have evolved mechanisms against such antimicrobials for survival.<sup>7</sup> These organisms are coined intrinsically resistant and are not the focus of the antimicrobial resistance issue. Rather, bacteria that were originally susceptible of antibiotic treatment but then acquired resistance is the focus of this epidemic.

## **I.2. Mechanisms Of Antibiotic Resistance**

Antibiotic resistance can occur via two major genetic strategies by bacteria. The first strategy is acquisition of foreign DNA coding for resistance through horizontal gene transfer (HGT).<sup>7</sup> Bacteria can acquire external genetic material through three situations, a) transformation (incorporation of naked DNA), b) transduction (phage mediated) and, c) conjugation (bacterial “sex”).<sup>7</sup> The second strategy revolves around the mutations of gene(s) associated with the specific mechanism of action of the compound.<sup>7</sup> These genetic mutations can alter the antibiotic action of following mechanisms resulting in antimicrobial-resistance. These mechanisms include, a) modifications of the antibiotic molecule, b) a decrease in drug uptake and increase of efflux, c) changes of target site and, d) global changes in important metabolic pathways via modulation of regulatory networks.<sup>6,7</sup> Each of these mechanisms will be further discussed below.

**I.2.1. Modifications of the antibiotic molecule.** This mechanism is one of the most successful bacterial strategies to fight against the presence of antibiotics. The organism produces enzymes that either inactivates the drug by adding specific chemical moieties to the antibiotic or complete destruction of the antibiotic itself.<sup>7</sup> Both situations have the antibiotic unable to bind

with target site. In the case of chemical alterations, the production of enzymes that introduce chemical changes to the antibiotic is well-known mechanism used by gram-positive and gram-negative bacteria. The chemical changes to these compounds are a result of enzyme-required biochemical reactions such as acetylation, phosphorylation, and adenylation.<sup>7, 8</sup> The resulting effect is often correlated to steric hindrance, causing lower affinity of binding between the antibiotic and target site. The other modification of the antibiotic molecule pertains to the destruction of the antibiotic molecule. In the scenario of  $\beta$ -lactam antibiotic resistance (these include antibiotics such as penicillin derivatives, cepheems, monobactams, carbapenems, and carbacephems) via  $\beta$ -lactamases, these enzymes destroy the amide bond of the  $\beta$ -lactam ring, inactivating the drug.<sup>6, 9, 10</sup>

**I.2.2. Decrease Of Drug Uptake And Increase Of Efflux.** Most antibiotics have targets located inside the bacterial cell; therefore, the antibiotic compound must penetrate the outer and/or cytoplasmic membrane in order to use its antimicrobial effect.<sup>7</sup> Bacteria have created a defense mechanism to prevent the uptake of antibiotics through the modification of porins. Porins are water diffusion channels that allow passage through the outer membrane of gram-negative bacteria.<sup>11</sup> Porin modifications that lead to a decrease in permeability, hence increasing antibiotic resistance include, a) shifts in the type of porins expressed, b) changes in level of porin expressed, and c) impairment of porin function.<sup>7</sup> If a bacterium has allowed antibiotic inside the cell, efflux pumps are used to extrude toxic compounds as a form of antibiotic resistance. One of the first efflux pumps described<sup>12</sup> a system with encoded plasmids, RP1, R222, R144, and RA1, used to facilitate extrusion of tetracycline out of *E. coli*. Since that study, many efflux pumps have been discovered and characterized in both gram-positive and gram-negative bacteria. These

systems can be substrate specific (i.e. tetracycline) or broad substrate specificity seen in MDR bacteria.<sup>7, 14</sup>

**I.2.3. Changes in target sites.** This mechanism is a common strategy for bacteria to acquire resistance as it avoids the antimicrobial effect by interfering with the target site of the antibiotic. There are a couple pathways in which interference of the target site can occur. The first pathway is through target protection. This protection is caused by inhibition of the target site with specific proteins used in elongation factors in protein synthesis<sup>14</sup> which “protects” the target site from the antibiotic. The second pathway modifies the target site to lower the affinity of binding between the antibiotic and target site. These target site changes include, a) point mutations in the genes encoding the target site, b) modification due to enzymatic reactions, c) replacement or bypass of the original target.<sup>7</sup>

**I.2.4. Resistance due to global cell adaptations.** The final mechanism discussed is developed by bacteria that need to cope with certain environmental stressors and pressures in order to survive hostile environments, such as the human body. If bacteria are inside host, the bacteria organisms are attacked by the hosts immune system. For these bacteria to survive, they need to adapt and cope with such stressful situations. These pathogens have created very complex mechanisms to remove the interference with crucial cellular processes like cell wall synthesis and membrane homeostasis.<sup>6, 7</sup>

### **I.3. Further Complications With Antibiotic Resistance**

The resistance of MDRs can also be attributed towards the environmental exposure caused by malpractice of qualified and unqualified medical practitioners and the patients that receive antibiotic treatment. Whether it is a physician prescribing antibiotic indiscriminately or

patients disobeying prescription plans, both lead to the increase of resistant microbes. The misuse of antibiotic treatment causes the exposure of more than 15 million kilograms of antibiotics annually in the US alone.<sup>4</sup>

Research and development for new antibiotic drugs have been terminated by most pharmaceutical companies.<sup>3</sup> As a result, there has been a 90% decline in novel FDA approved antibiotics in the past 30 years.<sup>15</sup> The emergence of bacterial antibiotic resistance is considered an epidemic. Suggested by a report, antibiotic resistance is estimated to cause roughly 300 million premature deaths by 2050, with a loss of up to \$100 trillion to the global economy.<sup>16</sup> There will be a time soon where antibiotic treatment will cease to defend humanity against these microbes. Therefore, a novel non-antibiotic treatment towards harmful bacteria must be found.

#### **I.4. Drug Discovery And The Search For New Antimicrobial Agents**

As stated previously, there is a growing problem for discovering new chemical compounds that are not only better antimicrobials, but do not originate from conventional antibiotic families. Simple small molecules such as organic compounds from different classes received a large amount of screening and preliminary assessment, but all failed due to intrinsic toxicity to mammals. Difficulties in modification of these organic compounds to tailor desired stability and solubility, result in prohibitive costs. The studied classes of organic compounds were heterocycles, aromatics, porphyrins/phthalocyanines,<sup>17</sup> carbohydrates,<sup>18</sup> and small peptides. Joseph Lister introduced phenol as a form of sterilization in surgery,<sup>19</sup> while some halogenated compounds - chloramines – have been shown to express antibacterial properties.<sup>20-22</sup>

Among classic antimicrobial inorganic compounds a large variety of silver (I),<sup>23</sup> mercury(I),<sup>24</sup> copper(II),<sup>25</sup> and zinc(II)<sup>26</sup> complexes were studied. Other than some silver(I)

derivatives, no elements were successfully applied as effective antimicrobial treatments. For example, silver(I) has been used in wound treatment fabric, as a colloidal solution for topical applications. Other silver-based compounds and compositions have various infection reducing properties. Silver alloys, silver oxides, and silver sulfadiazine are coated on surfaces of various implants, such as urinary and central venous catheters.<sup>27-29</sup> Other disinfection applications of silver(I) are silver-silica nanorattles used in implant cavity disinfection,<sup>30</sup> and silver ions dispersed on a proprietary polymer for disinfection of ventilator endotracheal tubes.<sup>31</sup>

Silver antimicrobial applications have been on the rise due to the increasing issue of MDR bacteria. A main contributor towards use of silver antimicrobials is their lower toxicity towards human cells and tissues.<sup>32</sup> Silver has shown to exhibit strong bacteriostatic and bactericidal effects, which are correlated by its interactions with bacterial DNA and deactivation of bacterial respiration enzymes.<sup>33</sup> Studies have also indicated that silver ion interactions can contribute to the generation of reactive oxygen species (ROS).<sup>34, 35</sup> In the case of silver nanoparticles (AgNPs), there is evidence of direct interaction with the cell surface, allowing penetration through the cell membrane causing leakage and eventual cell death.<sup>36, 37</sup> Interference with membrane permeability and inhibition of transcription and translations have also been reported.<sup>38, 39</sup> Even though silver antimicrobials in clinical treatment have shown promise, there are several hurdles with the application. The largest hurdle for silver(I) inorganic compounds corresponds to the reduction of the metal cation to elemental Ag(0), when exposed to light and heat.<sup>40, 41</sup> Overall, organometallic compounds have not been thoroughly investigated as antimicrobial agents, but they represent a suitable combination of chemical stability, lipophilicity, and novelty. These characteristics pose a threat towards antibiotic-resistant microbes as these bacteria have yet to develop resistance toward organometallics.



## II. LITERATURE REVIEW

### II.1. Introduction Of Bioinorganic Chemistry

Bioinorganic chemistry is a young field of the science and is concerned with the roles that inorganic elements pose in biological systems and processes.<sup>42</sup> Metal ions can have roles incorporated in structures, catalytic reactions, transportation (heme group with O<sub>2</sub>), or all the above. Representation of elements found in the human body can be seen in Table 1. Bioinorganic chemistry officially began with the revolutionary work done by Paul Ehrlich, Alfred Bertheim, and Sahachiro Hata when they developed the first successful antimicrobial arsenic-based drug, *Salvarsan*. This drug was one out of more than 300 arsenic compounds which was toxic towards the microbe that caused syphilis, but not towards the human host. A dose response curve can be attributed to determination of optimal concentration of doses with certain elements (Figure 1). Studying the change in growth of cells with respect to concentration of dosage is crucial to determine which concentrations are safe, optimal, and hazardous. In the case of antimicrobial activity, it is important to find the ideal concentration of inhibition towards microbe growth (Figure 2). These tools are very useful in progressing development of antimicrobial, antibacterial, and antifungal treatments.

### II.2. Antimony: Chemistry And Applications

Antimony is a metalloid chemical element with the symbol Sb and an atomic number of 51. Antimony has been known since ancient times. The element “antimony” was named around ~50 AD, where the Roman scholar Pliny gave the name *stibium*. The original discoverer of

antimony is not known, but many people attribute antimony with Nicolas Lemery, a French chemist that performed one of the earliest studies on the element. Other writings attributed to the

Table 1. Elements and weight percentages found in the human body.<sup>a</sup>

Element	Percentage (by weight)	Element	Percentage (by weight)
Oxygen	53.6	Silicon, Magnesium	0.04
Carbon	16.0	Iron, fluorine	0.005
Hydrogen	13.4	Zinc	0.003
Nitrogen	2.4	Copper, bromine	$2. \times 10^{-4}$
Sodium, potassium, sulfur	0.10	Selenium, manganese, arsenic, nickel	$2. \times 10^{-5}$
Chlorine	0.09	Lead, cobalt	$9. \times 10^{-6}$

<sup>a</sup>Data from Ref. 42.

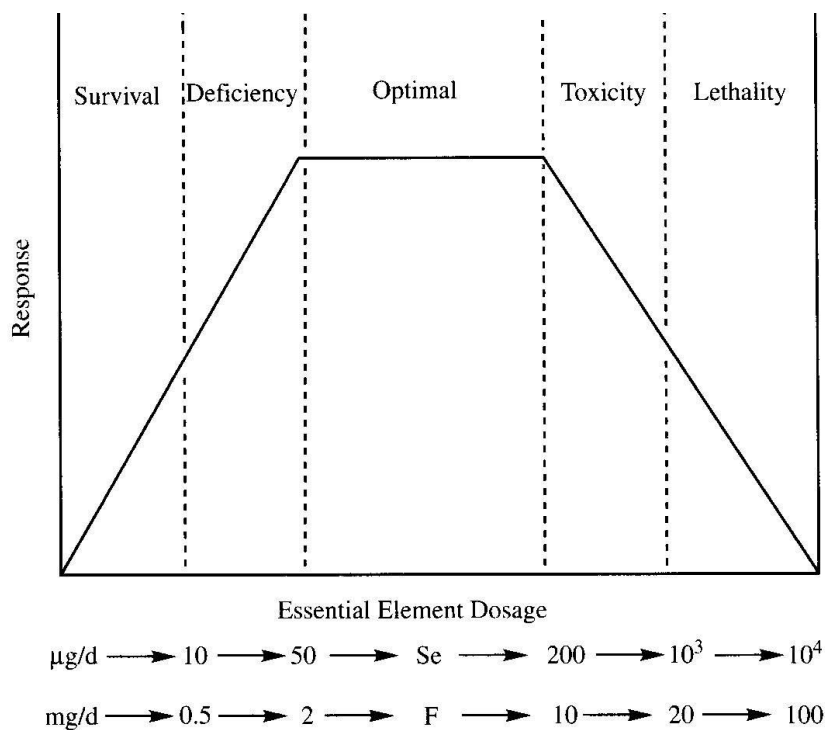


**Figure 1.** An example of a dose-response curve. Copied from Ref 42.

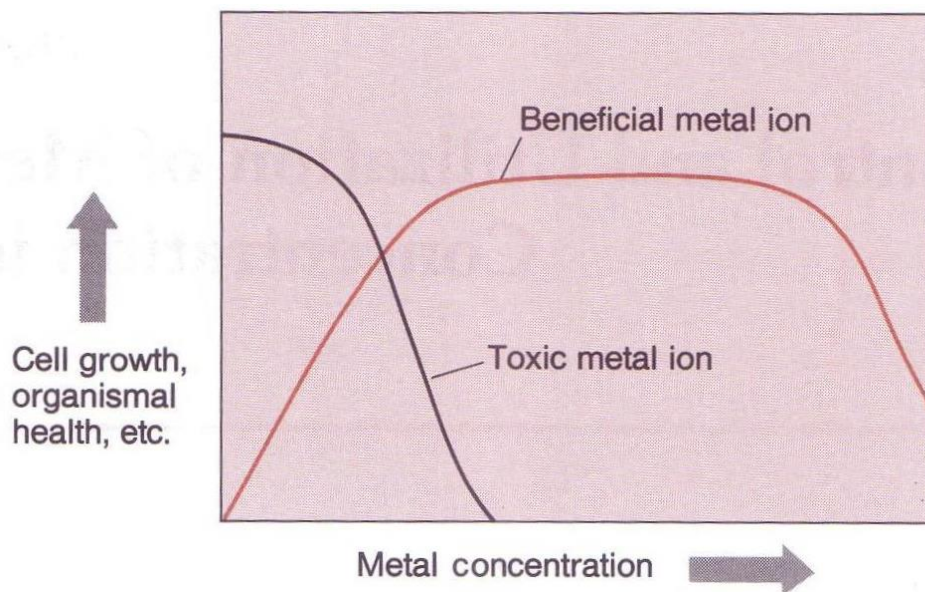


**Figure 2.** Representation of the concentration dependence of toxic and beneficial effects of metal ions on cell growth. Reprinted from Ref 42.

Arabic father of chemistry Jabir ibn Hayyan used the name *antimonium*.<sup>43</sup> Antimony has the electronic structure  $[\text{Kr}] 4d^{10} 5s^2 5p^3$  and has readily accessible oxidation states of -3, 0, +3, and +5. The trivalent and pentavalent oxidation states of antimony are the most important as they are found more commonly in nature. There are two stable isotopes of antimony,  $^{121}\text{Sb}$  with a natural abundance of 57.36% and  $^{123}\text{Sb}$  with a natural abundance of 42.64%. There are also, 35 radioisotopes, with the longest-living isotope being  $^{125}\text{Sb}$  with a half-life of 2.75 years.<sup>44</sup> As antimony is chemically reactive, it forms numerous chemical compounds. Values of various bond energies of electron withdrawing elements with antimony can be found in Table 2.

**II.1.1. Applications of antimony.** Antimony can be found naturally as sulphide and oxide ores, which are present in two forms, stibnite ( $\text{Sb}_2\text{S}_3$ ) and valentinite ( $\text{Sb}_2\text{O}_3$ ).<sup>43, 45</sup> These ores can be found in large quantities in China, South Africa, Mexico, Bolivia, and Chile. Less common sulfide ores include ullmanite ( $\text{NiSbS}$ ), livingstonite ( $\text{HgSb}_4\text{S}_8$ ), tetrahedrite ( $\text{Cu}_3\text{SbS}_3$ ), wolfsbergite ( $\text{CuSbS}_2$ ), and jamesonite ( $\text{FePb}_4\text{Sb}_6\text{S}_{14}$ ). One of the traditional treatment methods

occurs by roasting stibnite or valentinite ore with charcoal or coke to promote a volatile oxide fume ( $\text{Sb}_4\text{O}_6$ ), which can then be refined into pure antimony.<sup>46</sup> During ancient times, stibnite was commonly used for cosmetic purposes in Egypt. The distribution of domestic antimony consumption is estimated as follows: nonmetal products (including ceramics, glass, and rubber products), 22%; flame retardants, 40%; and metal products, such as antimonial lead and ammunition, 39%.<sup>47</sup>

One of the important uses of antimony metal is as a hardener in lead alloys for storage batteries. Antimony metal has other applications in solders and other metal alloys. Some other uses for antimony alloys include “type metal”, which is used in printing presses, bullets, and cable sheathing.<sup>43</sup> Stibine ( $\text{SbH}_3$ ), a gaseous compound used in semiconductor technology, where the purified gas serves as a n-type dopant for silicon. One of the most commercially relevant antimony compounds used today is the trivalent antimony trioxide  $\text{Sb}_2\text{O}_3$ . The compound is processed from the metalloid and is used in polyethylene terephthalate and flame-retardant production, and as an additive in paints, pigments, and ceramics.<sup>43</sup> Some flame-retardant applications are used in aircraft and automobile seat covers and children’s clothing and toys.<sup>43, 49</sup>

**II.1.2. Medicinal applications of antimony.** Organoantimony compounds have shown significant antimicrobial,<sup>50</sup> antitumor,<sup>51-53</sup> and antifungal activity.<sup>54, 55</sup> Organoantimony compounds also show antitumor activity in some diphenylorganoantimony(V) thiophosphates such as  $\text{Ph}_2\text{Sb}\{\text{S}_2\text{-PR}_2\}$  ( $\text{Ph} = \text{C}_6\text{H}_5$ ,  $\text{R} = \text{Ph}$ ,  $i\text{-OC}_3\text{H}_7$ )<sup>56, 57</sup> and methylantimony(III) complexes like  $(\text{CH}_3)\text{SbL}$  ( $\text{L} =$  derivatives of meta-substituted salicylic acid).<sup>58</sup> Due to similarity of the mechanism, cytostatic activity<sup>59</sup> is attributed to these complexes, which is correlative to cisplatin. Furthermore, the biological toxicity of organoantimony is much less than that of Pt and Pd in the case of anticancer

**Table 2.** Bond energies between Sb and halogens, chalcogens and N - typical ligands in organoantimony compounds taken from reference.<sup>a</sup>

Sb – E	E, kcal/mol
Sb-F	105 ± 23
Sb-Cl	86 ± 12
Sb-Br	75 ± 14
Sb-O	103.7 ± 10
Sb-S	90.5
Sb-Te	66.3 ± 0.9
Sb-N	110 ± 20

<sup>a</sup>Data from Ref. 48.

substances.<sup>60</sup> In addition, antimony compounds have been used in treatment against the parasitic disease leishmaniasis for about a century.

Leishmaniasis is caused by the protozoan parasite under the genus *Leishmania* which then multiplies in certain vertebrates.<sup>61</sup> The parasite is transmitted to humans through the bite of sandflies that are infected. Multiple forms of the disease exist, the two most known are cutaneous leishmaniasis (CL) the most common form and visceral leishmaniasis (VL) the most severe. The earliest treatment reported of CL used a trivalent antimonial, tartar emetic, in 1913.<sup>62</sup> Over a decade after the report, tartar emetic was criticized as an antimonial due to side effects such as heavy coughing, chest pain, and severe depression.<sup>61</sup> In addition, the compound was found to be very unstable in a tropical climate and highly toxic.<sup>63</sup> The disadvantages posed by trivalent antimonials lead to the discovery of treatment with pentavalent antimonials. These included urea stibamine.<sup>64,65</sup> antimony gluconate,<sup>66</sup> and sodium stibogluconate.<sup>67</sup> Currently, the most commonly used organoantimony compounds against leishmaniasis are the pentavalent sodium antimony gluconate (Pentostam) and meglumine antimoniate (Glucantime).

The most accepted, proposed mechanism of pentavalent antimonial is their behavior as prodrugs.<sup>68</sup> The pentavalent prodrug undergoes *in vivo* biological reduction into a much more active/toxic trivalent antimony. This  $\text{Sb}^{5+}$  to  $\text{Sb}^{3+}$  reduction requires thiol compounds of both mammalian and parasitic origin.<sup>69-71</sup> Mammalian thiols include glutathione (GSH), cysteine (Cys), and cysteinyl-glycine (Cys-Gly). Glutathione is the main thiol in the cytosol, while cysteine and cysteinyl-glycine are the predominant thiols within lysosomes of mammalian cells.<sup>72, 73</sup> The parasitic thiol compound required is trypanothione ( $\text{T}(\text{SH})_2$ ), this complex consists of glutathione and spermidine. Intake of pentavalent antimony into parasitic cells has been suggested to occur by monoadduct formation between  $\text{Sb}^{5+}$  and nucleotides.<sup>74</sup> This can be attributed to nucleotides containing vicinal *cis*-hydroxyl groups (i.e. adenosine, cytidine, guanosine, uridine, and AMP), where binding occurs at the deprotonated hydroxyl group of the ribose moiety.<sup>75</sup> The complexation leads to nucleotides acting as carriers for  $\text{Sb}^{5+}$  into parasites via lipophospholycan (LPG) transporter.<sup>74</sup> Figure 3 represents the intake of metal compounds and ions into the cell either through passive diffusion or an ion specific channel. Once inside the parasitic cell, the application of a prodrug can proceed. The reduction can occur enzymatically (through ACR2 or TDR1 reductase) or non-enzymatically. Once the reduction has occurred complexation between glutathione or trypanothione.

The first site of interference is with the trypanothione/TR system. This system maintains trypanothione in the reduced state to balance the oxidoreductive balance in the *Leishmania* parasite. This balance protects the cell from oxidative stress damage, toxic heavy metals, and delivers reducing power for DNA synthesis.<sup>76, 77</sup> Trivalent antimonials interfere with trypanothione metabolism by inhibiting trypanothione reductase (TR) and inducing rapid efflux of intracellular trypanothione and glutathione into unaffected *Leishmania cells* which lead to

apoptosis. The second site of attack by trivalent antimony is with the CCHC zinc finger domain. Zinc fingers can be characterized by the coordination of zinc with several amino acid residues, typically cysteine and histidine. This domain has purpose in a variety of diverse functions such as DNA recognition and replication and structure and repair,<sup>78</sup> RNA packing, protein folding and assembly, lipid binding, transcriptional activation, cell differentiation, cell growth, and regulation of apoptosis.<sup>79</sup> Once trivalent antimony is bound to the zinc finger domain, promotion of efflux of  $Zn^{2+}$  occurs, leading to apoptosis.<sup>80</sup> Figure 4 illustrates the prodrug model.

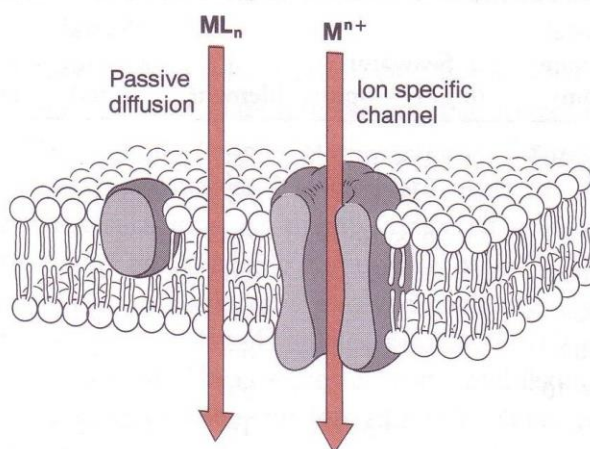


**Figure 3.** Schematic representation of how chemical compounds enter the cell, taken from literature. Reprinted from Ref 74.

### II.3. Coordination Compounds: An Introduction

Coordination compounds, often referred to as “Werner-type” (Figure 5), contain a central atom and ligands. The central atom is usually a metal ion, such as Cu, Ni, Fe, or metalloids, such as Sb, As, and Ge. While the ligands can be various types of inorganic molecules such as  $H_2O$ ,  $NH_3$ ,  $SO_2$ ,  $N_2$ , inorganic anions ( $Cl^-$ ,  $OH^-$ ,  $F^-$ ,  $Br^-$ ,  $NCS^-$ ,  $N_3^-$ ,  $CN^-$ ), or small organic molecules

(pyridine, 1,2-ethylendiamine, amino acids, *etc.*). In general the organic ligands can vary heavily, but the most interesting are mixed-donor ligands, allowing the opportunity to construct new structure with higher complexity.<sup>42</sup> Among the latter ligands, oximes have a special role of being: a) multidentate ligands, and b) possess biological activity. Types of oximes are shown in Figure 6.

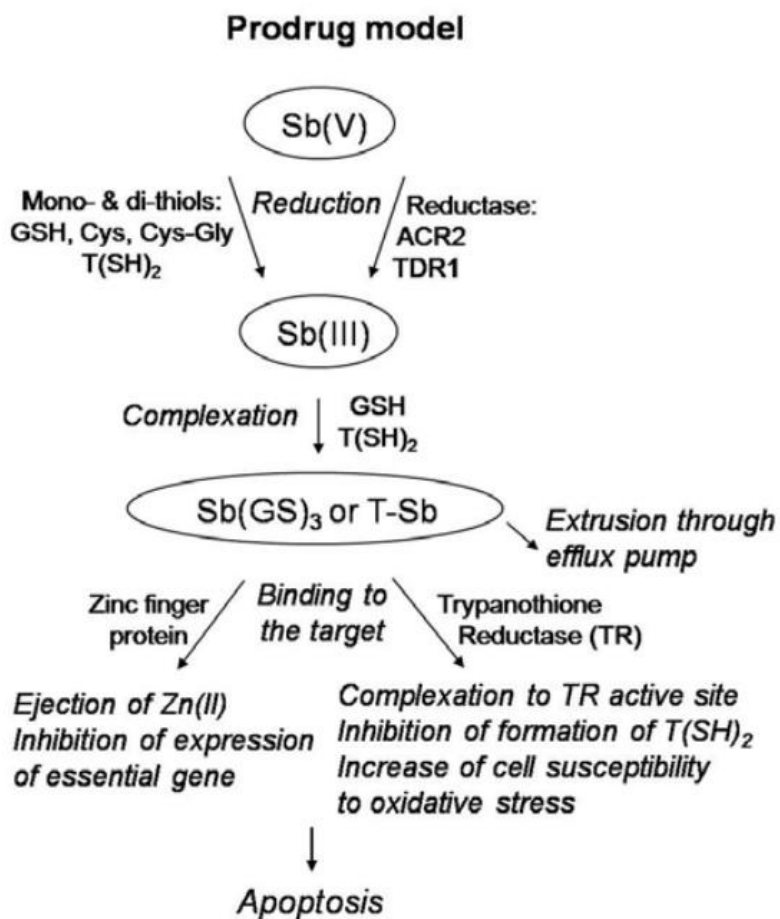


**Figure 4.** Model of pentavalent antimonials as prodrugs taken from literature. Transferred from Ref 81.



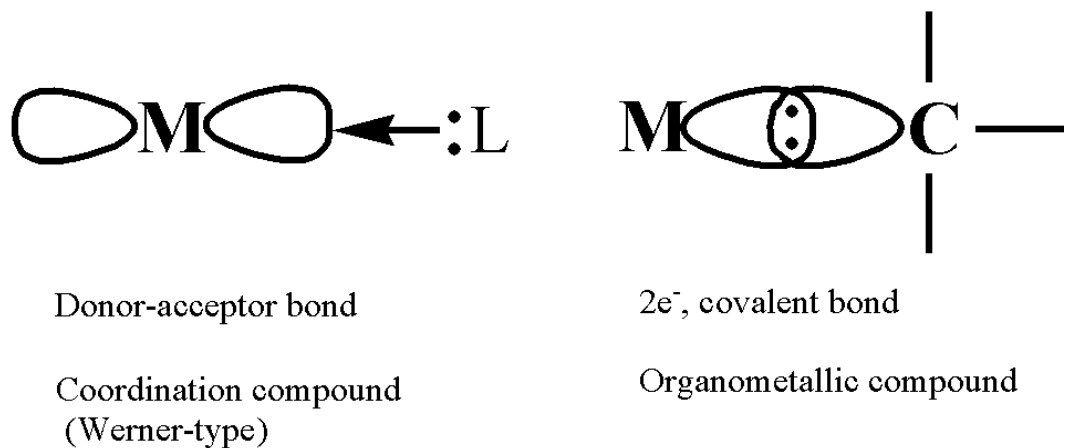


**Figure 5.** Types of bonding found in coordination and organometallic compounds.

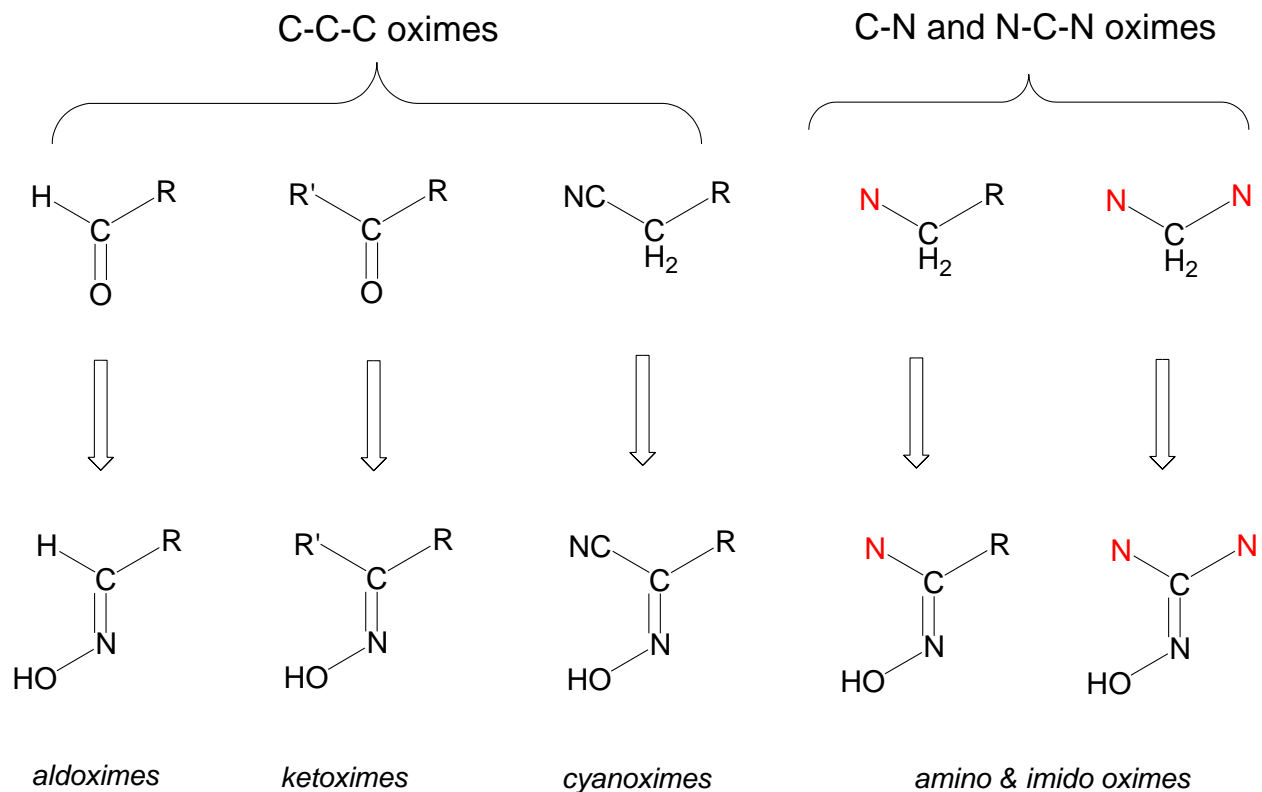


**Figure 6.** Currently known types of cyanoximes and their precursors.

## II.4. Cyanoximes: Ligands For Coordination Compounds

Oximes are ampolydentate organic ligands, which have known biological activity. As of events in the Spring of 2020, there are now newly developed antiviral oxime-containing compounds that showed activity against HIV, SARS-CoV-2, and MERS-CoV-2, which are now in different stages of clinical trials.<sup>82</sup> The structures of these oxime compounds are shown in Figure 7. This ampolydentate behavior can be seen with the  $\text{ACO}^-$  cyanoxime anion with various metals (Figure 8). All cyanoximes represent not only ampolydentate ligands, but also demonstrate rich stereochemistry. Therefore, we observed with years of study of these compounds four distinctive geometries shown in Figure 9. Each isomer was confirmed by X-ray analysis. No interconversion of these isomers was observed.

Cyanoximes represent a new, unique class of biologically active compounds capable of binding to various metals.<sup>83</sup> The general structure for cyanoximes is  $\text{HO-N=C(CN)-R}$ , where R represents the varying electron withdrawing group, typically O, N, or S. The presence of the electron-hungry nitrile (CN) group significantly increases the Lewis acidity making them better ligands to bind metals ions in solution than regular monoximes.<sup>60</sup> The nitrile group allows deprotonation of the cyanoxime in alkaline medium very facile in aqueous and polar organic solvents.<sup>84-86</sup> The color originates from a ground state to a low-lying excited state  $n \rightarrow \pi^*$  in the *nitroso*-chromophore in the visible region of the spectrum.<sup>87-89</sup> Figure 10 represents the deprotonation behavior. In addition, cyanoximes have a resonance system delocalization of charge with its anions allowing more stable structures (Figure 11).

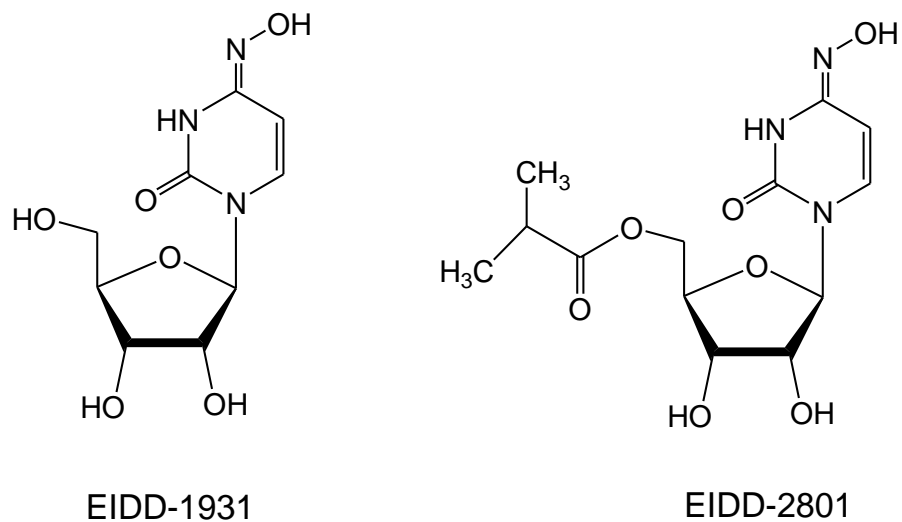


**Figure 7.** Structure of newly developed oxime-bearing compounds with antiviral properties.

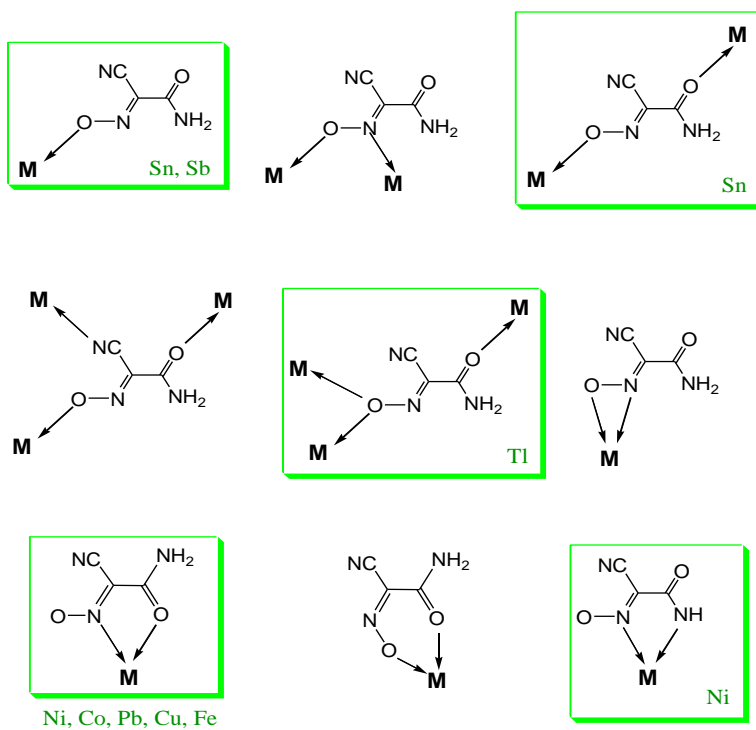


**Figure 8.** Examples of amplydentate binding of the  $\text{ACO}^-$  anion taken from literature. Used from Ref. 91.

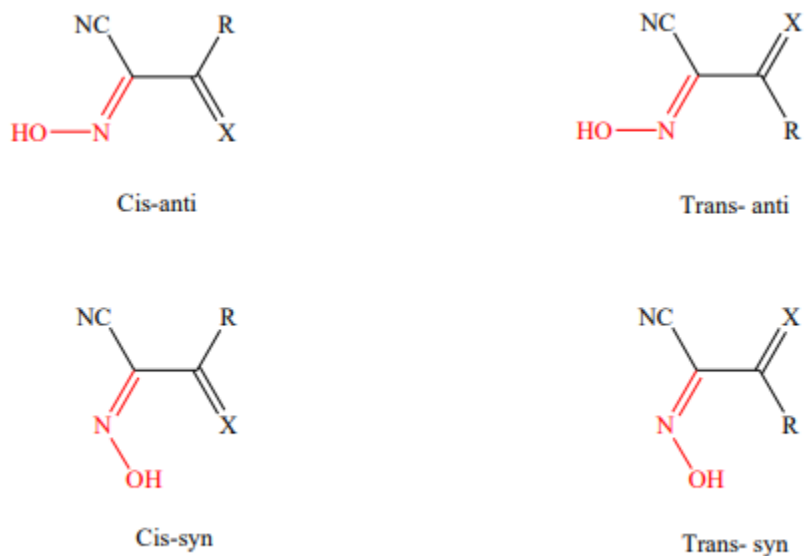


**Figure 9.** Geometrical isomers of cyanoximes.

Cyanoximes were found to have shown significant biological activity such as antimicrobial,<sup>93,94</sup> growth-regulating,<sup>95</sup> and detoxifying agricultural pesticide properties<sup>96</sup> making them useful in a variety of applications. Earlier data demonstrated no intrinsic *in vitro* cytotoxicity of free cyanoximes.<sup>97-99</sup> Also, cyanoximes have shown antimicrobial activity with some of their Ag(I) salts and the sulfur-containing thioamide-cyanoxime, HO-N=C(CN)-C(S)NH<sub>2</sub>, and its K<sup>+</sup>, Na<sup>+</sup>, Cu<sup>2+</sup>, Ni<sup>2+</sup> salts.<sup>100,101</sup> There are 44 known cyanoximes today (Figure 12), where eight of those ligands were selected for current studies from the library as discussed in Part II (Figure 13). The ligands were chosen based off known biological activity and those with some water solubility.

The source of antimony for the organoantimony(V) cyanoximates is from Sb(Ph)<sub>4</sub>Br. The [Sb(Ph)<sub>4</sub>] moiety was selected due to its commercial availability as a colorless and crystalline solid compound. We realized that the tetraphenyl antimony possesses considerable lipophilicity,

but we needed to prove the concept that the combination of known biological cyanoxime ligands and the  $[\text{Sb}(\text{Ph})_4]$  moiety will produce useful compounds. Regardless, it was important to develop a viable synthetic route of organoantimony(V) cyanoximates in general. Therefore, to summarize, this research was conducted for the purpose to try to combine the biological properties of both organoantimony and cyanoximes ligands, in the hope development of new antimicrobial compounds of non-antibiotic nature.

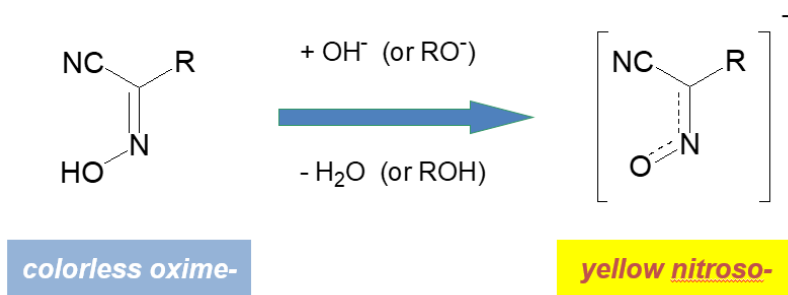


**Figure 10.** Deprotonation of cyanoximes with metal carbonates, hydroxides, and oxides in aqueous and polar organic solvents.

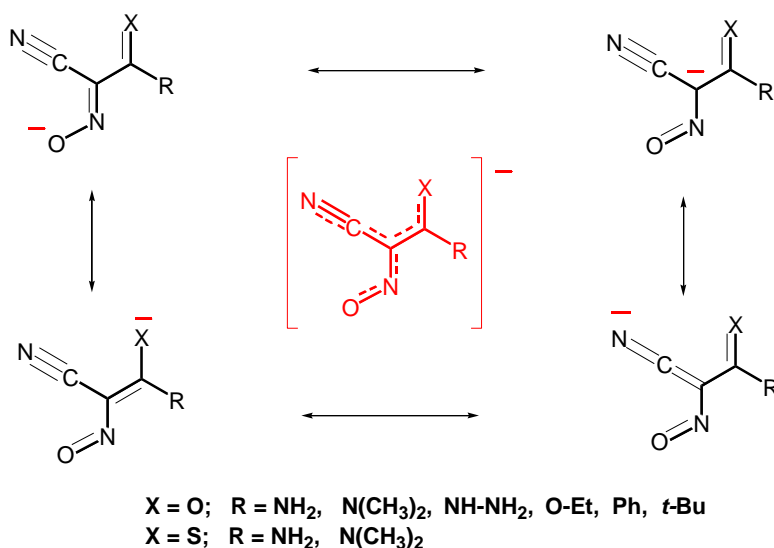


**Figure 11.** Charge delocalization in yellow cyanoxime anion involving several resonance forms. Taken from Ref. 91.

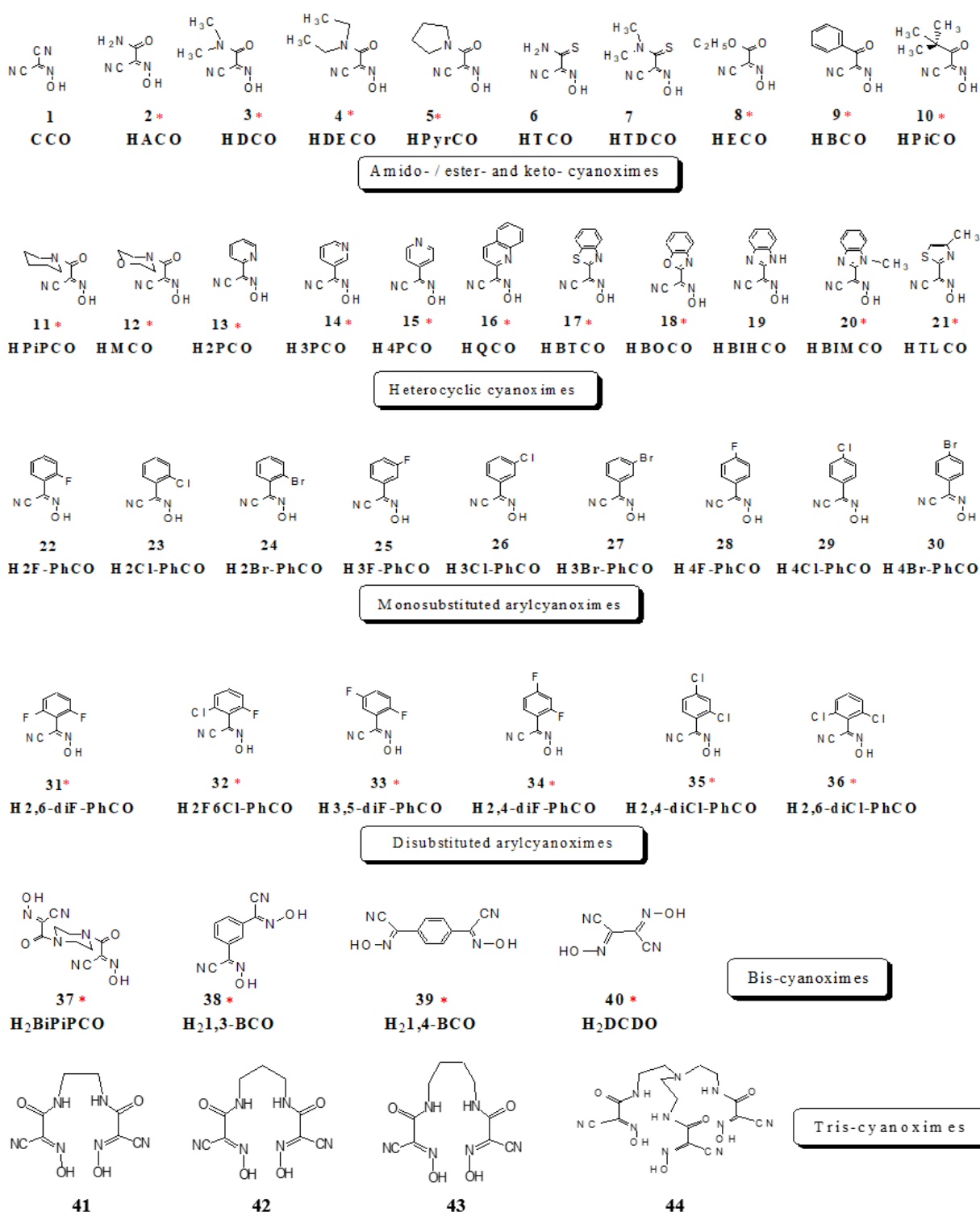


**Figure 12.** List of known cyanoximes ligands. Asterisks indicate compounds for which crystal structures were determined.

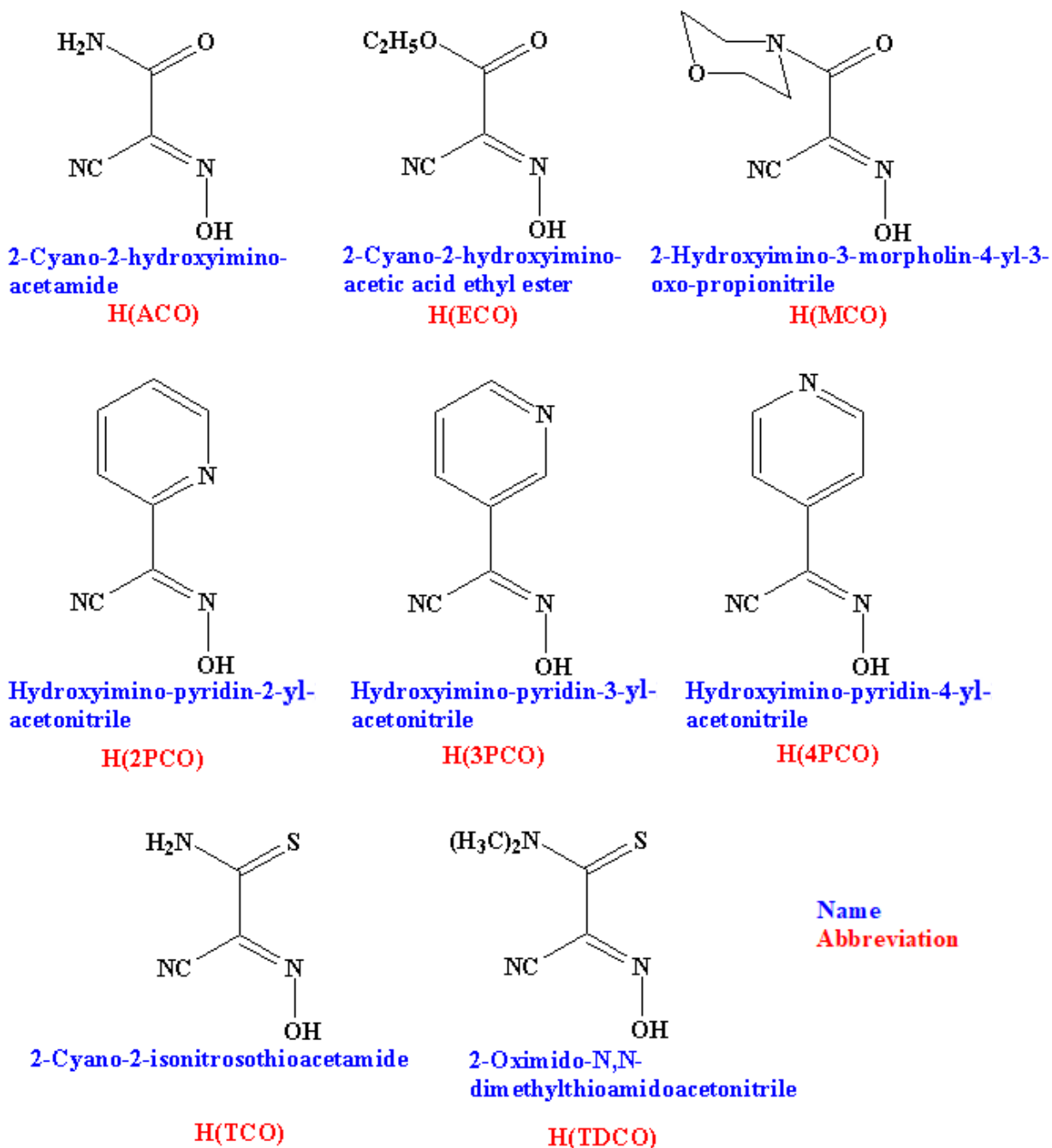


**Figure 13.** Chemical structures of selected cyanoxime ligands and their commonly used abbreviations.

### III. RESEARCH GOALS

My work proposes novel research in Dr. N. Gerasimchuk's lab. It was focused on the synthesis of eight new organoantimony (V) cyanoximates with the purpose of performing antimicrobial studies against Methicillin-resistant *Staphylococcus aureus* strain NRS70, *Escherichia coli* strain S17, and *Pseudomonas aeruginosa* strain PAO1. Therefore, we wanted to investigate the preparative and coordination chemistry of our tetraphenyl organoantimony (V) with a group of selected cyanoximes (Figure 13). Literature review described the importance of a new nonantibiotic treatment against resistant, harmful strains. Therefore, incorporating the medicinal applications of antimonials and antimicrobial activity of silver(I) cyanoximes will further develop this field of research. Hence, are the following goals for this research project:

1. To synthesize a series of eight novel compounds and conduct their characterization using available spectroscopic methods and X-ray analysis.
2. Submit pure and fully characterized compounds for *in vitro* antimicrobial and antifungal studies at a collaborative university – Oklahoma State University, Stillwater (Prof. M. Patrauchan and Dr. K. Wozniak, respectively).



## IV. EXPERIMENTAL

### IV.1. Experimental And Characterization Methods

**IV.1.1. Reagents and general considerations.** Reagent grade morpholine (C<sub>4</sub>H<sub>9</sub>NO), toluene (C<sub>7</sub>H<sub>8</sub>), ethyl cyanoacetate (C<sub>5</sub>H<sub>7</sub>NO<sub>2</sub>), chloroform (CH<sub>3</sub>Cl), and our source of organoantimony, Sb(C<sub>6</sub>H<sub>5</sub>)<sub>4</sub>Br at ~95% purity, was purchased from Sigma Aldrich. All other chemicals and organic solvents – isopropyl alcohol (*i*-PrOH), acetonitrile (CH<sub>3</sub>CN), diethyl ether, sodium nitrite (NaNO<sub>2</sub>), concentrated sulfuric acid (H<sub>2</sub>SO<sub>4</sub>), and concentrated hydrochloric acid (HCl) from Fisher Scientific and sodium metal from Fluka – were of sufficient quality, and used without additional purification.

Cyanoximes and their silver(I) derivatives selected for current studies were either taken from a bank of ligands in Dr. Gerasimchuk's research laboratory or obtained using published procedures from starting substituted acetonitriles. Therefore, compounds such as H(2PCO), Ag(3PCO), Ag(4PCO), Ag(ACO) and Ag(ECO), were used for syntheses of organoantimony(V) cyanoximates from previous investigations<sup>1</sup>, while H(MCO) was prepared and purified in this research. The thioamides-based cyanoximes H(TCO), H(TDCO) as well as all Tl(I)-cyanoximates were prepared by Dr. Gerasimchuk in order to avoid graduate students' exposure to stench or toxic chemical compounds. Melting points were determined with the help of pre-calibrated apparatus with urea and naphthalene standards Digi-Melt (MPA106 SRS) in open melting point capillaries, and reported without correction. Elemental analysis on C, H, N (and S with thioamide-based cyanoximes) content was conducted at the Atlantic Microlab (Norcross, GA).

---

<sup>1</sup> Mark Whited, Daniela Marcano, Jeff Morton

**IV.1.2. Vibrational spectroscopy.** The IR-spectra of all compounds reported herein were samples of studied compounds with the help of Bruker ATR FT spectrophotometer. The resolution was set to be  $4\text{ cm}^{-1}$  with 64 scans in the range of  $400 - 4000\text{ cm}^{-1}$ . An atmospheric compensation and baseline correction were applied for data treatment.

**IV.1.3. UV-visible spectra.** The electronic spectra of selected organoantimony(V) cyanoximate compounds were recorded in solutions using the HP 8354 diode array UV-visible spectrophotometer operating in the range of  $200 - 1100\text{ nm}$  typically at room temperature. In cases where variable temperature spectra were needed, a high precision Peltier Quantum Northwest thermocontroller was used with  $1\text{ cm}$  quartz cuvettes. Data of spectroscopic studies are presented in appropriate places in the thesis.

**IV.1.4. NMR spectra.** The spectra were obtained on a Varian INova-400 MHz spectrometer at room temperature in  $\text{DMSO-d}_6$  and  $\text{CDCl}_2$  solutions for  $^1\text{H}$  and  $^{13}\text{C}$ , respectively.

**IV.1.5. X-ray crystallography.** Suitable single crystals of organoantimony(V) cyanoximates were grown at  $+4^\circ\text{C}$  exclusively using the vapor diffusion method: acetonitrile solutions of compounds were placed into the inner tube and vapors of anhydrous ether were used as crystallizing agent from the outer tube with a screw cap. Normally within 2-3 weeks after setting up, transparent, well-shaped crystals appeared on the walls in the inner tube suitable for crystallographic studies. All crystals selected for studies were placed on plastic MiTeGen holders attached to the copper-pin on the goniometer head of the Bruker APEX-2 diffractometer, equipped with a SMART CCD area detector. The intensity data were collected at low temperature. Data collection was done in  $\omega$  scan mode using the Mo tube ( $\text{K}_\alpha$  radiation;  $\lambda = 0.71073\text{ \AA}$ ) with a highly oriented graphite monochromator. Intensities were integrated from 4 series of 364 exposures, each covering  $0.5^\circ$  steps in  $\omega$  at  $20 - 60$  seconds of exposition time

depending on the crystal diffracting power, with the total data set being a sphere. The space group determination was done with the aid of the XPREP software. The absorption correction was performed by a crystal face indexing procedure with a help of a video microscope followed by numerical input into the SADABS program. Both cited programs are included in the Bruker AXS software package. All structures were solved by direct methods and refined by least squares on weighted  $F^2$  values for all reflections with  $I > 3\sigma(I)$  using the SHELXTL program. In several structures it was possible to identify all H-atoms on the electron density map due to the high quality of crystals. However, in some structures H-atoms were placed in calculated positions in accordance with the hybridization state of a hosting carbon atom and were refined isotropically. No apparent problems or complications were encountered during the structures' solutions and refinement as evident from very positive PLATON checkCIF reports. Values of selected bond lengths and valence angles are presented in respective Tables following the discussion of crystal structures. A representative drawing of the crystal structures and packing diagrams was done using the ORTEP 3v2 and Mercury software packages. All determined crystal structures have been deposited at CCDC (England), with PLATON checkCIF reports.

**IV.1.6. Thermal Stability Studies.** Thermal stability of the obtained metal complexes was assessed using Q-600 TG/DSC analyzer (TA Instruments) under  $N_2$  flow of 100 mL/min at  $10^\circ/\text{min}$  heat rate. Appendix A-1 briefly explains the use of the instrument. Heating of samples was carried out to  $800^\circ\text{C}$  at which the samples' complete decomposition was attained. Some of the results of thermal analyses studies are presented in during discussion section with the rest of data given in Appendix B.

## **IV.2. Synthesis Of HMCO: Synthesis Of 3-Morpholin-4-yl-3-oxopropionitrile, The HMCO Cyanoxime Precursor, Pre-MCO**

Preparation of this ligand represents a two-step procedure (Figure 14), where we used two methods for the amide precursor preparation. The first method for synthesis of pre-MCO used dichloromethane as the solvent, and a mixture of morpholine, ethyl cyanoacetate, and dichloromethane 1:1:1 (gram based) was prepared in a 25 mL amber glass bottle. Nitrogen gas was then bubbled into the solution under stirring for 10 minutes. The bottle was then capped, wrapped in parafilm, and placed in the freezer at a temperature of 0°C until crystallization of the target amide. Crystallization of the desired pre-MCO compound occurred between one to two weeks. The crystals were then filtered and washed with 35 mL of toluene followed by 35 mL of hexane and dried in a desiccator charged with concentrated sulfuric acid for a week. The yield was 82% (1.434 g): calculations of which were based on ethyl cyanoacetate as the limiting reagent.

A second method for the synthesis of pre-MCO used chloroform as the solvent, as a similar procedure previously mentioned. A mixture of morpholine, ethyl cyanoacetate, and chloroform 1:1:1 (gram based) was prepared in a 25 mL amber glass bottle. Synthesis follows as previously mentioned. Crystallization of the desired pre-MCO amide compound occurred between one to two weeks. The crystals were filtered and then washed with 35 mL of toluene and then 35 mL of hexane and dried in a desiccator charged with concentrated sulfuric acid for a week. The yield was 77% (1.224 g): Similarly, calculations of yield were based on ethyl cyanoacetate as the limiting reagent. The two methods of preparation of the pre-MCO amide compound can be found in Figure 14A.

### IV.3. Synthesis Of H(MCO): From Its Precursor (pre-MCO)

Nitrosation of the pre-MCO was performed at room temperature by bubbling methylnitrite in basic conditions explained in published procedures (Figure 14B).<sup>[101]</sup> Yield of the final product was 65% (1.11 g) from 1.434g pre-MCO, mp.: 170-173 °C, and  $R_f = 0.36$  in EtOAc/hexane = 3:1 mobile phase. The  $^{13}\text{C}\{^1\text{H}\}$  NMR spectra of H(MCO) were recorded in DMSO- $d_6$ . Where the  $^1\text{H}$  NMR, in ppm, had chemical shifts of 14.27 (OH), ring protons - 3.32 ( $\text{CH}_2$  next to O), and 2.54 ( $\text{CH}_2$  next to N). The  $^{13}\text{C}$  NMR chemical shifts were analogous with previous literature reported in.<sup>101</sup> Bands in IR spectrum of H(MCO), in  $\text{cm}^{-1}$ , were: 3422, 2969, 2831, 2239, 1621, and 1006.

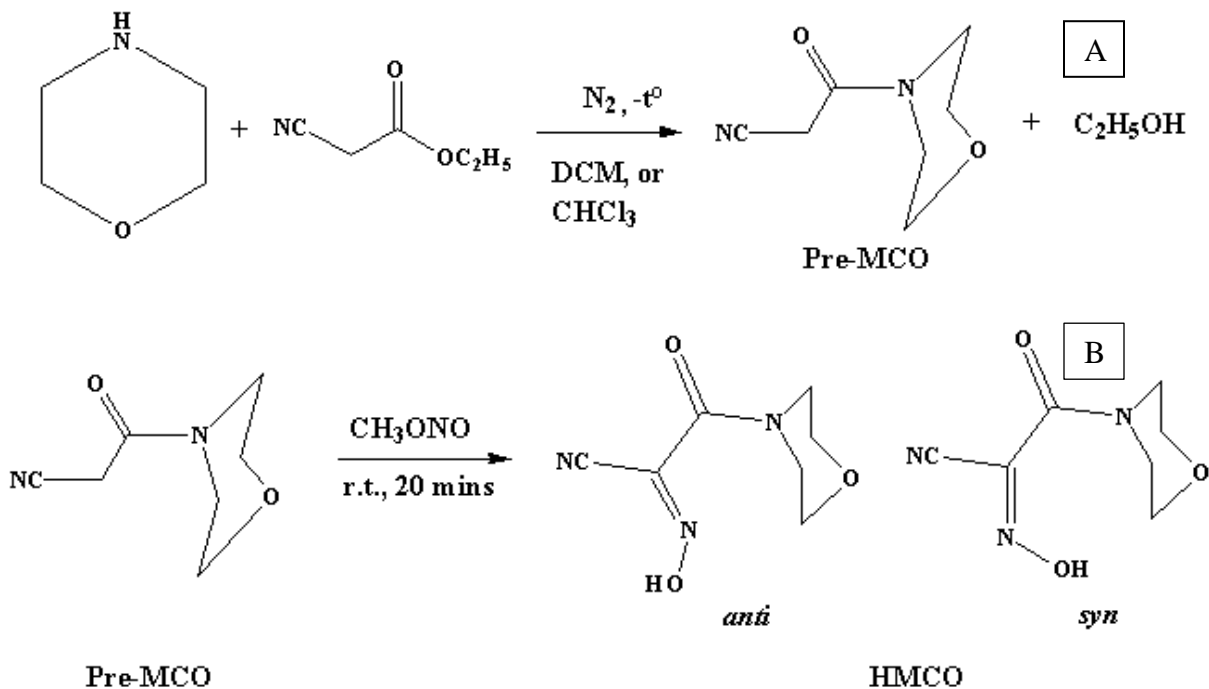


**Figure 14.** A, Synthesis of the H(MCO) from its precursor obtained in two different ways. B, nitrosation of pre-MCO amide compound into protonated cyanoxime ligand.

### IV.4. Synthesis Of Ag(I)L Salts From HL Acids

There were some AgL (L = cyanoxime anion ligand) available from previous investigations in our laboratory, which were needed for organoantimony(V) cyanoximates. Ag(MCO) and Ag(2PCO) were prepared in this research, while all other silver(I) salts were

retrieved from the library of compounds in our lab. Preparation of Ag(I) complexes began with deprotonation with  $K_2CO_3$ , followed by coordination with Ag through addition of  $AgNO_3$  (Figure 15). The typical synthesis of silver(I) derivatives is shown as an example for only one compound. Thus, white H(2PCO) in the amount of 0.4605 g (2.46 mmol) was dissolved in a mixture of 10 mL of EtOH, then diluted with 10 mL of water, heated to 55°C, and then added dropwise to a solution of 0.169 g (1.22 mmol) of  $K_2CO_3$  in 10 mL of  $H_2O$ . The color of the solution immediately turned yellow signifying the presence of the nitroso anion. The reaction mixture was placed for 2 min into an ultrasound bath to accelerate the evolution of  $CO_2$ . A solution of 0.4183 g (2.46 mmol) of  $AgNO_3$  in 10 mL of water was added dropwise under intensive stirring to a solution of K(2PCO) above. Mixing resulted in a very fine yellow precipitate, which after an additional 20 min of stirring was filtered, washed with three portions of 10 mL of water, and then dried in a vacuum desiccator charged with  $H_2SO_4$  (conc.) for 3 days. Analytical data for desired Ag(MCO) and Ag(2PCO) were reported in a MS thesis from a previous lab member<sup>101</sup> and published work,<sup>102</sup> respectively.

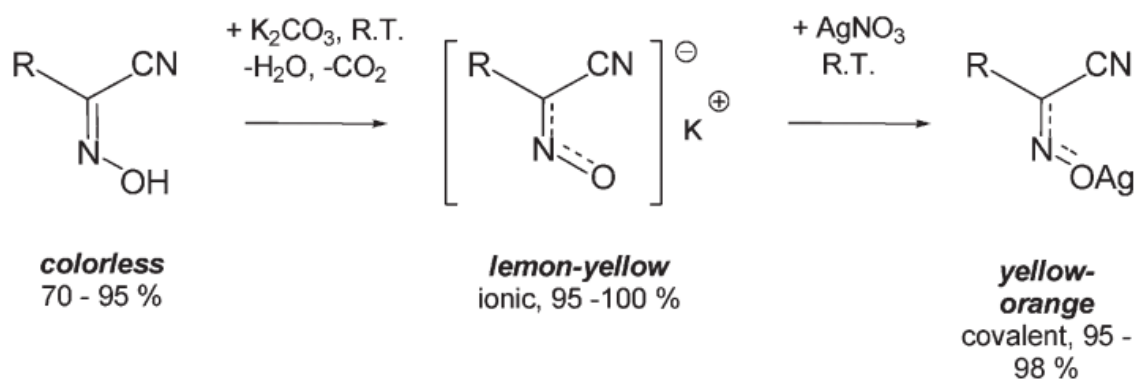


**Figure 15.** General synthesis of silver(I) salts of cyanoxime ligands from their protonated precursor. R represents the different cyanoximes.

#### IV.5. Synthesis of Sb(Ph)<sub>4</sub>L, The Metathesis Reaction

Tetraphenylantimony(V) cyanoximates were obtained using a metathesis reaction of previously prepared Ag(I) salts and tetraphenylantimony(V) bromide described in literature (Figure 16).<sup>60</sup> This method was found to be the most convenient way to synthesize organoantimony(V),<sup>60</sup> organotellurium (IV),<sup>103</sup> and organotin(IV)<sup>97</sup> compounds. The initial compound SbPh<sub>4</sub>Br is a commercially available source of pentavalent antimony. One typical synthesis of organoantimony(V) cyanoximates is depicted below. The preparation of Sb(Ph)<sub>4</sub>(ACO) was conducted by adding 0.201 g (0.394 mmol) of Sb(Ph)<sub>4</sub>Br to 10 mL of dry acetonitrile (CH<sub>3</sub>CN) in a 25-mL Erlenmeyer flask then swirled until completely dissolved. Then under a red-light emitting lamp, 0.0865 g (0.414 mmol) of finely grinded, solid Ag(ACO) was added in small portions to the flask and sonicated for five minutes for efficient mixing of this heterogeneous reaction. Following sonication, filtration of the white AgBr precipitate was done using two methods in the dark: a) by vacuum filtration and b) centrifugation with nylon 0.45 micron membrane, Eppendorf tubes (Figure 17).

In the vacuum filtration method, the first colorless filtrate was transferred in Erlenmeyer flask for storage and crystal growth. The product was washed with 5 mL portions of CH<sub>3</sub>CN, until the filtrate did not glow under UV light when spotted on a TLC plate. This technique was a way of controlling completeness of washing our desired product while filtering out the AgBr byproduct. Once all product was filtrated out and washed, each portion was added to the storage flask, and put into a desiccator with paraffin until acetonitrile was evaporated. This is possible, as paraffin wax absorbs alkanes like our solvent CH<sub>3</sub>CN. As for filtration through centrifugation, the cloudy solution of our desired organoantimony(V) cyanoximate and AgBr was transferred into filtered nylon Eppendorf tubes and centrifuged in a Thermo Scientific Sorvall Legends

Micro 17 at 10,000 rpm for three minutes. Following centrifugation, AgBr can be visibly seen at the bottom of the Eppendorf tubes in a clear solution. The transfer of the mentioned clear solution was placed inside a beaker and put into a desiccator with paraffin for crystallization. The progression of centrifuge filtration for Sb(Ph)<sub>4</sub>(MCO) is shown in Figure 18. Synthesis information regarding compounds' color, yields, and data of elemental composition determination presented in Table 3.

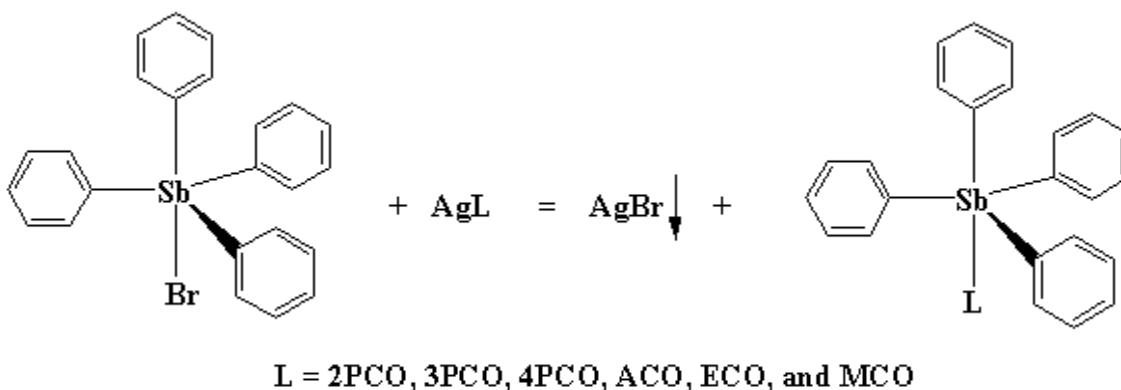


**Figure 16.** General synthesis of organoantimony(V) cyanoximates using the metathesis reaction with silver(I) salts. L represents the variety of ligands chosen for study.



**Figure 17.** Instrumentation and accessories used for isolation of organoantimony(V) cyanoximates from Ag(I)Br. A Thermo Scientific centrifuge (left) with filtered nylon Eppendorf tubes (right).



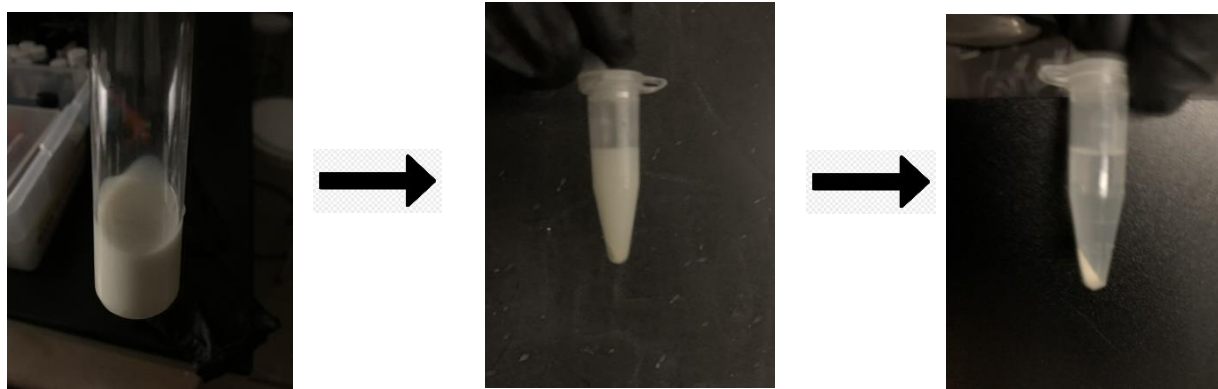


**Figure 18.** Progression of filtration using centrifugation a homogenous mixture of  $\text{Sb}(\text{Ph})_4(\text{MCO})$  and  $\text{AgBr}$  in  $\text{CH}_3\text{CN}$  (left), transferred into an Eppendorf tube (middle), and after centrifugation (right).

#### IV.6. Synthesis Of Thioamide $\text{Sb}(\text{Ph})_4\text{L}'$ , From $\text{TIL}'$ Salts

Two thioamides  $\text{TCO}^-$  and  $\text{TDCO}^-$  do not form  $\text{Ag}(\text{I})$  derivatives because of the fast decomposition reaction resulting in a black  $\text{Ag}_2\text{S}$  precipitate formation. Therefore, a methathesis reaction using  $\text{TIL}'$  was incorporated for the thioamide containing ligands. Contrary to  $\text{Ag}(\text{I})$  complexes of some cyanoximes,<sup>104</sup>  $\text{Tl}(\text{I})$  compounds are light-stable and readily formed with thiols and thioamides.<sup>105</sup>

For preparation of  $\text{Sb}(\text{Ph})_4(\text{TCO})$ , 0.155 g (0.304 mmol) of white  $\text{Sb}(\text{Ph})_4\text{Br}$  was dissolved in 8 mL of  $\text{CH}_3\text{CN}$ . Then 0.101 g (0.304 mmol) of a solid, yellow powder  $\text{Tl}(\text{TCO})$  (Figure 19) was suspended in 4 mL of  $\text{CH}_3\text{CN}$  and mixed with first solution. Sonication was used to insure proper mixing of the solution and suspension at room temperature. After 10 minutes of sonication, filtration via centrifugation went exactly as mentioned previously, receiving a clear yellow solution and a colorless  $\text{TlBr}$  precipitate. The filtered solution was then placed in a beaker and stored in a charged desiccator, with paraffin wax (for  $\text{CH}_3\text{CN}$  absorption), for crystallization. The crystallized product is shown in Figure 20. Thus, preparation of  $\text{Sb}(\text{Ph})_4\text{L}'$

( $L' = \text{TCO}^-$ ,  $\text{TDCO}^-$ ) was accomplished using the metathesis reaction shown in Figure 21. This is accomplished easily as Tl(I) halides (similar to Ag(I) halides) readily precipitate in aqueous and nonaqueous solutions. Synthesis of both thioamide containing cyanoximates follows.

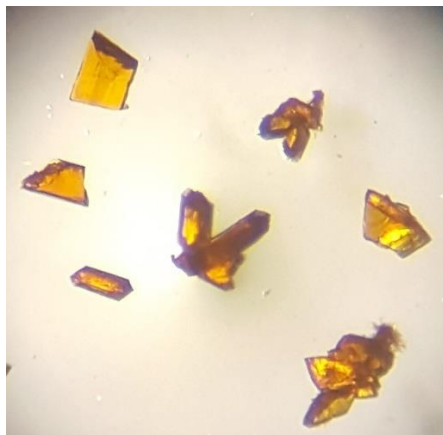


**Figure 19.** Microscopic image of the Tl(TCO) salt.

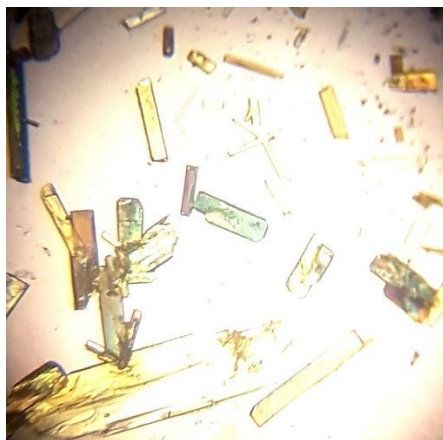


**Figure 20.** Microscopic image of desired crystalline organoantimony(V) cyanoximate, Sb(Ph)<sub>4</sub>(TCO).

As for the synthesis of Sb(Ph)<sub>4</sub>(TDCO), 0.206 g (0.404 mmol) of white Sb(Ph)<sub>4</sub>Br was dissolved in 8 mL of CH<sub>3</sub>CN. Then, 0.143 g (0.404 mmol) of finely grinded, orange Tl(TDCO) was readily dissolved in 4 mL of CH<sub>3</sub>CN. The two solutions were sonicated for 10 minutes,

filtered via centrifuge, and left for crystallization in the same procedure as before generating a yellow-plate crystalline product (Figure 22).

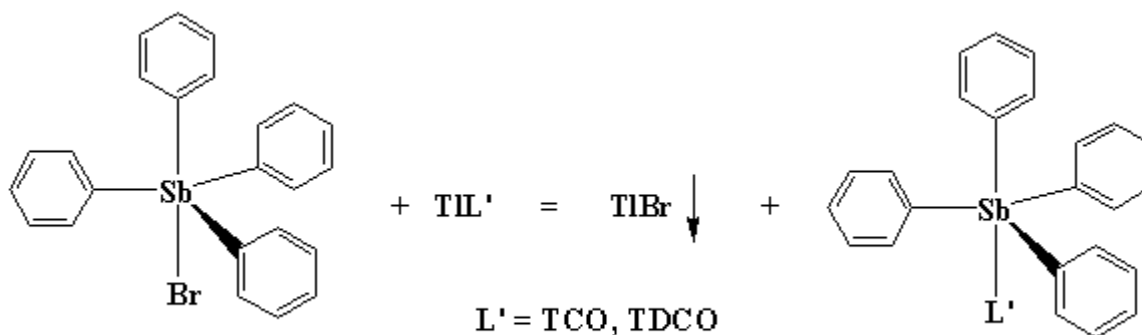


**Figure 21.** General synthesis of organoantimony(V) cyanoximates using the metathesis reaction with thallium(I) salts. L' represents the thioamide containing ligands.

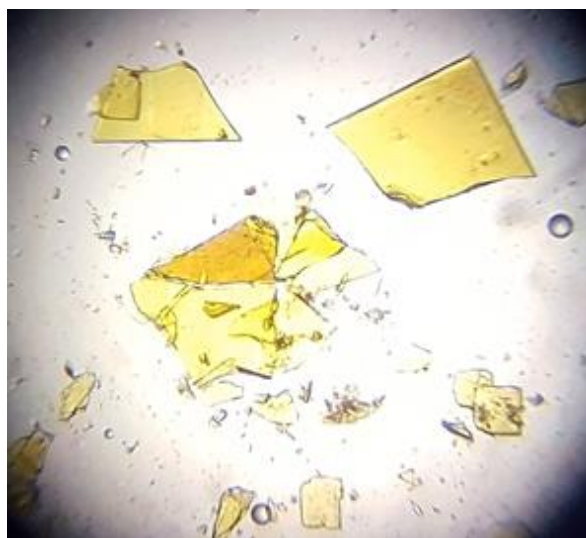


**Figure 22.** Microscopic image of desired crystalline organoantimony(V) cyanoximate,  $\text{Sb(Ph)}_4(\text{TDCO})$ .

#### IV.7. Antimicrobial Studies: Kirby-Bauer Single Disk Test

The  $\text{Sb(Ph)}_4(\text{MCO})$ ,  $\text{Sb(Ph)}_4(\text{ECO})$ ,  $\text{Sb(Ph)}_4(\text{TCO})$ ,  $\text{Sb(Ph)}_4(\text{TDCO})$ , and  $\text{Sb(Ph)}_4(\text{ACO})$  compounds were chosen for initial inhibition zone measurements. One of the precursors of the

metathesis reaction,  $\text{Sb}(\text{Ph})_4\text{Br}$ , was used as a control. The procedure of applying compounds to disks follows. Using 100% cotton paper, disks were cut with a hole-punch. 25  $\mu\text{l}$  aliquot samples of three different concentrations (stock, x2, and x4 dilution factor) of compounds dissolved in acetonitrile were transferred onto paper disks and left to dry on a Teflon surface for 20 minutes. Following disk preparation, inhibition zone measurements were conducted at another institute, Oklahoma State University. Methicillin-resistant *Staphylococcus aureus* strain NRS70, *Escherichia coli* strain S17, and *Pseudomonas aeruginosa* strain PAO1 were used. Precultures were prepared by inoculating 3 mL of LB medium with a strain culture. The mixture was then incubated at 37 °C at 200 rpm for 12 hours via a Thermo scientific MaxQ 4000. Before plate inoculation, the cultures were collected and diluted to obtain an optical density of 600 (OD600) at 0.1. Next, 100  $\mu\text{l}$  of normalized culture was spread onto LB agar plates (15 mL of LB in each plate). 10  $\mu\text{l}$  of phosphate buffered saline (PBS) was then applied on the plate followed by placement of compound-adsorbed disks. Fully prepared plates were then incubated at 37°C for 24 hours, after incubation clearance zones were measured.

#### **IV.8. Antimicrobial Broth Dilution Minimal Inhibition Concentration (MIC) Assays**

The same strains selected in the previous antimicrobial assay were used for broth dilution MIC studies. The strains were tested against 4 compounds:  $\text{Sb}(\text{Ph})_4(\text{MCO})$ ,  $\text{H}(\text{MCO})$ ,  $\text{H}(\text{ECO})$ , and  $\text{Na}[\text{H}(\text{ACO})_2]$ . MIC assays were determined using a similar published procedure.<sup>107</sup> Precultures of the selected strains were grown for 12 hours in Mueller Hinton broth (MHB) at 37°C 200 rpm. The four compounds previously mentioned were put into 10 different concentrations, starting at 0 to 500  $\mu\text{g}/\text{mL}$  in increments of 50. The compounds were dissolved in DMSO ranging from 0 to 10% in increments of 1% for the gradient. The cultures were then

normalized to an OD of 0.1 using a spectrophotometer, then 120  $\mu\text{L}$  of OD 0.1 was diluted 50X. Next, 100  $\mu\text{L}$  of the dilution inoculate solution was placed into a 100  $\mu\text{L}$  well plate with the appropriate antimicrobial compound solution. The wells were then incubated again at 37°C and 200 rpm until two time intervals occurred, 6 and 24 hours. Once reaching both time slots, the OD600 was then measured.

#### **IV.9. Antifungal Studies: Kirby-Bauer Single Disk Test And MIC Assays**

The protonated ligands  $\text{Na}[\text{H}(\text{ACO})_2]$ ,  $\text{H}(\text{MCO})$ ,  $\text{H}(\text{ECO})$ , and the organoantimony cyanoximate  $\text{Sb}(\text{Ph})_4(\text{MCO})$  were chosen for inhibition zone and MIC determination assays. Fungi used in these experiments were *Cryptococcus neoformans* and *Candida albicans*. For all experiments, both MIC and disk diffusion, the fungi were grown in Yeast Extract-Peptone-Dextrose (YDP) broth at 30°C for 16-18 hours. Then fungi were washed three times with PBS before adjusting to required concentration for the specific assay. In the MIC assays, the media was RPMI-MOPS, at a pH of 7.4, and with a fungal concentration of  $0.5 \times 10^3$  cells/mL. In addition, fungi were incubated for 48 hours at 35°C, then visually inspected the plate and took optical density readings on a platereader to confirm visual inspection. For the disk diffusion assays, the media was PBS and the fungal concentration used was  $1 \times 10^6$  cells/mL. The disk was applied to the center of a YPD plate previously spread with the specific fungal culture. The plate and disk were then incubated at 30°C for 48 hours, then zone of inhibition around the disk was measured. Results of antimicrobial and antifungal studies will be presented and discussed in the following chapters.

**Table 3.** Color, yield, and elemental analysis of synthesized organoantimony(V) cyanoximates and their precursors.

Compound	Color	Yield (%)	Elemental analysis, element %			
			C, % Calc. (Found)	H, % Calc. (Found)	N, % Calc. (Found)	S, % Calc. (Found)
pre-MCO	white	65	-	-	-	-
HMCO	off-white	82	-	-	-	-
Ag(MCO)	yellow		28.99 (28.19)	2.78 (2.81)	14.49 (14.06)	-
Sb(Ph) <sub>4</sub> (MCO)	colorless	90	60.81 (59.48)	4.61 (4.52)	8.86 (6.47)	-
Sb(Ph) <sub>4</sub> (2PCO)·H <sub>2</sub> O	colorless	45	64.61 (64.34)	4.20 (4.07)	7.29 (7.19)	-
Sb(Ph) <sub>4</sub> (3PCO)	colorless	84	64.61 (62.17)	4.20 (3.99)	7.29 (6.51)	-
Sb(Ph) <sub>4</sub> (4PCO)	colorless	46	64.61 (63.93)	4.20 (3.93)	7.29 (7.31)	-
Sb(Ph) <sub>4</sub> (ACO)	colorless	79	59.81 (58.39)	4.09 (4.16)	7.75 (7.29)	-
Sb(Ph) <sub>4</sub> (ECO)	colorless	91	60.86 (60.59)	4.58 (4.44)	4.89 (4.94)	-
Sb(Ph) <sub>4</sub> (TDCO)	golden yellow	51	59.40 (58.84)	4.47 (4.37)	7.17 (6.20)	5.47 (4.64)
Tl(TCO)	yellow		10.84 (10.77)	0.61 (0.54)	12.64 (12.71)	9.64 (9.52)
Sb(Ph) <sub>4</sub> (TCO)	yellow	51	58.08 (57.93)	3.97 (3.84)	7.53 (7.42)	5.74 (5.59)

## V. RESULTS AND DISCUSSION

### V.1. X-Ray Single Crystal Analysis

The crystals of all complexes were successfully grown using two different methods: 1) by slow crystallization through evaporation of a CH<sub>3</sub>CN solvent, or 2) through the vapor diffusion when ether helped with crystallization. Most compounds were simple and easy to crystallize with method 1, while some hard to crystallize compounds were accomplished with 2. The Sb(Ph)<sub>4</sub>L complexes of H(2PCO), H(3PCO), H(4PCO), H(ECO), H(MCO), H(TCO), and Tl(TDCO) were crystallized and analyzed. Most crystal structures were initially determined by Dr. Gerasimchuk, while later determination of the full crystal report was accomplished by me for learning purposes. The structures were solved using direct methods incorporated into the SHELXS – 2013 and refined using the Bruker SHELXTL Software Packages.<sup>108</sup> In the case of crystal twins, application of the detwinning procedure followed by absorption correction was accomplished with the help of TWINABS.<sup>109</sup> Some of the drawings of molecular structures were done with ORTEP 3v2,<sup>110</sup> while the other molecular structures and packing diagrams for structures were performed using the Mercury Program.<sup>111</sup> Below we present brief descriptions of crystallographic results in this study. All the presented structures were assigned Cambridge Crystallographic Data Centre (CCDC) numbers, the checkCIF reports for each structure can be found in Appendix C 1-9.

**V.1.1. Trends found in Sb(Ph)<sub>4</sub> cyanoximates crystal structure.** All tetraphenyl organoantimony(V) cyanoximates have an Sb(V) core that adopts a distorted trigonal bipyramid geometry. This can be seen in every Oak Ridge Thermal Ellipsoids Program (ORTEP) diagram shown in this chapter. Coordination polyhedra of organoantimony(V) cyanoximates are similar

to those as previously determined compounds  $\text{Sb(Ph)}_4\text{OCH}_3$  and  $\text{Sb(Ph)}_4\text{OH}$  referenced.<sup>60</sup> Some peculiarities of the pentavalent coordination can be described for each crystal structure determined in this work. Thus, there are three phenyl rings in the equatorial position of the distorted trigonal bipyramid, where they adopt the most sterically favored three blade propeller-type configuration. These equatorial phenyl rings are also slightly tilted towards the coordinated monodentate cyanoxime ligand bound in the axial position to the  $\text{Sb(V)}$  atom.

In total, nine crystal structures of organoantimony(V) cyanoximtes were determined. In six cases, there were only one molecule located in the asymmetric unit (ASU), while in three cases we observed multiple crystallographically independent molecules in the ASU. All determined and finalized crystal structures were registered at the world-wide Cambridge Crystallographic Data Centre (CCDC) in England. Quality of data has been verified in Holland by using the PLATON checkCIF program and results are present in Appendix C.

**V.1.2. Crystal structure of  $\text{Sb(Ph)}_4(\text{ACO})$ .** The  $\text{Sb(Ph)}_4(\text{ACO})$  crystal and refinement data are presented in Table 4. The coordination compound crystallized as a clear colorless block-like specimen. The cyanoxime moiety adopts the *trans-anti* conformation with respect to the position of the N-O of the oxime and pyridyl ring along the C2-C3 bond (Figure 23). The *trans-anti* configuration agreed with previous determination of previously described  $\text{Sb(Ph)}_4(\text{ACO})$  crystal structure determined in.<sup>60</sup> The  $\text{ACO}^-$  oxime anion is planar, signifying no dihedral angle, and in agreement with the previously mentioned publication and other data for this ligand. In this study a low temperature structure was the same. This crystal structure is stabilized by H-bonding between one of the amide's Hydrogens and the cyanoximes N from N-O-Sb (Figure 24). The geometry of the coordination polyhedron of the  $\text{Sb(V)}$  atom was a distorted trigonal bipyramid coordinated was observed (Figure 25). The cyano group of the oxime is linear with atoms C1 -



C2 - N2 = 175.9° (Table 5). Bond distances for cyano group C2 - N2 = 1.144 Å, oxime group N1-O1 = 1.337 Å, and C1 - N1 = 1.278 Å. CCDC 2011862 contains the supplementary crystallographic data for this compound found in Appendix C-1.

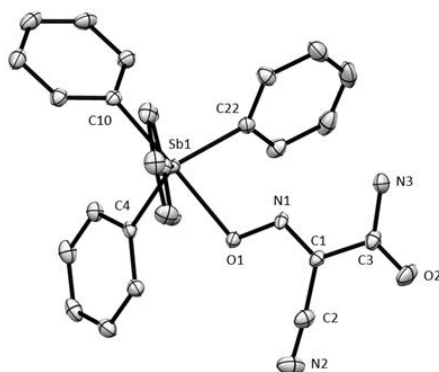


**Figure 23.** Molecular structure and numbering scheme of principal atoms in the crystal structure of  $\text{Sb}(\text{Ph})_4(\text{ACO})$ . An ORTEP representation at 50% thermal ellipsoid probability. H-atoms omitted for clarity.

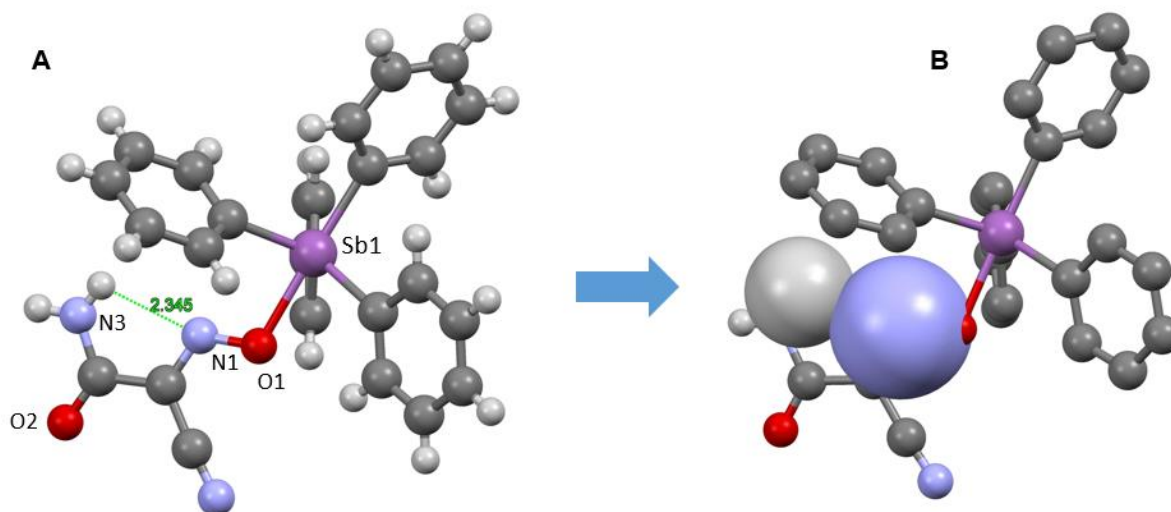


**Figure 24.** Two least obstructed views of  $\text{Sb}(\text{Ph})_4(\text{ACO})$  showing structure stabilization through intramolecular H-bonding of H1a and N1, **A**, along with the space filling model, **B**.

**Table 4.** Crystal data and structure refinement of Sb(Ph)<sub>4</sub>(ACO).

Parameter	Sb(Ph) <sub>4</sub> (ACO)
Empirical formula	C <sub>27</sub> H <sub>22</sub> N <sub>3</sub> O <sub>2</sub> Sb
F.W., g mol <sup>-1</sup>	542.22
Color	Colorless
Crystal size, mm	0.188 mm x 0.127 mm x 0.104 mm
Temperature, K	120(2)
Crystal system	monoclinic
Space group, #	P 1 21/c 1
Unit cell, Å, °	a = 14.8336(8)      α = 90 b = 9.9060(6)      β = 112.7130(10) c = 17.3977(10)      γ = 90
Unit Cell volume, Å <sup>3</sup>	2358.2(2)
Z	4
Density (calc.) Mg m <sup>-3</sup>	1.527 g/cm <sup>3</sup>
Absorp. Coeff., mm <sup>-1</sup>	1.199
F(000)	1088
Θ range, °	1.49 to 33.02°
Index ranges	-22 ≤ h ≤ 22 -14 ≤ k ≤ 15 -26 ≤ l ≤ 26
<b>Structure solution</b>	
Reflections collected	38365
Independent reflections	8465 [R(int) = 0.0278]
Completeness to Θ, (%)	33.02° (95.0)
Absorption correction	Multi-scan
T <sub>max</sub> and T <sub>min</sub>	0.880 and 0.683
<b>Refinement method</b>	
Data/restraints/parameters	8465 / 0 / 386
Goodness-of-fit on F <sup>2</sup>	1.172
Final R indices [I > 2σ(I)]	R1 = 0.0288 wR2 = 0.0636
R indices (all data)	R1 = 0.0391 wR2 = 0.0726
Largest peak/hole, e Å <sup>-3</sup>	2.183 and -0.806
Extinction coefficient	n/a
Structure volume, Å <sup>3</sup> (%)	1507.5 (63.92)

**Table 5.** Selected bond lengths (Å) and angles (°) of the cyanoxime and metal complex center in Sb(Ph)<sub>4</sub>(ACO).

Bond length (Å)	Valence angle (°)
Cyanoxime:	
C1 - C2 = 1.441(3)	O1 - N1 - C1 = 116.81(17)
N2 - C2 = 1.144(3)	N1 - C1 - C2 = 121.02(19)
C1 - C3 = 1.498(3)	N1 - C1 - C3 = 119.22(19)
C3 - O2 = 1.227(3)	C1 - C2 - N2 = 175.9(3)
C3 - N3 = 1.339(3)	C1 - C3 - N3 = 114.25(19)
O1 - N1 = 1.337(2)	C1 - C3 - O2 = 121.0(2)
N1 - C1 = 1.278(3)	N3 - C3 - O2 = 124.8(2)
Metal Center:	
Sb1 - O1 = 2.2529(14)	C4 - Sb1 - O1 = 81.29(7)
	C10 - Sb1 - O1 = 176.48(6)
	C16 - Sb1 - O1 = 84.74(7)
	C22 - Sb1 - O1 = 83.43(7)
	C10 - Sb1 - C4 = 95.71(8)
	C16 - Sb1 - C4 = 118.80(8)
	C22 - Sb1 - C4 = 120.76(8)
	C16 - Sb1 - C10 = 98.35(8)
	C16 - Sb1 - C22 = 116.21(8)
	C22 - Sb1 - C10 = 96.62(8)

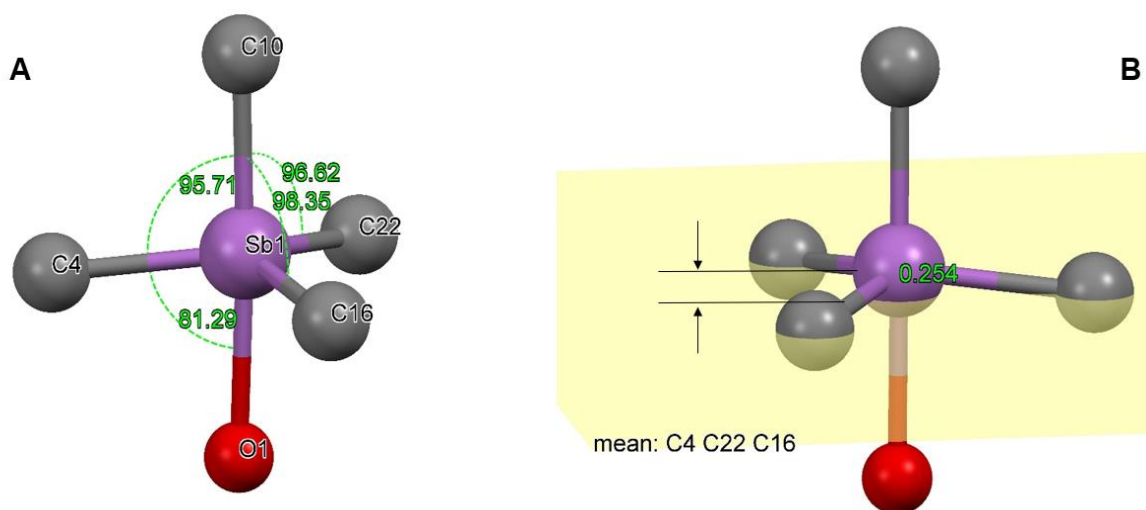


**Figure 25.** **A**, analysis of the angles of the coordination polyhedron of Sb(V) in Sb(Ph)<sub>4</sub>(ACO). **B**, analysis of planarity between Sb(V) core and equatorial *ipso* carbons of the phenyl rings.

**V.1.3. Crystal structure of Sb(Ph)<sub>4</sub>(2PCO).** The Sb(Ph)<sub>4</sub>(2PCO) crystal and refinement data are presented in Table 6. The coordination compound crystallized as a colorless block-like specimen (Figure 26). The cyanoxime moiety adopts the *trans-anti* conformation with respect to the position of the N-O of the oxime and pyridyl ring along the C2-C3 bond (Figure 27). The *trans-anti* configuration does not agree with that of the free cyanoxime H(2PCO) previously described.<sup>112</sup> H(2PCO) and its Fe and Ni complexes.<sup>113</sup> The oxime anion is nonplanar as there are two planes: a) with the main cyanoxime structure O1-N1-C1-C2-N2, and b) the pyridyl ring. These planes have a dihedral angle of 22.63°. This crystal structure is stabilized through intramolecular short electrostatic contact from one of the hydrogen and the  $\pi$ -system of one of the equatorial phenyl rings (Figure 28). The cyano group of the oxime is linear with atoms C1 - C2 - N2 = 179.3° (Table 7). Bond distances for cyano group C2 - N2 = 1.147 Å, oxime group N1-O1 = 1.336 Å, and C1 - N1 = 1.301 Å. The CCDC number for this compound is 2011861. Quality of the obtained structure is shown in Appendix C-2.

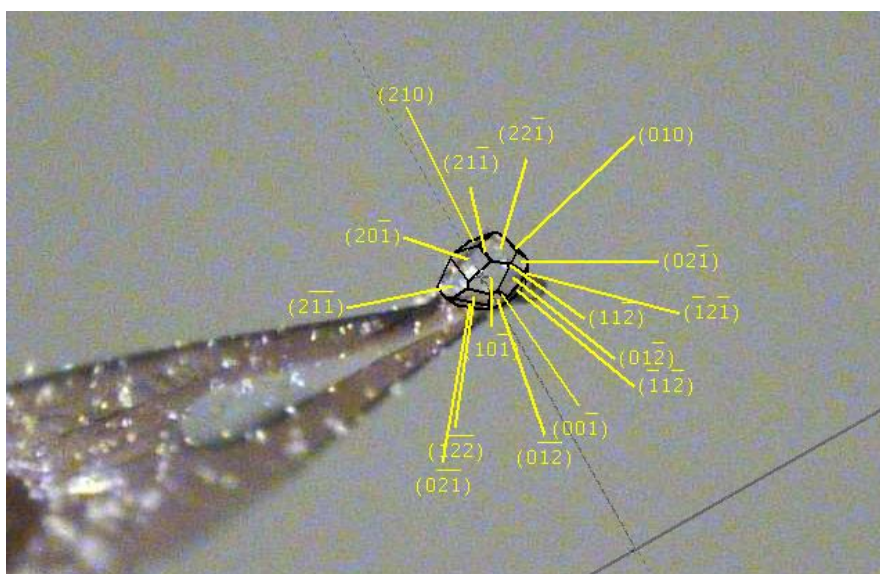


**Figure 26.** Video microscope image of the crystal of Sb(Ph)<sub>4</sub>(2PCO) with indexed faces.

**Table 6.** Crystal data and structure refinement of Sb(Ph)<sub>4</sub>(2PCO).

Parameter	Sb(Ph) <sub>4</sub> (2PCO)
Empirical formula	C <sub>31</sub> H <sub>24</sub> N <sub>3</sub> OSb
F.W., g mol <sup>-1</sup>	576.28
Color	Colorless
Crystal size, mm	0.084 x 0.127 x 0.171
Temperature, K	120(2)
Crystal system	Monoclinic
Space group, #	P 1 21/n 1
Unit cell, Å, °	a = 12.6032(8)      α = 90 b = 14.4421(9)      β = 104.9640(10) c = 14.6699(9)      γ = 90
Unit Cell volume, Å <sup>3</sup>	2579.6(3)
Z	4
Density (calc.) Mg m <sup>-3</sup>	1.484 g/cm <sup>3</sup>
Absorp. Coeff., mm <sup>-1</sup>	1.098
F(000)	1160
Θ range, °	1.90 to 30.57°
Index ranges	-18 ≤ h ≤ 18 -20 ≤ k ≤ 20 -20 ≤ l ≤ 20
<b>Structure solution</b>	
Reflections collected	41038
Independent reflections	7900 [R(int) = 0.0675]
Completeness to Θ, (%)	30.57° (99.7)
Absorption correction	Multi-scan
T <sub>max</sub> and T <sub>min</sub>	0.9130 and 0.8340
<b>Refinement method</b>	
Data/restraints/parameters	7900/0/421
Goodness-of-fit on F <sup>2</sup>	1.057
Final R indices [I > 2σ(I)]	R1 = 0.0445 wR2 = 0.0900
R indices (all data)	R1 = 0.0778 wR2 = 0.1098
Largest peak/hole, e Å <sup>-3</sup>	2.388 and -1.442
Extinction coefficient	n/a
Structure volume, Å <sup>3</sup> (%)	1623.92(62.95)

**Table 7.** Selected bond lengths (Å) and angles (°) of the cyanoxime and metal complex center in  $\text{Sb}(\text{Ph})_4(2\text{PCO})$ .

Bond length (Å)	Valence angle (°)
<b>Cyanoxime:</b>	
C1 - N1 = 1.301(4)	C1 - N1 - O1 = 113.3(3)
C1 - C3 = 1.473(5)	C1 - C2 - N2 = 179.3(4)
C2 - N2 = 1.147(5)	C2 - C1 - C3 = 118.6(3)
C3 - N3 = 1.338(4)	C7 - N3 - C3 = 117.4(3)
C7 - N3 = 1.348(5)	N1 - C1 - C3 = 120.4(3)
N1-O1 = 1.336(4)	C2 - C1 - N1 = 121.0(3)
<b>Metal Center:</b>	
Sb - O1 = 2.226(2)	C8 - Sb1 - O1 = 176.09(11)
	C14 - Sb1 - O1 = 81.88(11)
	C20 - Sb1 - O1 = 86.01(11)
	C26 - Sb1 - O1 = 94.14(12)
	C14 - Sb1 - C8 = 96.48(12)
	C20 - Sb1 - C8 = 97.90(13)
	C26 - Sb1 - C8 = 94.14(12)
	C20 - Sb1 - C14 = 115.26(13)
	C20 - Sb1 - C26 = 118.21(13)
	C26 - Sb1 - C14 = 123.15(13)

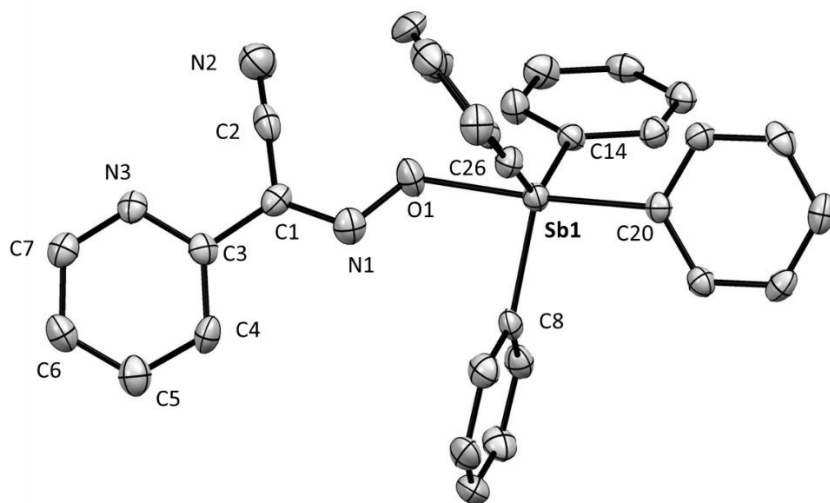


**Figure 27.** An ORTEP drawing at 50% thermal ellipsoids probability level for the ASU  $\text{Sb}(\text{Ph})_4(2\text{PCO})$  showing the numbering of principal atoms. H-atoms are omitted for clarity.

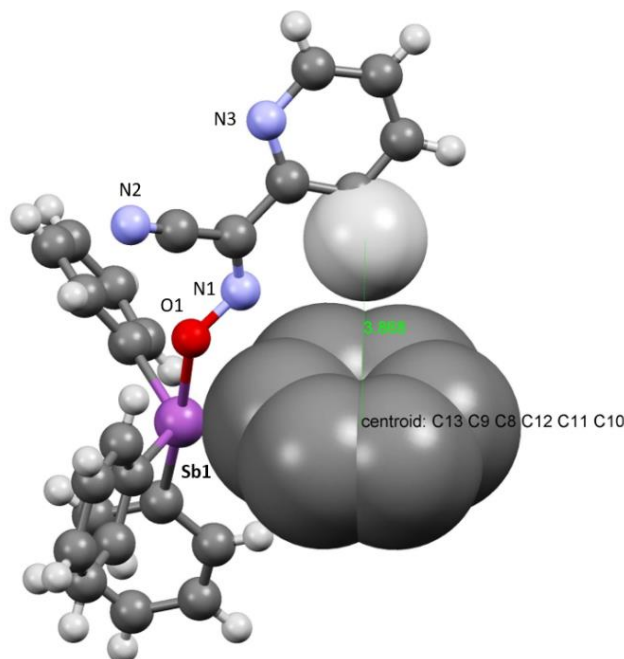


**Figure 28.** Structure of intramolecular stabilization through electrostatic contact of equatorial phenyl ring  $\pi$ -system and pyridyl hydrogen of  $\text{Sb}(\text{Ph})_4(2\text{PCO})$ . Involved atoms are expressed in a space-filling mode.

**V.1.4. Crystal structure of  $\text{Sb}(\text{Ph})_4(3\text{PCO})$ .** The  $\text{Sb}(\text{Ph})_4(3\text{PCO})$  crystal and refinement data are presented in Table 8. The coordination compound crystallized as a colorless block-like specimen. The cyanoxime moiety adopts the *trans-anti* conformation with respect to the position of the N-O of the oxime and pyridyl ring along the C2-C3 bond (Figure 29). The *trans-anti* configuration agrees with previous determination of the free cyanoxime  $\text{H}(3\text{PCO})$  previously described.<sup>112</sup> The oxime anion is completely planar in this structure. This crystal structure is stabilized through intramolecular H-bonding from one of the hydrogens from the pyridyl ring and N1 of the cyanoxime (Figure 30). The cyano group of the oxime is linear with atoms C1 - C2 - N2 = 177.3° (Table 9). Bond distances for cyano group C2 - N2 = 1.134 Å, oxime group N1-O1 = 1.339 Å, and C1 - N1 = 1.295 Å. The geometry of the coordination polyhedron and off plane trigonal distance of the distorted trigonal bipyramid polyhedron of  $\text{Sb}(\text{Ph})_4(3\text{PCO})$  can be seen in Figures 31-32. The CCDC number assigned for this structure is 201180, while the checkCIF report is presented in Appendix C-3.

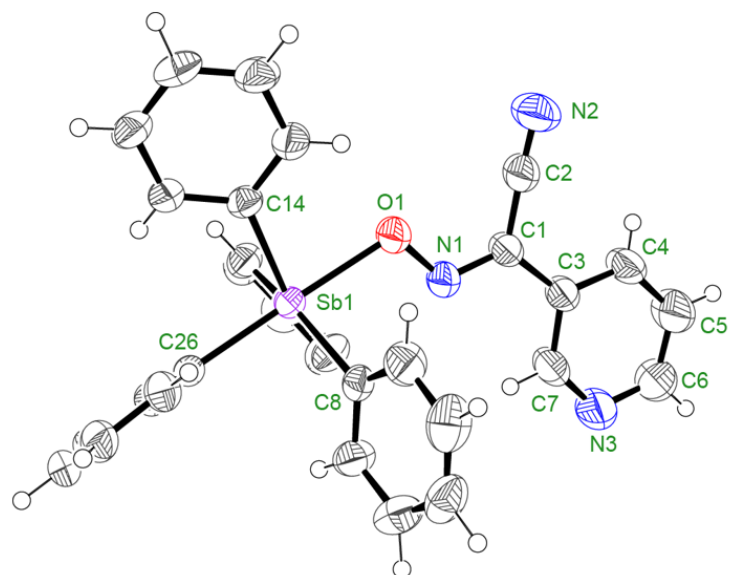


**Figure 29.** An ORTEP drawing at 50% thermal ellipsoids probability level for the ASU  $\text{Sb}(\text{Ph})_4(3\text{PCO})$  showing the numbering of principal atoms.

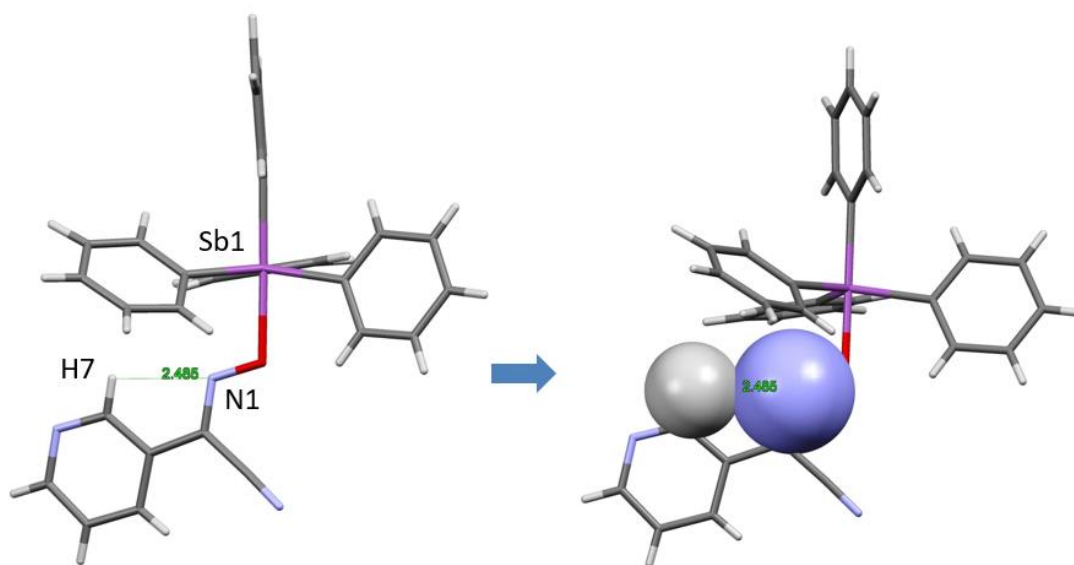


**Figure 30.** The least obstructed view of the ASU of  $\text{Sb}(\text{Ph})_4(3\text{PCO})$  showing intramolecular electrostatic contact of the pyridyl hydrogen (H7) with the nitrogen (N1) of the cyanoximes moiety.



**Table 8.** Crystal data and structure refinement of Sb(Ph)<sub>4</sub>(3PCO).

Parameter	Sb(Ph) <sub>4</sub> (3PCO)
Empirical formula	C <sub>31</sub> H <sub>24</sub> N <sub>3</sub> OSb
F.W., g mol <sup>-1</sup>	576.28
Color	Colorless
Crystal size, mm	0.086 x 0.103 x 0.144
Temperature, K	296(2)
Crystal system	Triclinic
Space group, #	P - 1
Unit cell, Å, °	a = 10.0228(4)      α = 69.3240(10) b = 10.498(4)      β = 72.0860(10) c = 13.8258(5)      γ = 83.9710
Unit Cell volume, Å <sup>3</sup>	2579.6(3)
Z	2
Density (calc.) Mg m <sup>-3</sup>	1.483 g/cm <sup>3</sup>
Absorp. Coeff., mm <sup>-1</sup>	1.098
F(000)	580
Θ range, °	1.65 to 28.00°
Index ranges	-13 ≤ h ≤ 13 -13 ≤ k ≤ 13 -18 ≤ l ≤ 18
<b>Structure solution</b>	
Reflections collected	18032
Independent reflections	6218[R(int) = 0.0263]
Completeness to Θ, (%)	28.00(99.9)
Absorption correction	Multi-scan
T <sub>max</sub> and T <sub>min</sub>	0.7465 and 0.6966
<b>Refinement method</b>	
Data/restraints/parameters	6218/0/421
Goodness-of-fit on F <sup>2</sup>	1.055
Final R indices [I > 2σ(I)]	R1 = 0.0242 wR2 = 0.0567
R indices (all data)	R1 = 0.0278 wR2 = 0.0585
Largest peak/hole, e Å <sup>-3</sup>	0.598 and -0.302
Extinction coefficient	n/a
Structure volume, Å <sup>3</sup> (%)	811.86 (62.92)

**Table 9.** Selected bond lengths (Å) and angles (°) of the cyanoxime and metal complex center in  $\text{Sb}(\text{Ph})_4(3\text{PCO})$ .

Bond length (Å)	Valence angle (°)
Cyanoxime:	
C1 - N1 = 1.295(3)	C1 - N1 - O1 = 115.64(17)
C1 - C3 = 1.466(3)	C1 - C2 - N2 = 177.3(3)
C2 - N2 = 1.134(3)	C2 - C1 - C3 = 119.55(17)
C6 - N3 = 1.318(4)	C7 - N3 - C6 = 116.6(2)
C7 - N3 = 1.318(3)	N1 - C1 - C3 = 119.33(18)
N1-O1 = 1.339(2)	C2 - C1 - N1 = 121.11(19)
Metal Center:	
Sb - O1 = 2.226(2)	C8 - Sb1 - O1 = 85.79(6)
	C14 - Sb1 - O1 = 83.77(6)
	C20 - Sb1 - O1 = 86.72(6)
	C26 - Sb1 - O1 = 177.39(6)
	C14 - Sb1 - C8 = 123.50(7)
	C20 - Sb1 - C8 = 118.71(7)
	C26 - Sb1 - C8 = 92.04(7)
	C20 - Sb1 - C14 = 115.89(7)
	C20 - Sb1 - C26 = 95.61(7)
	C26 - Sb1 - C14 = 96.23(7)

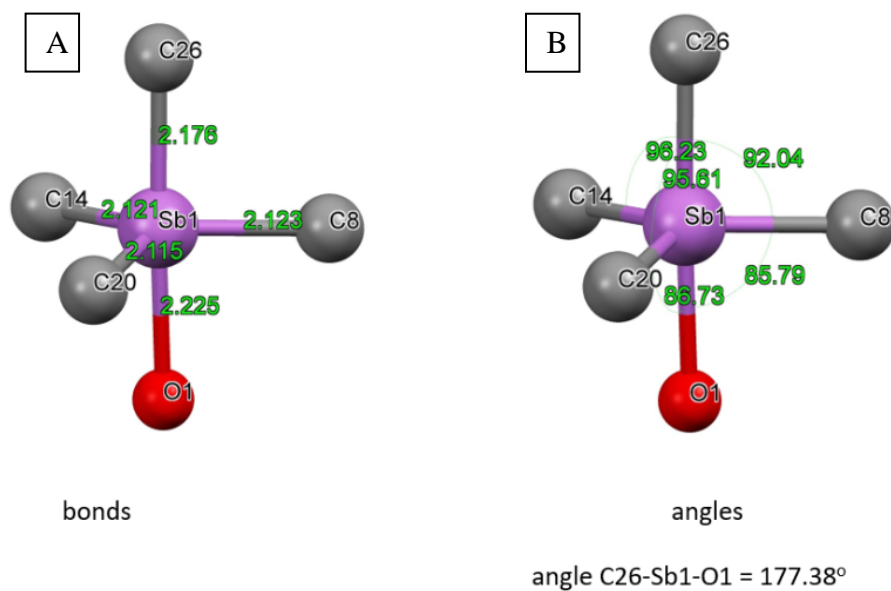


**Figure 31.** Geometry of the pentavalent antimony complex  $\text{Sb}(\text{Ph})_4(3\text{PCO})$ , showing a distorted trigonal bipyramid polyhedron coordination. Important bond lengths (A) and angles (B) of coordination are shown.

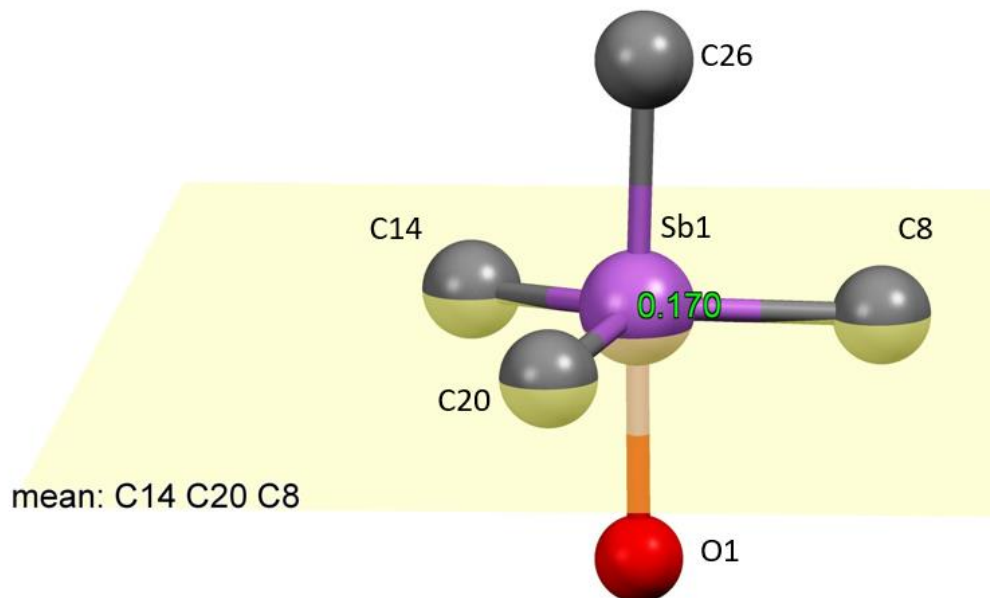


**Figure 32.** View of the off-plane distance in the distorted trigonal-bipyramid coordination polyhedron of  $\text{Sb}(\text{Ph})_4(3\text{PCO})$ .

**V.1.5. Crystal structure of  $\text{Sb}(\text{Ph})_4(4\text{PCO})$ .** The  $\text{Sb}(\text{Ph})_4(4\text{PCO})$  crystal and refinement data are presented in Table 10. The coordination compound crystallized as a clear, colorless block-like specimen. The oxime anion is completely planar (Figure 33). Crystal packing of this crystal structure is stabilized by H-bonding from two separate hydrogens of two phenyl rings to a phenyl ring and pyridyl  $\pi$ -system (Figure 34). The cyano group of the oxime is linear with atoms  $\text{C1} - \text{C2} - \text{N2} = 177.10^\circ$  (Table 11). Bond distances for cyano group  $\text{C2} - \text{N2} = 1.146 \text{ \AA}$ , oxime group  $\text{N1} - \text{O1} = 1.339 \text{ \AA}$ , and  $\text{C1} - \text{N1} = 1.304 \text{ \AA}$ . The CCDC number for this compound is 2011863, while details of checkCIF report are in Appendix C-4.

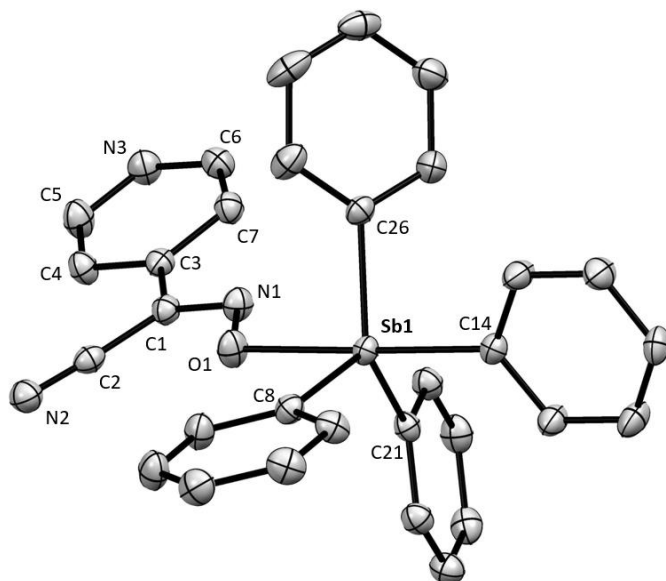


**Figure 33.** An ORTEP drawing at 50% thermal ellipsoids probability level for the ASU  $\text{Sb}(\text{Ph})_4(4\text{PCO})$  showing the numbering of principal atoms. H-atoms are omitted for clarity.

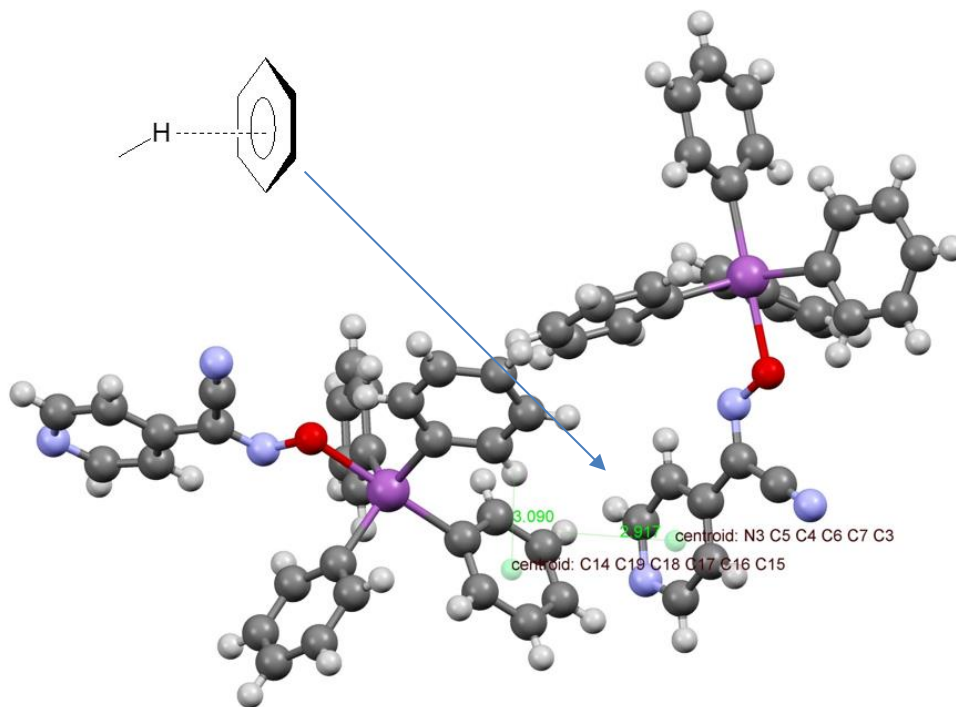


**Figure 34.** Packing of two structures of  $\text{Sb}(\text{Ph})_4(4\text{PCO})$  showing stabilization short electrostatic contact between the centers of the 4-pyridyl centroid and phenyl rings with phenyl hydrogens.

**Table 10.** Crystal data and structure refinement of Sb(Ph)<sub>4</sub>(4PCO).

Parameter	Sb(Ph) <sub>4</sub> (4PCO)
Empirical formula	C <sub>31</sub> H <sub>24</sub> N <sub>3</sub> OSb
F.W., g mol <sup>-1</sup>	576.28
Color	Colorless
Crystal size, mm	0.212 x 0.228 x 0.700
Temperature, K	120(2)
Crystal system	Monoclinic
Space group, #	P 1 21/n 1
Unit cell, Å, °	a = 15.3351(10)      α = 90 b = 9.7845(6)        β = 108.4590(10) c = 18.0770(11)     γ = 90
Unit Cell volume, Å <sup>3</sup>	2572.8(3)
Z	4
Density (calc.) Mg m <sup>-3</sup>	1.488 g/cm <sup>3</sup>
Absorp. Coeff., mm <sup>-1</sup>	1.101
F(000)	1160
Θ range, °	1.52 to 28.00°
Index ranges	-20 ≤ h ≤ 20 -12 ≤ k ≤ 12 -23 ≤ l ≤ 23
<b>Structure solution</b>	
Reflections collected	33177
Independent reflections	6190 [R(int) = 0.0197]
Completeness to Θ, (%)	28.00(100)
Absorption correction	Multi-scan
T <sub>max</sub> and T <sub>min</sub>	0.8000 and 0.5130
<b>Refinement method</b>	
Data/restraints/parameters	6190/0/409
Goodness-of-fit on F <sup>2</sup>	1.057
Final R indices [I > 2σ(I)]	R1 = 0.0213 wR2 = 0.0543
R indices (all data)	R1 = 0.0236 wR2 = 0.0556
Largest peak/hole, e Å <sup>-3</sup>	1.015 and -0.281
Extinction coefficient	n/a
Structure volume, Å <sup>3</sup> (%)	1640.11 (63.74)

**Table 11.** Selected bond lengths (Å) and angles (°) of the cyanoxime and metal complex center in  $\text{Sb(Ph)}_4(4\text{PCO})$ .

Bond length (Å)	Valence angle (°)
Cyanoxime:	
C1 - N1 = 1.304(2)	C1 - N1 - O1 = 113.82(13)
C1 - C3 = 1.470(2)	C1 - C2 - N2 = 177.10(17)
C2 - N2 = 1.146(2)	C2 - C1 - C3 = 118.60(13)
C5 - N3 = 1.339(2)	C6 - N3 - C5 = 115.71(15)
C6 - N3 = 1.339(2)	N1 - C1 - C3 = 120.33(14)
N1-O1 = 1.3390(17)	C2 - C1 - N1 = 121.11(19)
Metal Center:	
Sb - O1 = 2.226(2)	C8 - Sb1 - O1 = 84.25(5)
	C14 - Sb1 - O1 = 178.65(5)
	C20 - Sb1 - O1 = 82.58(5)
	C26 - Sb1 - O1 = 84.37(5)
	C14 - Sb1 - C8 = 96.82(6)
	C20 - Sb1 - C8 = 121.08(6)
	C26 - Sb1 - C8 = 117.11(6)
	C20 - Sb1 - C14 = 97.57(6)
	C20 - Sb1 - C26 = 118.25(6)
	C26 - Sb1 - C14 = 94.40(6)

**V.1.6. An unexpected result: crystal structure of  $\text{Sb(Ph)}_3(\text{ECO})$   $\mu$ -oxo-dimer.** With some mistakes in the world of science, sometimes a surprise can occur with failure. This is the case with one of my early synthesis with  $\text{Sb(Ph)}_4(\text{ECO})$ . By misjudging how much water was needed for the basic solution of  $\text{K}_2\text{CO}_3$  during a preparation of  $\text{Ag}(3\text{PCO})$ , it ended up hydrolyzing  $\text{Sb(Ph)}_4(\text{ECO})$  into the  $[\text{Sb(Ph)}_3(\text{ECO})]_2$   $\mu$ -oxo-dimer which was later discovered after solving its crystal structure (Figure 35). There is a *trans-effect* of the coordinated oxime that facilitates addition of a hydroxo-group to the  $\text{Sb(V)}$  core (Figure 36A) followed by the dimerization of the triphenyl(V) hydroxide with elimination of water (Figure 36B). Stereospecific reactions with substitutions in the *trans*- position are common in inorganic and organometallic chemistry, and well documented in chemistry of  $\text{Pt(II)}$  and other kinetically inert metal centers.

For the crystal structure determination, a clear colorless, prism-like specimen was selected. The  $\text{Sb}(\text{Ph})_3(\text{ECO})$  oxo-dimer crystal and refinement data are presented in Table 12. It was a surprise to find out the formation of an oxygen-bridging dimeric system. This  $\mu$ -oxo-bridge is linear as the angle of  $\text{Sb1} - \text{O1BR} - \text{Sb2} = 180.0^\circ$  (Table 13). One of the interesting features about this structure is the anionic oxime moieties are completely planar. The cyano group is linear  $\text{C1} - \text{C2} - \text{N2} = 177.43^\circ$ . Bond lengths for the cyano group were  $\text{C2} - \text{N2} = 1.145 \text{ \AA}$ , oxime group  $\text{N1} - \text{O1} = 1.337 \text{ \AA}$ , and  $\text{C1} - \text{N1} = 1.299 \text{ \AA}$ . As for both Sb-O bond lengths that are incorporated into the oxo-bridge  $\text{Sb1} - \text{OBr}$  and  $\text{Sb2} - \text{OBr}$  were  $1.95274$  and  $1.95276 \text{ \AA}$ , respectively (Table 13). The CCDC assigned number is 2012154 for this compound. The checkCIF report is present in Appendix C-5.

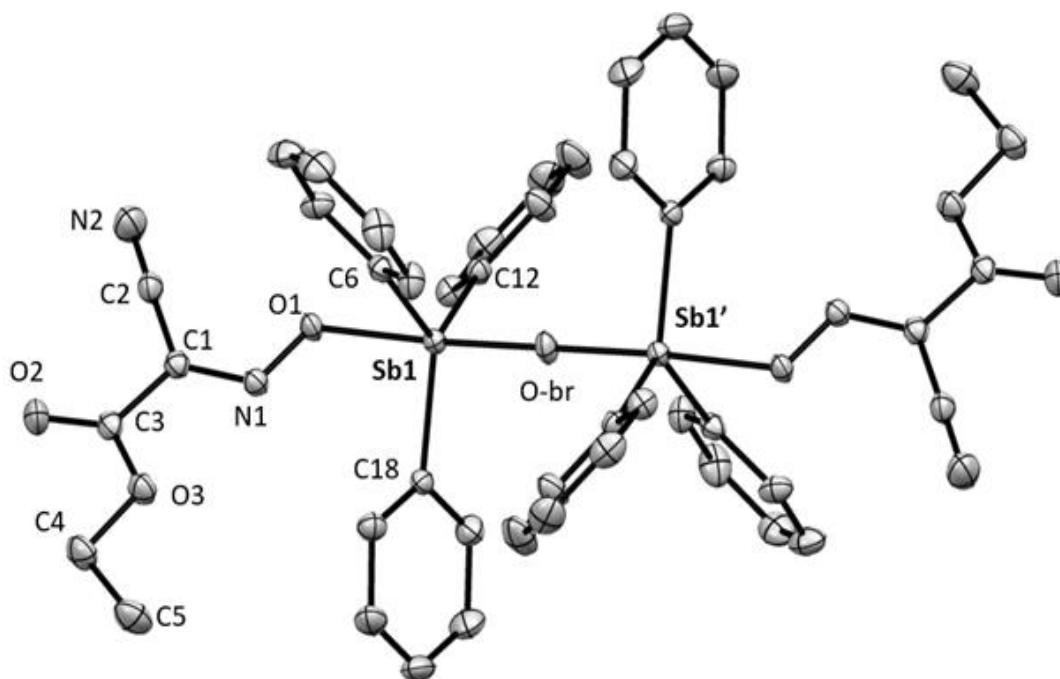
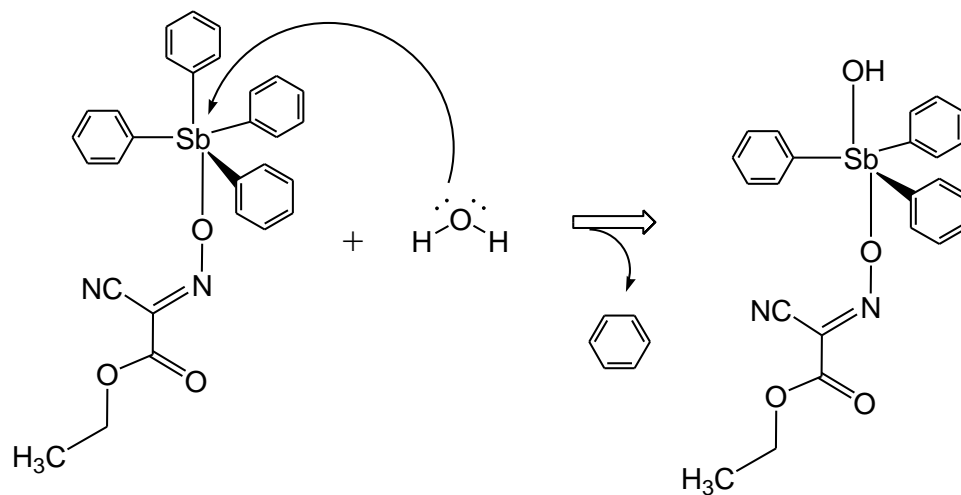


**Figure 35.** An ORTEP drawing at 50% thermal ellipsoids probability level for the ASU in the structure of  $\text{Sb}(\text{Ph})_3(\text{ECO})$   $\mu$ -oxo-dimer showing the numbering of principal atoms. H-atoms are omitted for clarity.

### A hydrolysis



### B dimerization

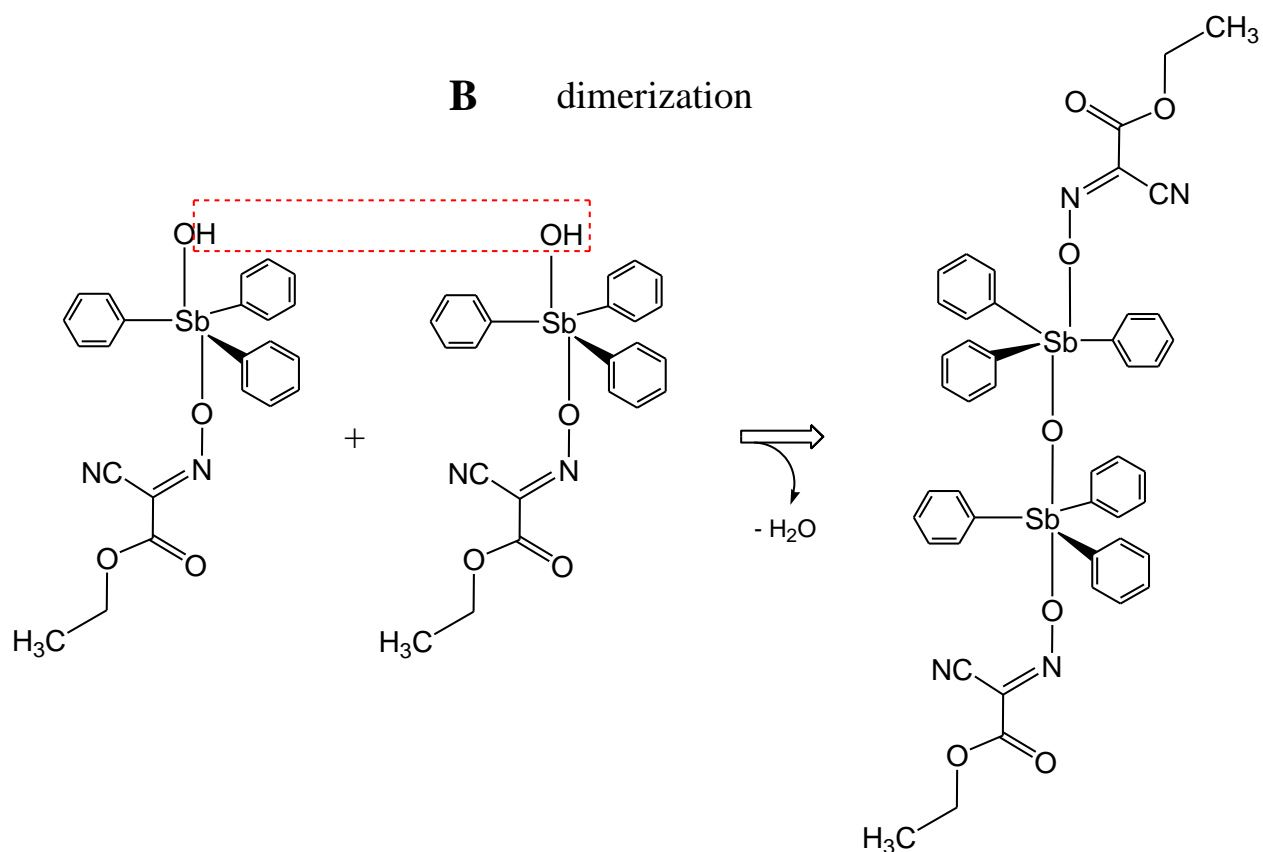


**Figure 36.** Scheme of suggested path for hydrolysis, **A**, and the dimerization, **B**, of organoantimony(V) in moist conditions.



**Table 12.** Crystal data and structure refinement of the Sb(Ph)<sub>3</sub>(ECO) oxo-dimer.

Parameter	Sb(Ph) <sub>4</sub> (ECO) dimer	
Empirical formula	C <sub>46</sub> H <sub>40</sub> N <sub>4</sub> O <sub>7</sub> Sb <sub>2</sub>	
F.W., g mol <sup>-1</sup>	1004.32	
Color	Colorless	
Crystal size, mm	0.180 x 0.228 x 0.984	
Temperature, K	120(2)	
Crystal system	Triclinic	
Space group, #	P - 1	
Unit cell, Å, °	a = 9.1829(9)	α = 111.9570(10)
	b = 10.0829(10)	β = 103.200(2)
	c = 13.4714(16)	γ = 95.4050(10)
Unit Cell volume, Å <sup>3</sup>	1103.8(2)	
Z	1	
Density (calc.) Mg m <sup>-3</sup>	1.511 g/cm <sup>3</sup>	
Absorp. Coeff., mm <sup>-1</sup>	1.277	
F(000)	502	
Θ range, °	1.70 to 30.51°	
Index ranges	-13 ≤ h ≤ 13	
	-14 ≤ k ≤ 14	
	-19 ≤ l ≤ 19	
<b>Structure solution</b>		
Reflections collected	17209	
Independent reflections	6688 [R(int) = 0.0159]	
Completeness to Θ, (%)	30.51° (99.2)	
Absorption correction	Multi-scan	
T <sub>max</sub> and T <sub>min</sub>	0.8030 and 0.3660	
<b>Refinement method</b>		
Data/restraints/parameters	6688/0/348	
Goodness-of-fit on F <sup>2</sup>	1.079	
Final R indices [I > 2σ(I)]	R1 = 0.0188	
	wR2 = 0.0433	
R indices (all data)	R1 = 0.0206	
	wR2 = 0.0447	
Largest peak/hole, e Å <sup>-3</sup>	1.545 and -0.613	
Extinction coefficient	n/a	
Structure volume, Å <sup>3</sup> (%)	677.92 (61.42)	

**Table 13.** Selected bond lengths (Å) and angles (°) of the cyanoxime and metal complex center in Sb(Ph)<sub>3</sub>(ECO) oxo-dimer. BR denotes the bridge oxygen connecting the dimer.

Bond length (Å)	Valence angle (°)
Cyanoxime:	
C1 - C2 = 1.441(2)	N2 - C2 - C1 = 177.43(17)
N2 - C2 = 1.145(2)	C1 - N1 - O1 = 115.11(12)
N1 - C1 = 1.2993 (18)	N1 - C1 - C2 = 122.83(13)
N1 - O1 = 1.3370 (15)	
C1 - C3 = 1.488(2)	
Metal Center:	
O1BR-Sb1 = 1.95274(16)	Sb1 - O1BR - Sb2 = 180.0
O1BR-Sb2 = 1.95276 (16)	

**V.1.7. Crystal structure of the monomeric Sb(Ph)<sub>4</sub>(ECO).** Oposing the failure that gave rise to the  $\mu$ -oxo-dimer, the monomer of Sb(Ph)<sub>4</sub>(ECO) was successfully prepared and crystallized. The crystalline compound is also a clear colorless block-like specimen. Crystal structure of this compound is different and interesting because contrary to earlier described structures, it contains two independent molecules in the ASU (Figure 37). The crystal packing can be seen in Figure 38. Both molecules **A** and **B** cannot be superimposed by any symmetry operations in this group. Therefore, they are called *crystallographically independent* molecules. The Sb(V) atom is in a special position and is located directly on the only symmetry element present in the crystal - a gliding plane (Figure 39).

Regarding the configuration of the oxime ligand, it adopts *trans-anti* conformation in both structures. Structure and refinement data of the monomer crystal structure is shown in Table 14. Molecule **A** has linear cyano group C1A - C2A - N2A = 179.2° (Table 15). Molecule **B** adopts a linear cyano group as well with C1B - C2B - N2B = 177.5° (Table 16). Bond lengths for the cyano group were C2A - N2A = 1.144 Å, oxime group N1A-O1A = 1.324 Å, and C1A - N1A =

1.308 Å for molecule **A**, and C2B - N2B = 1.144 Å, oxime group N1B-O1B = 1.323 Å, and C1B - N1B = 1.302 Å for molecule **B**. Both independent molecules have the ECO<sup>-</sup> anion with a planar configuration cyanoximes core structure. As an interesting peculiarity, we will mention that the C-O-C atoms of the ethoxy-group are ion plane with only the CH<sub>3</sub> group being out of plane. We may attribute this behavior to the demands of crystal packing. This structure has received the CCDC number 2012153 and quality of the structure has been validated in the checkCIF report shown in Appendix C-6.

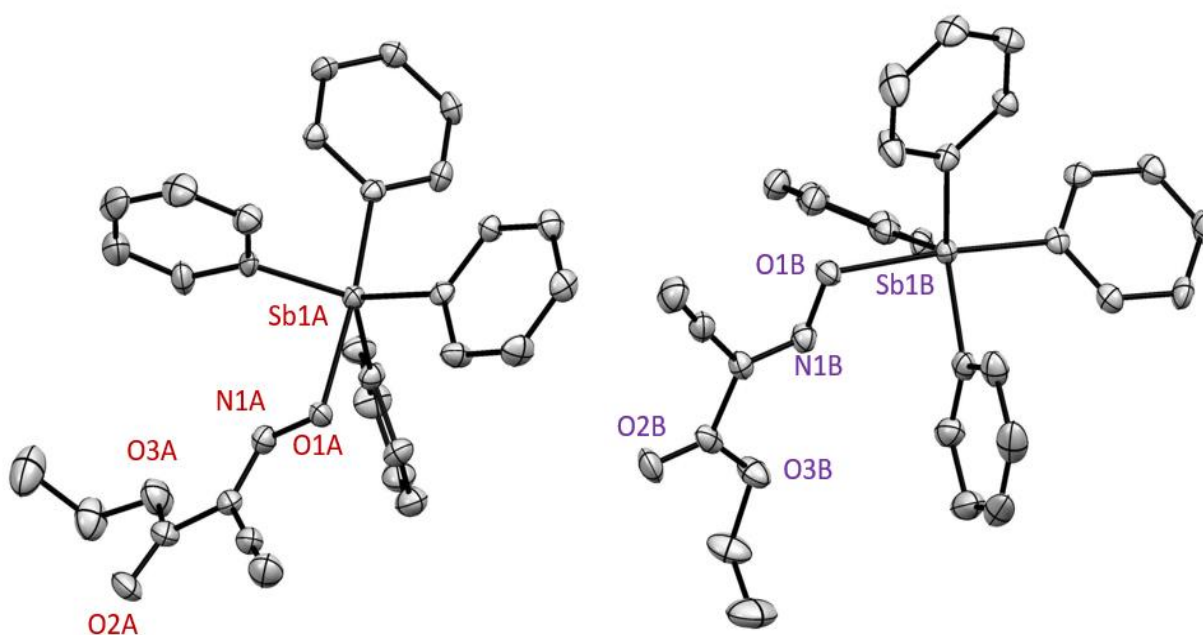


**Figure 37.** An ORTEP drawing at 50% thermal ellipsoids probability level for the two crystallographically independent molecules in the ASU of Sb(Ph)<sub>4</sub>(ECO) monomer showing the numbering of principal atoms. H-atoms are omitted for clarity.

**Table 14.** Crystal data and structure refinement of monomeric Sb(Ph)<sub>4</sub>(ECO).

Parameter	Sb(Ph) <sub>4</sub> (ECO )
Empirical formula	C <sub>29</sub> H <sub>25</sub> N <sub>2</sub> O <sub>3</sub> Sb
F.W., g mol <sup>-1</sup>	571.26
Color	Colorless
Crystal size, mm	0.091 x 0.099 x 0.128
Temperature, K	100(2)
Crystal system	Monoclinic
Space group, #	P 1 n 1
Unit cell, Å, °	a = 9.7871(6)      α = 90 b = 14.9208(9)      β = 94.613(10) c = 17.6984(11)      γ = 90
Unit Cell volume, Å <sup>3</sup>	2576.1(3)
Z	4
Density (calc.) Mg m <sup>-3</sup>	1.473 g/cm <sup>3</sup>
Absorp. Coeff., mm <sup>-1</sup>	1.103
F(000)	1152
Θ range, °	1.37 to 33.08°
Index ranges	-13 ≤ h ≤ 13 -14 ≤ k ≤ 14 -19 ≤ l ≤ 19
<b>Structure solution</b>	
Reflections collected	9092
Independent reflections	6688 [R(int) = 0.0159]
Completeness to Θ, (%)	33.08° (93.2)
Absorption correction	Multi-scan
T <sub>max</sub> and T <sub>min</sub>	0.7454 and 0.6801
<b>Refinement method</b>	
Data/restraints/parameters	9092 / 2 / 654
Goodness-of-fit on F <sup>2</sup>	1.193
Final R indices [I > 2σ(I)]	R1 = 0.0351 wR2 = 0.00709
R indices (all data)	R1 = 0.0404 wR2 = 0.0774
Largest peak/hole, e Å <sup>-3</sup>	2.218 and -1.311
Extinction coefficient	n/a
Structure volume, Å <sup>3</sup> (%)	1615.90 (62.73)

**Table 15.** Selected bond lengths (Å) and angles (°) of the cyanoxime and metal complex center in Sb(Ph)<sub>4</sub>(ECO) molecule A.

Bond length (Å)	Valence angle (°)
Cyanoxime:	
C1A - N1A = 1.308(6)	C1A - N1A - O1A = 116.0(4)
C1A - C3A = 1.483(7)	C1A - C2A - N2A = 179.2(6)
C2A - N2A = 1.144(8)	C2A - C1A - C3A = 118.0(4)
C3A - O3A = 1.352(8)	C3A - O3A - C4A = 115.9(5)
C4A - O3A = 1.456(7)	N1A - C1A - C3A = 119.3(5)
N1A-O1A = 1.324(5)	C2A - C1A - N1A = 122.7(5)
Metal Center:	
Sb1A - O1A = 2.373(3)	C6A - Sb1A - O1A = 83.06(17)
	C12A - Sb1A - O1A = 174.59(15)
	C18A - Sb1A - O1A = 80.13(15)
	C24A - Sb1A - O1A = 84.05(16)
	C12A - Sb1A - C6A = 96.4(2)
	C18A - Sb1A - C6A = 125.3(2)
	C24A - Sb1A - C6A = 114.09(18)
	C18A - Sb1A - C12A = 95.91(18)
	C18A - Sb1A - C24A = 115.29(18)
	C24A - Sb1A - C12A = 101.03(19)

**Table 16.** Selected bond lengths (Å) and angles (°) of the cyanoxime and metal complex center in Sb(Ph)<sub>4</sub>(ECO) molecule B.

Bond length (Å)	Valence angle (°)
Cyanoxime:	
C1B - N1B = 1.302(6)	C1B - N1B - O1B = 115.4(4)
C1B - C3B = 1.488(7)	C1B - C2B - N2B = 177.5(6)
C2B - N2B = 1.144(8)	C2B - C1B - C3B = 117.8(4)
C3B - O3B = 1.338(7)	C3B - O3B - C4B = 115.7(5)
C4B - O3B = 1.460(7)	N1B - C1B - C3B = 120.5(5)
N1B-O1B = 1.323(5)	C2B - C1B - N1B = 121.7(4)
Metal Center:	
Sb1B - O1B = 2.327(3)	C6B - Sb1B - O1B = 82.70(16)
	C12B - Sb1B - O1B = 175.94(17)
	C18B - Sb1B - O1B = 81.21(16)
	C24B - Sb1B - O1B = 83.28(17)
	C12B - Sb1B - C6B = 100.23(19)
	C18B - Sb1B - C6B = 115.2(2)
	C24B - Sb1B - C6B = 115.80(19)
	C18B - Sb1B - C12B = 94.96(19)
	C18B - Sb1B - C24B = 123.82(19)
	C24B - Sb1B - C12B = 97.86(18)

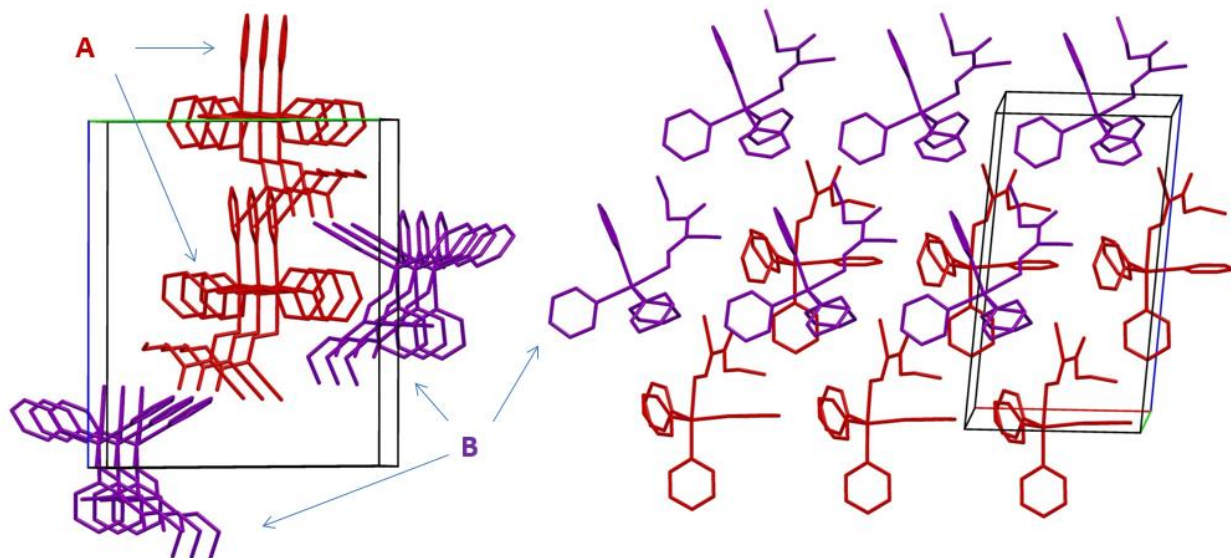


**Figure 38.** Two different views of the crystal packing in the unit cell in the structure  $\text{Sb}(\text{Ph})_4(\text{ECO})$  molecule **A** (red) and molecule **B** (purple).

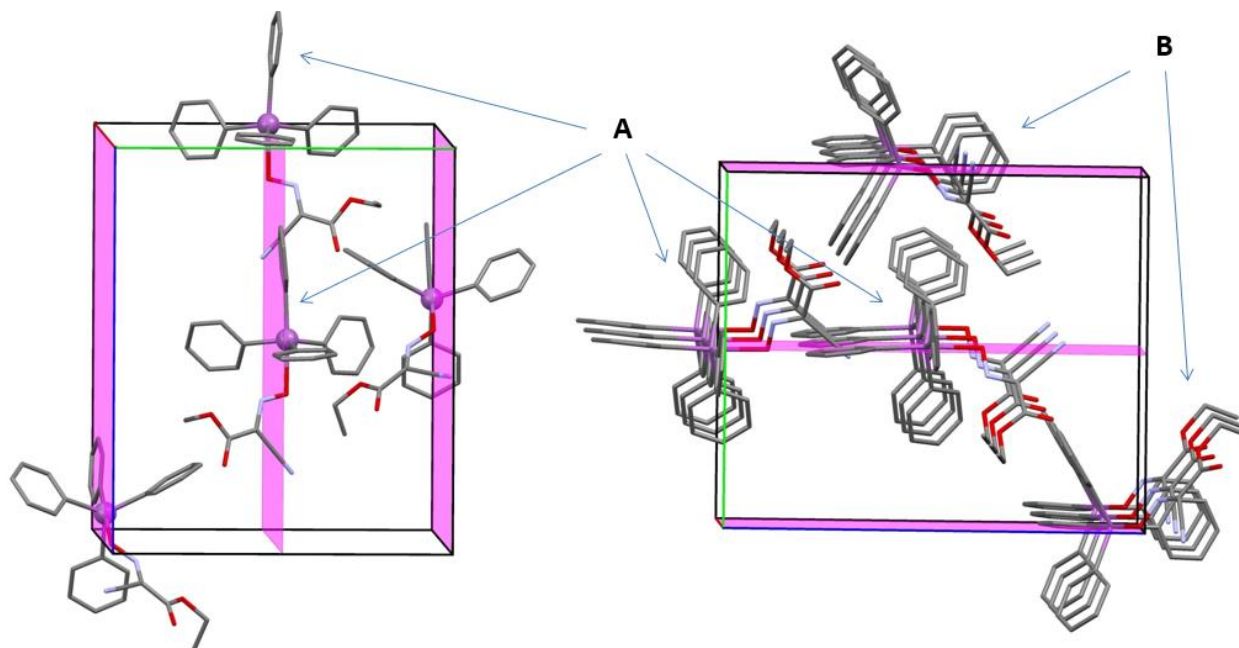


**Figure 39.** Two views of the crystal packing in the unit cell  $\text{Sb}$  atom on a special position gliding plane. Independent molecules **A** and **B** are drawn in different colors for clarity.

**V.1.8. Crystal structure of Sb(Ph)<sub>4</sub>(MCO).** For structure determination of this compound a clear, colorless, block-like crystal was selected. Similarly to the previous structure, in the structure of Sb(Ph)<sub>4</sub>(MCO) it was found to include two crystallographically independent molecules in the ASU which we also labeled as **A** and **B** (Figure 40). The crystal and refinement data for this structure are presented in Table 17. Different from most of the solved crystal structures, around half of the hydrogen atoms were found isotropically, the rest were attached based on hybridization states with carbon atoms. The cyanoximes moieties of molecules **A** and **B** are nonplanar. The morpholyl groups in molecules **A** and **B** adopted the chair conformation for stability. In both cases, the cyanoximes moieties in molecules **A** and **B** are heavily non-planar and their dihedral angles between the cyanoxime and amide fragments are 43.99° and 47.31° for **A** and **B**, respectively. This situation is different from other previously described Sb(V)-cyanoximates with ACO<sup>-</sup> and isomeric pyridyl-cyanoximes.

This compound is an example of a classical molecular crystallography, which only relies on van-der-Waals interactions in crystal packing. Molecules **A** and **B** have linear cyano group Bond lengths for the cyano group were C2A - N2A = 1.141 Å, oxime group N1A-O1A = 1.353 Å, and C1A - N1A = 1.289 Å for molecule **A** (Figure 41), and C2B - N2B = 1.157 Å, oxime group N1B-O1B = 1.339 Å, and C1B - N1B = 1.289 Å with molecule **B** (Table 18-19). The CCDC has assigned the number 2012156 for this structure. Quality of crystal data for this compound are presented in Appendix C-7.

**Table 17.** Crystal and refinement data for the crystal Sb(Ph)<sub>4</sub>(MCO).

Parameter	Sb(Ph) <sub>4</sub> (MCO)
Empirical formula	C <sub>31</sub> H <sub>28</sub> N <sub>3</sub> O <sub>3</sub> Sb
F.W., g mol <sup>-1</sup>	612.31
Color	Colorless
Crystal size, mm	0.120 X 0.120 X 0.140
Temperature, K	100(2)
Crystal system	Monoclinic
Space group, #	P 1 21/c 1
Unit cell, Å, °	a = 17.6451(4)      α = 90 b = 10.8777(3)      β = 94.8360(10) c = 28.3876(7)      γ = 90
Unit Cell volume, Å <sup>3</sup>	5429.3(2)
Z	8
Density (calc.) Mg m <sup>-3</sup>	1.498 g/cm <sup>3</sup>
Absorp. Coeff., mm <sup>-1</sup>	1.054
F(000)	2480
Θ range, °	1.16 to 26.52°
Index ranges	-22 ≤ h ≤ 22 -13 ≤ k ≤ 13 -35 ≤ l ≤ 35
<b>Structure solution</b>	
Reflections collected	75269
Independent reflections	11251 [R(int) = 0.0612]
Completeness to Θ, (%)	26.52° (99.8)
Absorption correction	Multi-scan
T <sub>max</sub> and T <sub>min</sub>	0.8840 and 0.8670
<b>Refinement method</b>	
Data/restraints/parameters	11251 / 0 / 750
Goodness-of-fit on F <sup>2</sup>	1.114
Final R indices [I > 2σ(I)]	R1 = 0.0447 wR2 = 0.1034
R indices (all data)	R1 = 0.0584 wR2 = 0.1109
Largest peak/hole, e Å <sup>-3</sup>	2.081 and -0.653
Extinction coefficient	n/a
Structure volume, Å <sup>3</sup> (%)	1623.92(62.95)



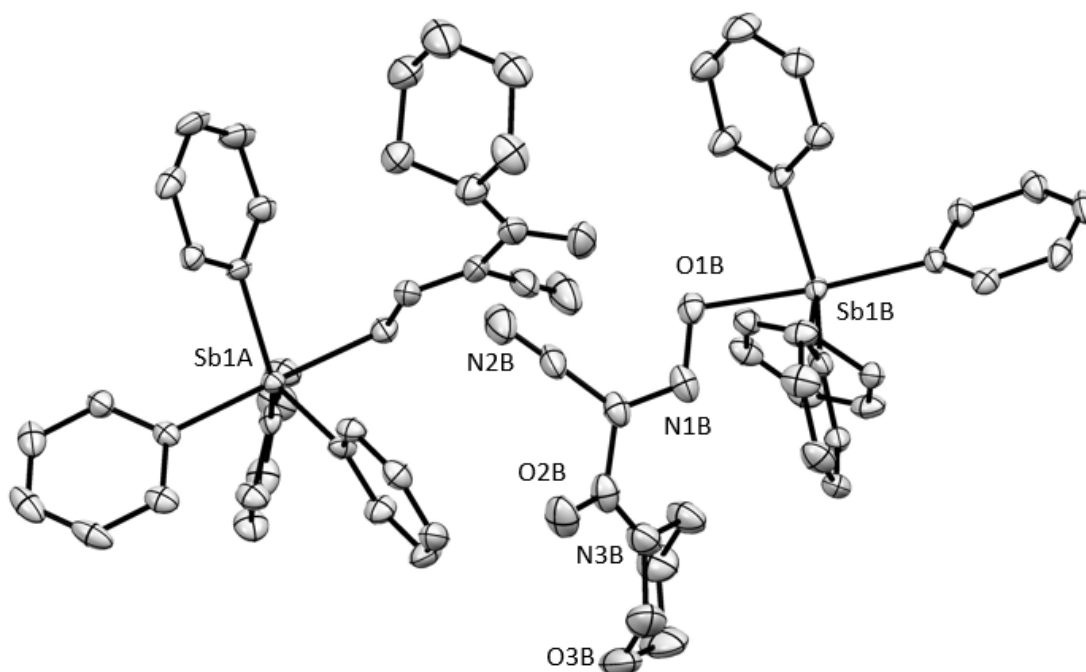


**Figure 40.** Two independent molecules in the ASU of the structure of  $\text{Sb}(\text{Ph})_4(\text{MCO})$ ; and ORTEP drawing at 50% thermal ellipsoids probability level. Principal atoms are labeled, with H atoms are omitted for clarity.

**Table 18.** Selected bond lengths ( $\text{\AA}$ ) and angles ( $^\circ$ ) of the cyanoxime and metal complex center in the first independent molecule A, in the ASU of  $\text{Sb}(\text{Ph})_4(\text{MCO})$ .

Bond length ( $\text{\AA}$ )	Valence angle ( $^\circ$ )
Cyanoxime:	
C1A - N1A = 1.289(5)	C1A - N1A - O1A = 114.8(4)
C1A - C3A = 1.496(6)	C1A - C2A - N2A = 178.6(6)
C2A - N2A = 1.141(6)	C2A - C1A - C3A = 115.2(4)
C3A - O2A = 1.240(5)	C1A - C3A - O2A = 116.6(4)
C3A - N3A = 1.337(6)	N1A - C1A - C3A = 122.2(4)
N1A-O1A = 1.353(5)	C2A - C1A - N1A = 122.3(4)
	O2A - C3A - N3A = 122.6(5)
Metal Center:	
Sb1A - O1A = 2.260(3)	C8A - Sb1A - O1A = 83.12(13)
	C14A - Sb1A - O1A = 177.76(12)
	C20A - Sb1A - O1A = 83.17(13)
	C26A - Sb1A - O1A = 85.89(13)
	C14 - Sb1A - C8A = 97.40(16)
	C20A - Sb1A - C8A = 113.89(16)
	C26A - Sb1A - C8A = 123.77(15)
	C20A - Sb1A - C14A = 94.64(15)
	C20A - Sb1A - C26A = 119.19(16)
	C26A - Sb1A - C14A = 95.59(15)

**Table 19.** Selected bond lengths (Å) and angles (°) of the cyanoxime and metal complex center in the second independent molecule B, in the ASU of Sb(Ph)<sub>4</sub>(MCO).

Bond length (Å)	Valence angle (°)
Cyanoxime:	
C1B - N1B = 1.289(5)	C1B - N1B - O1B = 115.3(4)
C1B - C3B = 1.493(7)	C1B - C2B - N2B = 178.4(5)
C2B - N2B = 1.157(6)	C2B - C1B - C3B = 117.1(4)
C3B - O2B = 1.233(5)	C1B - C3B - O2B = 118.4(4)
C3B - N3B = 1.343(6)	N1B - C1B - C3B = 119.1(4)
N1B-O1B = 1.339(5)	C2B - C1B - N1B = 123.3(4)
	O2B - C3B - N3B = 123.2(5)
Metal Center:	
Sb1B - O1B = 2.241(3)	C8B - Sb1B - O1B = 81.09(13)
	C14B - Sb1B - O1B = 175.06(13)
	C20B - Sb1B - O1B = 86.79(13)
	C26B - Sb1B - O1B = 84.06(14)
	C14B - Sb1B - C8B = 94.05(15)
	C20B - Sb1B - C8B = 120.45(16)
	C26B - Sb1B - C8B = 116.21(16)
	C20B - Sb1B - C14B = 96.53(15)
	C20B - Sb1B - C26B = 120.11(15)
	C26B - Sb1B - C14B = 97.35(16)

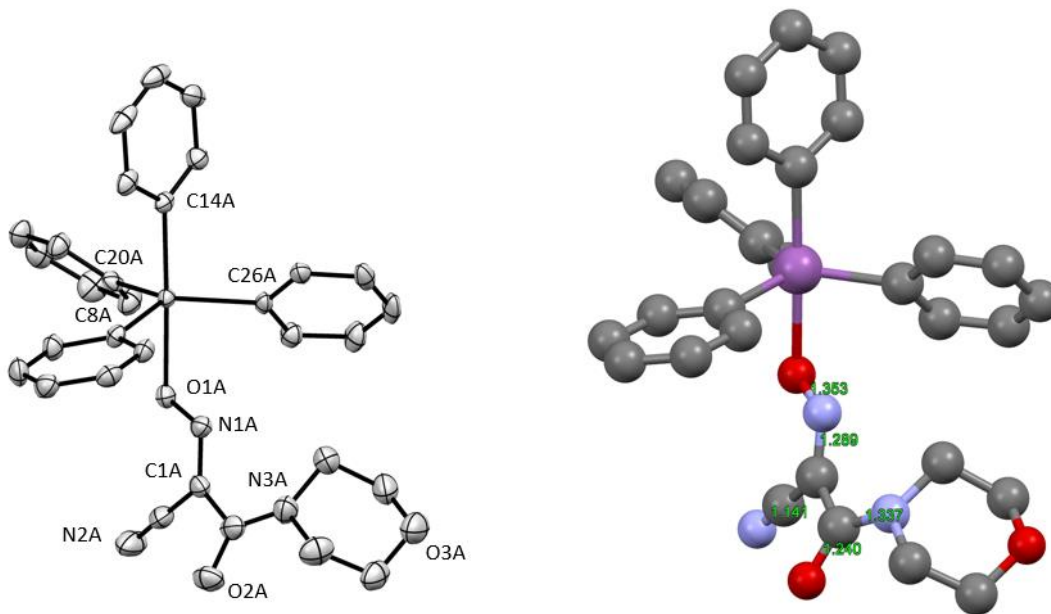


**Figure 41.** Molecular structure and labeling of principal atoms in the structure of Sb(Ph)<sub>4</sub>(MCO) molecule A on the left, and some selected important bond lengths on the right.

**V.1.9. Crystal structure of Sb(Ph)<sub>4</sub>(TCO), two polymorphs.** There were two different polymorphs of the Sb(Ph)<sub>4</sub>(TCO) obtained from the system involving the TCO<sup>-</sup> anion and Sb(Ph)<sub>4</sub><sup>+</sup> cation: polymorph *1* and polymorph *2*. The first contains two independent molecules in the ASU and crystallizes in the standard P2<sub>1</sub>/c monoclinic space group (Table 20). The second one contains *eight* independent molecules in the ASU and crystallizes in the Cc monoclinic space group (Table 21). The difference between these two systems generating 2 different polymorphs are the conditions of crystallization. Polymorph 1 was obtained after slow evaporation of the solvent CH<sub>3</sub>CN in a charged desiccator with paraffin. Utilizing this method of crystallization, crystals were obtained in a week. Polymorph 2 was collected through means of vapor diffusion when ether vapors assisted crystallization by pushing the compound from the CH<sub>3</sub>CN solution to the walls of the inner tube. The second method, using vapor diffusion, afforded suitable crystals for the X-ray analysis of crystals over a two-month period for crystal growth.

**Polymorph 1.** The coordination compound crystallized as a clear, yellow-bronze, plate-like specimen (Figure 42). The Sb(Ph)<sub>4</sub>(TCO) was discovered to have in both cases unusual geometry of the thio-oxime. In polymorph 1 there are two co-crystallized diastereomers, *trans-anti* and *trans-syn*, in the asymmetric unit (ASU) in the structure (Figure 43). The crystal and refinement data of this complex is shown in Table 20. The ratio between both diastereomers was found to be 81.7 and 18.3%, respectively (Figure 44). In both diastereomers, the TCO<sup>-</sup> cyanoxime ligand are practically planar. In the case of the *trans-anti* isomer, the first plane consists of every atom in the cyanoxime moiety except the amide electron withdrawing group (C3-N3-H3B) giving a small dihedral angle of 7.42°. The *trans-syn* isomer is a bit different in terms of what creates the planes of non-planarity. The first plane consists of O1A-N1A-N2A-

C2A-C1A-C3A, the second follows with the sulfur and nitrogen of the amide (S1A-N3A-H3A1). These two planes intersect forming a dihedral angle of  $17.27^\circ$ .

Another representation of the Sb(V) coordinated distorted trigonal bipyramid polyhedron can be seen in Figure 45. The *trans-anti* isomer has a linear cyano group  $C1 - C2 - N2 = 175.6^\circ$  (Table 21). The *trans-syn* isomer owns a linear cyano group with  $C1a - C2a - N2a = 173.0^\circ$  (Table 21). Bond lengths for the cyano group were  $C2 - N2 = 1.140 \text{ \AA}$ , oxime group  $N1-O1 = 1.345 \text{ \AA}$ , and  $C1 - N1 = 1.266 \text{ \AA}$  for the *trans-anti* diastereomer, and  $C2a - N2a = 1.15 \text{ \AA}$ , oxime group  $N1a-O1a = 1.273 \text{ \AA}$ , and  $C1a - N1a = 1.33 \text{ \AA}$  with the *syn* diastereomer. This structure received the CCDC number 2012155, and its quality is assessed in the checkCIF report in Appendix C-8.



**Figure 42.** Video microscope image of the crystal of  $Sb(Ph)_4(TCO)$ , polymorph **1**, with indexed faces.

**Table 20.** Crystal and refinement data for the crystal Sb(Ph)<sub>4</sub>(TCO), polymorph 1.

Parameter	Sb(Ph) <sub>4</sub> (TCO)
Empirical formula	C <sub>27</sub> H <sub>21</sub> N <sub>3</sub> OSb
F.W., g mol <sup>-1</sup>	557.28
Color	light yellow-bronze
Crystal size, mm	0.142 x 0.148 x 0.167
Temperature, K	120(2)
Crystal system	Monoclinic
Space group, #	P 1 21/c 1
Unit cell, Å, °	a = 14.6709(7)      α = 90 b = 9.8468(5)      β = 111.9940(10) c = 18.3414(9)      γ = 90
Unit Cell volume, Å <sup>3</sup>	2456.8(2)
Z	4
Density (calc.) Mg m <sup>-3</sup>	1.507 g/cm <sup>3</sup>
Absorp. Coeff., mm <sup>-1</sup>	1.232
F(000)	1116
Θ range, °	2.30 to 27.20°
Index ranges	-18 ≤ h ≤ 18 -12 ≤ k ≤ 12 -23 ≤ l ≤ 23
<b>Structure solution</b>	
Reflections collected	29603
Independent reflections	5476 [R(int) = 0.0351]
Completeness to Θ, (%)	27.20(99.9)
Absorption correction	Multi-scan
T <sub>max</sub> and T <sub>min</sub>	0.8440 and 0.8210
<b>Refinement method</b>	
Data/restraints/parameters	5476 / 0 / 391
Goodness-of-fit on F <sup>2</sup>	1.033
Final R indices [I > 2σ(I)]	R1 = 0.0308 wR2 = 0.0715
R indices (all data)	R1 = 0.0397 wR2 = 0.0764
Largest peak/hole, e Å <sup>-3</sup>	1.245 and -0.614
Extinction coefficient	n/a
Structure volume, Å <sup>3</sup> (%)	1614.42 (65.71)

**Table 21.** Selected bond lengths (Å) and angles (°) of the cyanoxime and metal complex center in the co-crystallized diastereomers of polymorph **1** of Sb(Ph)<sub>4</sub>(TCO) polymorph **1**, *trans-anti* (top) and *trans-syn* (bottom).

Bond length (Å)	Valence angle (°)
Cyanoxime:	
C1 - N1 = 1.266(5)	C1 - N1 - O1 = 113.9(17)
C1 - C3 = 1.480(5)	C1 - C2 - N2 = 175.6(5)
C2 - N2 = 1.140(7)	C2 - C1 - C3 = 119.2(3)
C3 - S1 = 1.636(5)	C1 - C3 - S1 = 121.9(3)
C3 - N3 = 1.336(5)	N1 - C1 - C3 = 118.9(4)
N1-O1 = 1.345(4)	C2 - C1 - N1 = 121.9(3)
	S1 - C3 - N3 = 124.1(3)
Metal Center:	
Sb1 - O1 = 2.304(2)	C4 - Sb1 - O1 = 84.23(10)
	C10 - Sb1 - O1 = 176.86(9)
	C16 - Sb1 - O1 = 83.09(10)
	C22 - Sb1 - O1 = 79.91(10)
	C10 - Sb1 - C4 = 97.81(10)
	C16 - Sb1 - C4 = 116.60(10)
	C22 - Sb1 - C4 = 122.04(10)
	C16 - Sb1 - C10 = 98.06(10)
	C16 - Sb1 - C22 = 116.18(10)
	C22 - Sb1 - C10 = 96.97(10)
Cyanoxime:	
C1a - N1a = 1.33(2)	C1a - N1a - O1a = 113.9(17)
C1a - C3a = 1.44(3)	C1a - C2a - N2a = 173.(2)
C2a - N2a = 1.15(3)	C2a - C1a - C3a = 121.7(18)
C3a - S1a = 1.82(3)	C1a - C3a - S1a = 111.8(17)
C3a - N3a = 1.27(3)	N1a - C1a - C3a = 128.(2)
N1a-O1a = 1.273(19)	C2a - C1a - N1a = 109.9(19)
	S1a - C3a - N3a = 123.1(16)
Metal Center:	
Sb1 - O1a = 2.370(14)	C4 - Sb1 - O1a = 78.3(3)
	C10 - Sb1 - O1a = 164.1(4)
	C16 - Sb1 - O1a = 70.7(3)
	C22 - Sb1 - O1a = 98.1(4)

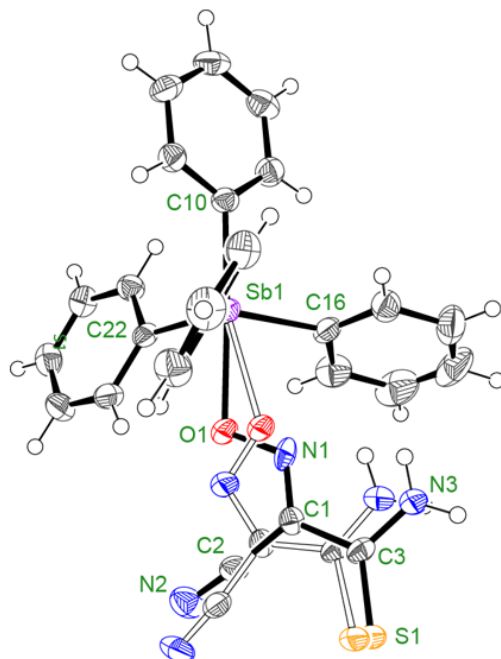


**Figure 43.** Two co-crystallized diastereomers, *trans-syn* and *trans-anti*, of the structure of  $\text{Sb}(\text{Ph})_4(\text{TCO})$  polymorph **1**; an ORTEP drawing at 50% thermal ellipsoids probability level. Principal atoms are labeled.

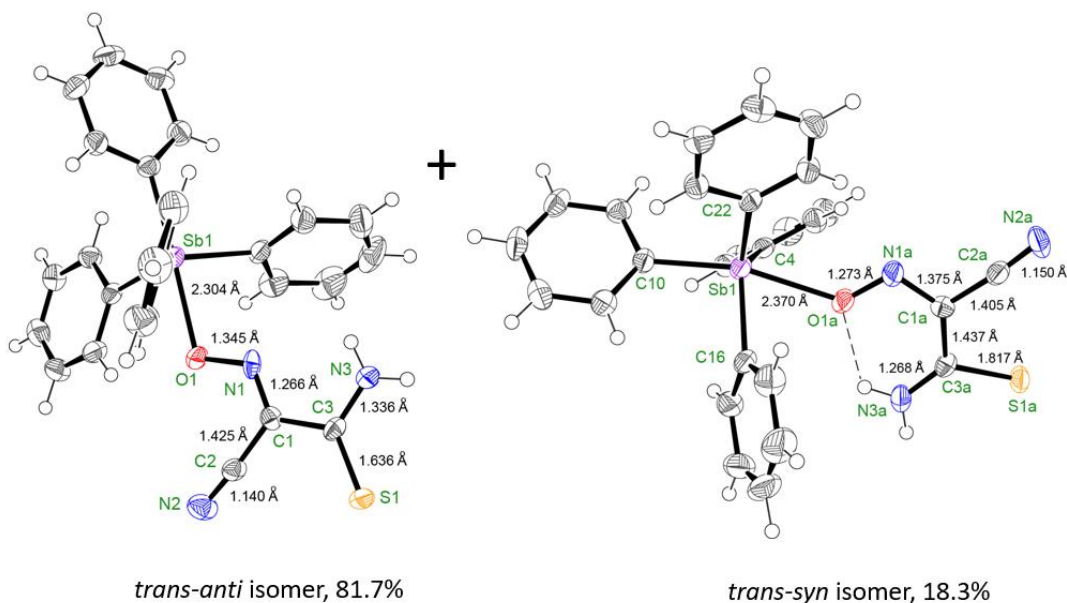


**Figure 44.** Two least obstructed views of the two diastereomers of  $\text{Sb}(\text{Ph})_4(\text{TCO})$  in the ASU representing H bonding stability between the amide hydrogen (N-H3a) and O1a. Ratios of diastereomers are shown.

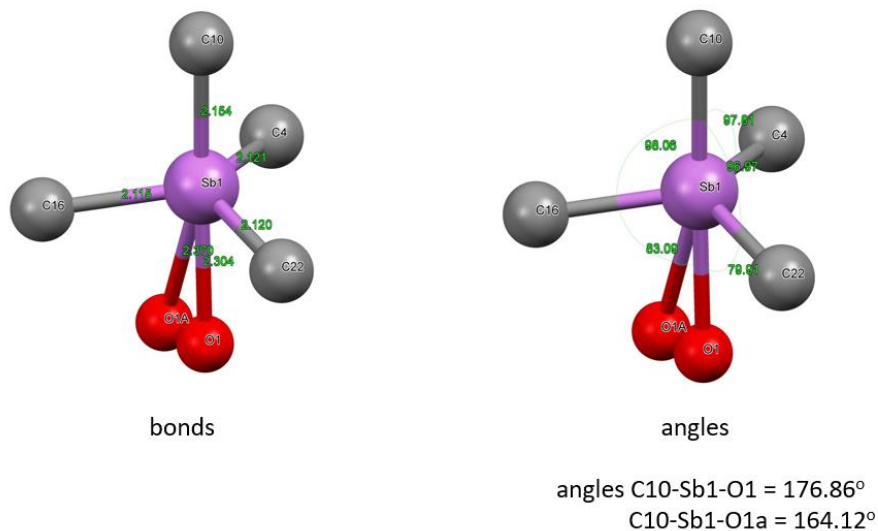


**Figure 45.** Geometry of the pentavalent antimony complex  $\text{Sb}(\text{Ph})_4(\text{TCO})$  diastereomers, showing a distorted trigonal bipyramid polyhedron coordination. Important bond lengths and angles of coordination are shown.

**Polymorph 2.** This crystalline compound formed as yellow almost square plates. A specimen with dimensions of 0.080 mm x 0.110 mm x 180 mm was selected for crystallographic work. We assigned it as polymorph 2. Contrary to the previous polymorph the ASU of polymorph 2 contained *eight* individual molecules as only *one* diastereomer, *trans-syn* (Figure 46). This is a unique occurrence, as the unit cell volume is incredibly larger,  $19\text{k } \text{\AA}^3$  compared to the previous  $2.5\text{k } \text{\AA}^3$  to be precise (Table 22)! With a Z value of 4, this contributes 32 molecules in one unit cell.

The lone diastereomer, *trans-syn*, stabilizes its structure through intramolecular H-bonding between the one of the equatorial phenyl ring's and amide's hydrogen to the only oxygen from the cyanoxime (Figure 47). The numbering scheme in the structure consisted of A, B, C, D, E, F, H, and Q independent molecules. Representation of molecule Q will be used for bonds and angles as an example. Other seven individual molecules can be retrieved from the



CCDC number 2012157 and seen in Appendix C-9. The diastereomer has a linear cyano group  $C1Q - C2Q - N2Q = 175.1^\circ$  (Table 23). Bond lengths for the cyano group were  $C2Q - N2Q = 1.151 \text{ \AA}$ , oxime group  $N1Q-O1Q = 1.315 \text{ \AA}$ , and  $C1Q - N1Q = 1.339 \text{ \AA}$  found in Table 23. Every individual molecule was found to be nonplanar in the cyanoxime anion. All of which had the same position of planes in the cyanoxime structure with the first plane being made up from  $N3-C3-S1A$  from the thioamide. The second plane consisted of  $N2-C2-O1-N1-C1$ . All dihedral angles from each individual molecule can be found with some statistical analysis in Table 24. This table also includes the bond lengths of Sb-O and angles, followed by analysis of off-plane Sb(V) core distance from the 3 *ipso* equatorial carbons of the phenyl rings.

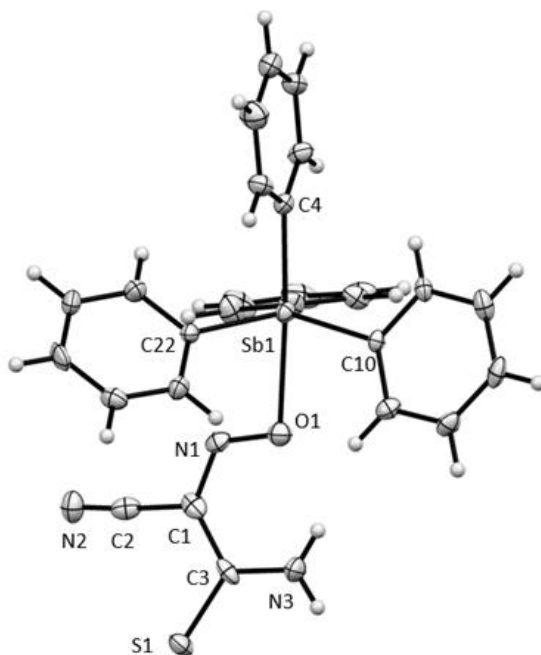


**Figure 46.** Molecular structure and numbering scheme for principal atoms in the one of the eight individual molecules in the ASU for the structure  $Sb(Ph)_4(TCO)$  polymorph 2. An adoption of the *trans-syn* configuration by the cyanoxime moiety is shown.

**Table 22.** Crystal and refinement data for another polymorph of crystalline Sb(Ph)<sub>4</sub>(TCO) polymorph 2.

Parameter	Sb(Ph) <sub>4</sub> (TCO) polyorph 2
Empirical formula	C <sub>216</sub> H <sub>176</sub> N <sub>24</sub> O <sub>8</sub> S <sub>8</sub> Sb <sub>8</sub>
F.W., g mol <sup>-1</sup>	4466.28
Color	fluorescent light colorless
Crystal size, mm	0.080 x 0.110 x 0.180
Temperature, K	100(2)
Crystal system	Monoclinic
Space group, #	C 1 c 1
Unit cell, Å, °	a = 24.517(4),      α = 90 b = 24.448(4),      β = 101.670(2) c = 32.958(5),      γ = 90
Unit Cell volume, Å <sup>3</sup>	19346.(5)
Z	4
Density (calc.) Mg m <sup>-3</sup>	1.533 g/cm <sup>3</sup>
Absorp. Coeff., mm <sup>-1</sup>	1.252
F(000)	8960
Θ range, °	1.19 to 29.48°
Index ranges	-33 ≤ h ≤ 33 -33 ≤ k ≤ 33 -45 ≤ l ≤ 43
<b>Structure solution</b>	
Reflections collected	145367
Independent reflections	49604 [R(int) = 0.0558]
Completeness to Θ, (%)	29.48(94.3)
Absorption correction	Multi-scan
T <sub>max</sub> and T <sub>min</sub>	0.9120 and 0.8160
<b>Refinement method</b>	
Data/restraints/parameters	49604 / 2 / 2379
Goodness-of-fit on F <sup>2</sup>	1.047
Final R indices [I > 2σ(I)]	R1 = 0.0569 wR2 = 0.1386
R indices (all data)	R1 = 0.0691 wR2 = 0.1472
Largest peak/hole, e Å <sup>-3</sup>	5.682 and -2.056
Extinction coefficient	n/a
Structure volume, Å <sup>3</sup> (%)	12444.5 (64.3)

**Table 23.** Selected bond lengths (Å) and angles (°) of the cyanoxime and metal complex center in Sb(Ph)<sub>4</sub>(TCO) polymorph **2** of the 8<sup>th</sup> independent molecule in the ASU, labeled as Q.

Bond length (Å)	Valence angle (°)
Cyanoxime:	
C1Q - N1Q = 1.339(13)	C1Q - N1Q - O1Q = 118.2(9)
C1Q - C3Q = 1.486(15)	C1Q - C2Q - N2Q = 175.1(11)
C2Q - N2Q = 1.151(14)	C2Q - C1Q - C3Q = 118.3(9)
C3Q - S1Q = 1.687(10)	C1Q - C3Q - S1Q = 120.0(7)
C3Q - N3Q = 1.326(13)	N1Q - C1Q - C3Q = 127.8(9)
N1Q - O1Q = 1.315(11)	C2Q - C1Q - N1Q = 113.8(9)
	S1Q - C3Q - N3Q = 123.1(9)
Metal Center:	
Sb1Q - O1Q = 2.430(7)	C4Q - Sb1Q - O1Q = 176.6(3)
	C10Q - Sb1Q - O1Q = 83.2(3)
	C16Q - Sb1Q - O1Q = 81.4(3)
	C22Q - Sb1Q - O1Q = 81.7(3)
	C10Q - Sb1Q - C4Q = 99.7(4)
	C16Q - Sb1Q - C4Q = 98.8(4)
	C22Q - Sb1Q - C4Q = 95.3(4)
	C16Q - Sb1Q - C10Q = 116.5(4)
	C16Q - Sb1Q - C22Q = 117.9(4)
	C22Q - Sb1Q - C10Q = 120.0(3)

**Table 24.** Analysis of bond lengths, bond and dihedral angles of the eight independent molecules of the Sb(Ph)<sub>4</sub>(TCO) polymorph **2** ASU.

Independent Molecule	Sb-O bond length (Å)	C-Sb-O angle (°)	Off-plane distance Sb and plane of 3 carbon atoms of Ph-rings	Dihedral angle of the cyanoxime moiety
Sb(Ph) <sub>4</sub> (TCO) - a	2.395	177.21	0.29	16.85
Sb(Ph) <sub>4</sub> (TCO) - b	2.392	178.75	0.297	18.64
Sb(Ph) <sub>4</sub> (TCO) - c	2.418	178.84	0.299	16.54
Sb(Ph) <sub>4</sub> (TCO) - d	2.408	178.03	0.296	17.42
Sb(Ph) <sub>4</sub> (TCO) - e	2.404	178.6	0.284	17.75
Sb(Ph) <sub>4</sub> (TCO) - f	2.433	177.06	0.316	15.31
Sb(Ph) <sub>4</sub> (TCO) - h	2.434	176.37	0.308	15.92
Sb(Ph) <sub>4</sub> (TCO) - q	2.43	176.61	0.29	16.31
Average	2.4143	177.6939	0.2975	16.8425
St. Dev.	0.017	0.9947	0.0104	1.0666

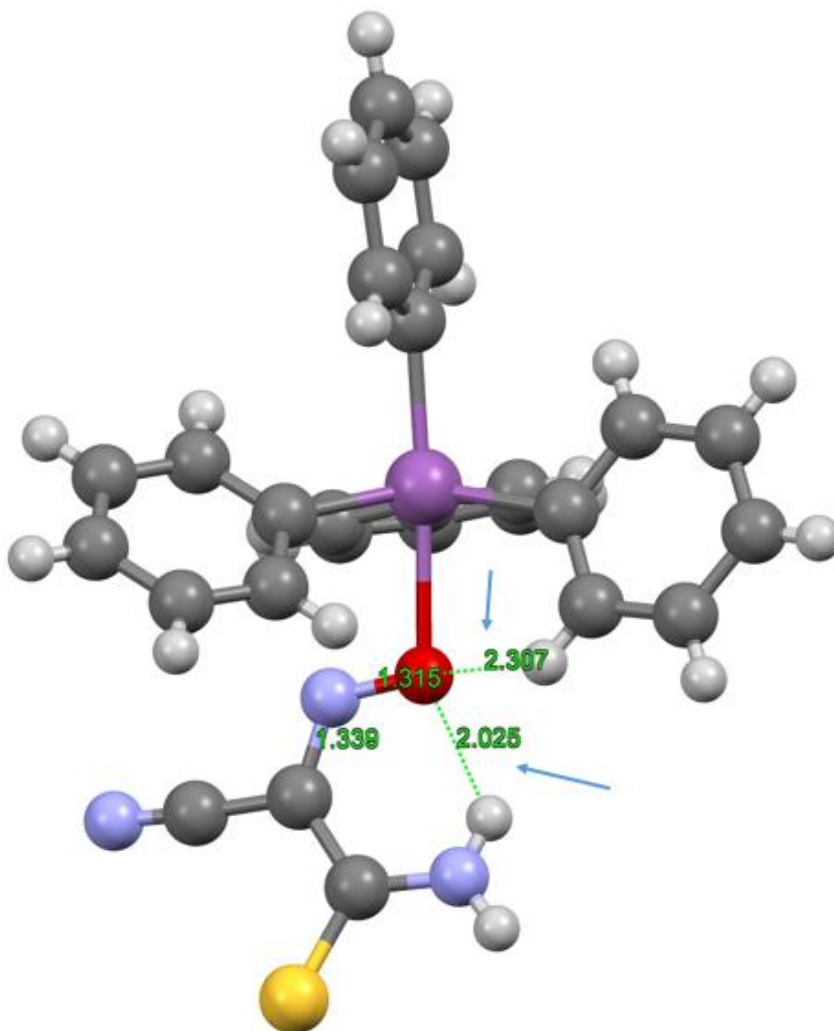


**Figure 47.** Structure of the Q (or 8<sup>th</sup>) different polymorph shown of  $\text{Sb}(\text{Ph})_4(\text{TCO})$  with representation of H-bonding between the amide and phenyl hydrogen's with the oxygen from the oxime moiety.

## V.2. Differential Scanning Calorimetry – Thermal Gravimetry Analysis (DSC/TGA)

This method was used to assess compounds' thermal stability and determine accurate phase transitions. The DSC-TGA analysis of the Sb(V) cyanoximates are described Table 25. A typical thermogram of the  $\text{Sb}(\text{Ph})_4(\text{ECO})$  monomer shows an endothermic peak of heat flow at  $144.7^\circ\text{C}$  representing an endothermic effect due to melting point (Figure 48). Every other thermogram contributing to Table 25 can be found in Appendix B, Figures B-1 to B-6.

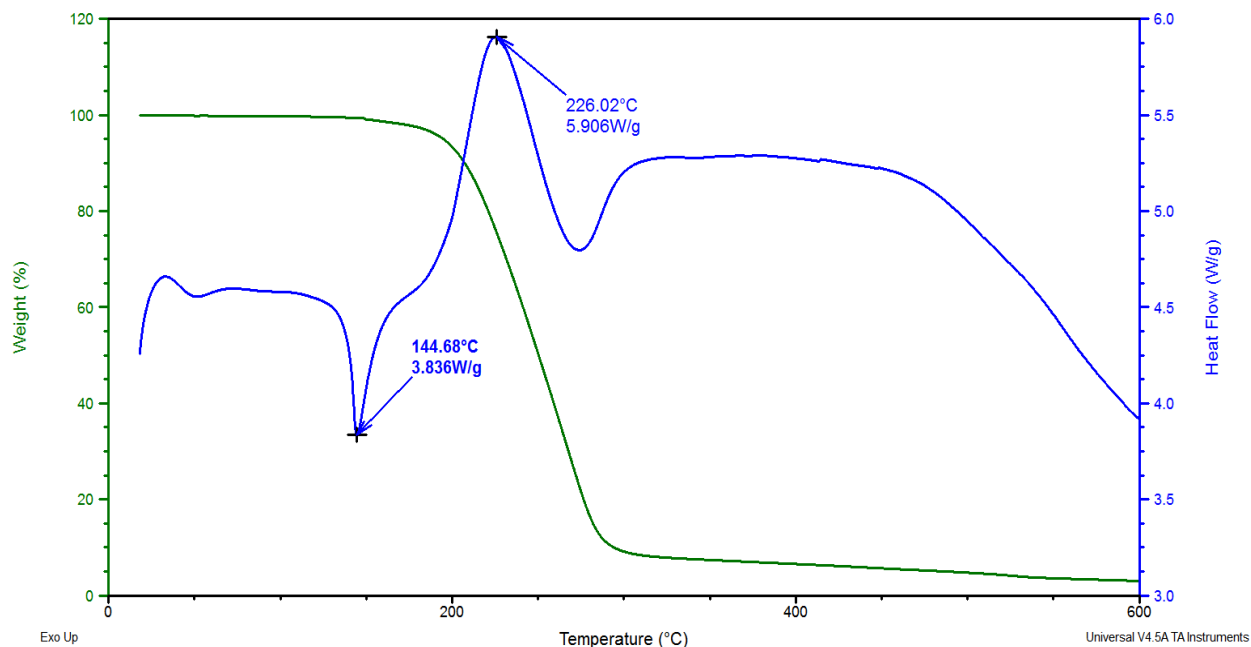


**Figure 48.** Traces of weight loss (green) and heat flow (blue for the  $\text{Sb}(\text{Ph})_4(\text{ECO})$  monomer showing the melting point of the compound at  $144^\circ\text{C}$  followed by its decomposition at  $\sim 220^\circ\text{C}$ .

### V.3. Vibrational Spectroscopy: Infrared Spectroscopy

Assignments of vibrations were completed on all synthesized organoantimony(V) cyanoximates and can be found in Table 26. For a majority of assignments referenced from,<sup>60, 112</sup> but for the low  $\text{cm}^{-1}$  bands for Sb-Ph vibrations literature<sup>114, 115</sup> were used.

### V.4. NMR Spectroscopy – $^{13}\text{C}\{^1\text{H}\}$ Results

All NMR spectra were recorded at room temperature for most of the organoantimony(V) cyanoximates except  $\text{Sb}(\text{Ph})_4(\text{TDCO})$  and  $\text{Sb}(\text{Ph})_4(\text{ACO})$ . The  $^{13}\text{C}\{^1\text{H}\}$  chemical shifts of these complexes can be found in Tables 27-28 below, along with Figure 49 demonstrating labeling on phenyl ring. Chemical shifts were assigned based on common knowledge of chemical shifts, previous work completed in the Dr. Gerasimchuk research group.<sup>102, 112, 116</sup> The technique of  $^{13}\text{C}\{^1\text{H}\}$  NMR spectroscopy is very useful as it can determine co-crystallized diastereomers, *syn* and *trans*, by recognizing the difference in the electronic structures of individual conformations

as two sets of resonances.<sup>117</sup> The less favorable conformation can be found as small satellite peaks close to the main signal, as there is a small difference in chemical shifts between the two isomers.  $^{13}\text{C}\{^1\text{H}\}$  NMR spectra can be used as a good approximation for the ratio between the two diastereomers and can be coupled with crystallography to clearly identify the percentages of said ratio.<sup>102</sup> In the case of  $\text{Sb}(\text{Ph})_4(\text{TCO})$ , satellites were present in the spectra, with chemical shifts shown in Table 28. Further investigation with  $^{13}\text{C}\{^1\text{H}\}$  chemical shifts of the organoantimony(V) cyanoximates, specifically the pyridylcyanoximates,

**Table 25.** Results of thermal analysis studies of organoantimony(V) cyanoximates.

Compound	Events, temperatures (°C)
$\text{SbPh}_4(2\text{PCO})\cdot\text{H}_2\text{O}^*$	weight loss for $\sim 1 \text{ H}_2\text{O}$ at $\sim 166$ <i>endo</i> -, melting at 204.2; decomposition, <i>exo</i> - at 249
$\text{SbPh}_4(3\text{PCO})$	<i>endo</i> -, melting at 146.9; decomposition, <i>exo</i> - at 199
$\text{SbPh}_4(4\text{PCO})$	<i>endo</i> -, melting at 145.4; decomposition, <i>exo</i> - at 224 and second decomposition, <i>exo</i> - at 283
$\text{SbPh}_4(\text{ACO})$	<i>endo</i> -, melting at 199.5; decomposition, <i>exo</i> - at 239
$\text{SbPh}_4(\text{ECO})$	<i>endo</i> -, melting at 144.7; decomposition, <i>exo</i> - at 226
$\text{SbPh}_4(\text{MCO})$	<i>endo</i> -, melting at 175.2; decomposition, <i>exo</i> - at 238
$\text{SbPh}_4(\text{TCO})$	<i>endo</i> -, melting at 185.6; decomposition, <i>endo</i> - at 239; and second decomposition, <i>endo</i> - at 286
$\text{SbPh}_4(\text{TDCO})$	<i>endo</i> -, melting at 148.7; decomposition, <i>exo</i> - at 221

\*- X-ray structure gives evidence of anhydrous behavior. Therefore, the complex most likely absorbed moisture from handling.

**Table 26.** Assignment of important vibrational frequencies ( $\text{cm}^{-1}$ ) for synthesized organoantimony(V) cyanoximates.

Compound	vibrations in cyanoxime group							$\text{C}_6\text{H}_5$ - group and Sb-Ph vibrations		
	$\nu(\text{NH}_2)$	$\nu(\text{C}\equiv\text{N})$	$\nu(\text{C}=\text{X})^{\text{a}}$	$\nu(\text{C}=\text{N})_{\text{pyr}}$	$\nu(\text{C}=\text{N})_{\text{ox}}$	$\nu(\text{N}-\text{O})$	$\rho(\text{NH}_2)$	$\nu_{\text{as}}(\text{C}-\text{H})$	$\gamma(\nu'_{1g})$	$\nu(\nu_8)$
$\text{Sb}(\text{Ph})_4(2\text{PCO})$	-	2213	-	1589	1463	1016	-	3094	463, 433	689
$\text{Sb}(\text{Ph})_4(3\text{PCO})$	-	2218	-	1574	1473	1065	-	3051	459, 444	687
$\text{Sb}(\text{Ph})_4(4\text{PCO})$	-	2216	-	1590	1468	1114	-	3057	454, 442, 431	687
$\text{Sb}(\text{Ph})_4(\text{ACO})$	3439, 3366	2222	1679	-	1478	1086	1580	3053	442	688
$\text{Sb}(\text{Ph})_4(\text{ECO})$	-	2217	1703	-	1477	1091	-	3052	458, 436	689
$\text{Sb}(\text{Ph})_4(\text{MCO})$	-	2223	1629	-	1497	1063	-	3061	443	690
$\text{Sb}(\text{Ph})_4(\text{TCO})$	3465, 3341	2220	889	-	1583	1067	1618	3062	450	692
$\text{Sb}(\text{Ph})_4(\text{TDCO})$	-	2216	973	-	1524	1069	-	3066	445	688

<sup>a</sup> X = sulfur atom (for  $\text{TCO}^-$  and  $\text{TDCO}^-$ ), oxygen atom (for  $2\text{PCO}^-$ ,  $3\text{PCO}^-$ ,  $4\text{PCO}^-$ ,  $\text{ACO}^-$ ,  $\text{ECO}^-$ ,  $\text{MCO}^-$ ). <sub>ox</sub> – oxime, <sub>pyr</sub> – pyridine

and free cyanoximes had a correlation with the acidity of the cyanoxime ligand. Figure 50 demonstrates this relationship between the chemical shifts of the *ipso* carbon with  $pK_a$  values.  $pK_a$  values were found from previous literature.<sup>117</sup> This relationship can be explained by the four inequivalent carbons found on a phenyl ring. It is important to note the pyridylcyanoximates have different delocalization of electron density when compared to other aliphatic amide-/keto-/ester-cyanoximes. Even though there are only three data points contributing to this linear relationship, it is still evident that the chemical shift of the *ipso* carbon is affected differently by each opposite axial cyanoxime ligand.

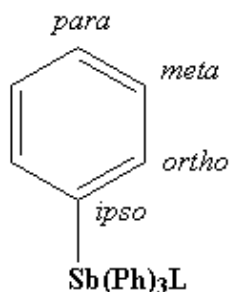


**Figure 49.** General Structure representing the substitution patterns for the phenyl ring of organoantimony(V) cyanoximates. L = ligands and Br, in the case of  $\text{Sb(Ph)}_4\text{Br}$ .

**Table 27.** Tabulated chemical shifts of  $^{13}\text{C}\{^1\text{H}\}$  NMR spectroscopy for the  $\text{Sb(Ph)}_4\text{Br}$  and organoantimony(V) cyanoximates' equivalent phenyl rings.

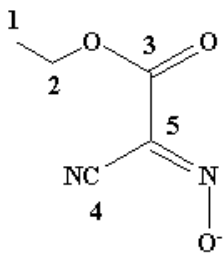
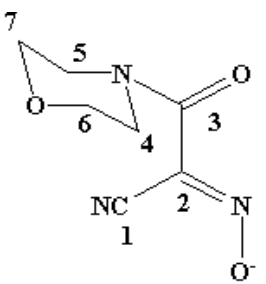
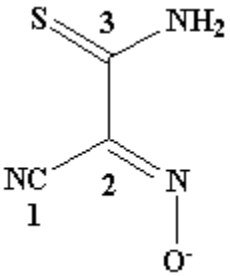
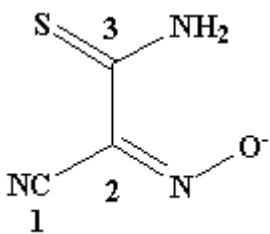
Compound	Assigned peak signals (ppm)			
	<i>ipso</i>	<i>ortho</i>	<i>meta</i>	<i>para</i>
$\text{Sb(Ph)}_4\text{Br}$	135.38	135.04	129.44	131.15
$\text{Sb(Ph)}_4(\text{ECO})$	133.97	135.57	129.207	136.96
$\text{Sb(Ph)}_4(2\text{PCO})$	135.79	135.65	129.02	130.54
$\text{Sb(Ph)}_4(3\text{PCO})$	131.53	135.48	129.17	130.75
$\text{Sb(Ph)}_4(4\text{PCO})$	129.01	135.54	129.12	149.69
$\text{Sb(Ph)}_4(\text{MCO})$	134.9	135.59	129.2	130.9
$\text{Sb(Ph)}_4(\text{TCO})$	133.45	135.34	129.52	131.29



**Table 28.** Tabulated values of chemical shifts of organoantimony(V) cyanoximates in the  $^{13}\text{C}\{^1\text{H}\}$  NMR spectra.

Compound	Structure	$\delta$ (ppm)
Sb(Ph) <sub>4</sub> (2PCO)		C <sub>1</sub> 112.03
		C <sub>2</sub> 132.38
		C <sub>3</sub> 152.24
		C <sub>4</sub> 148.79
		C <sub>5, C<sub>6</sub>, C<sub>7</sub></sub> 135.79
		122.46
118.24		
Sb(Ph) <sub>4</sub> (3PCO)		C <sub>1</sub> 111.55
		C <sub>2</sub> 128.52
		C <sub>3</sub> 127.99
		C <sub>4</sub> 149.05
		C <sub>5</sub> 145.76
		C <sub>6, C<sub>7</sub></sub> 129.17;
123.09		
Sb(Ph) <sub>4</sub> (4PCO)		C <sub>1</sub> 111.56
		C <sub>2</sub> 150.15
		C <sub>3</sub> 140.05
		C <sub>4, 4'</sub> 118.24
		C <sub>5, 5'</sub> 149.69

Table 28 (continued).

Compound	Structure	$\delta$ (ppm)
Sb(Ph) <sub>4</sub> (ECO)		C <sub>1</sub> 112.03 C <sub>2</sub> 132.38 C <sub>3</sub> 152.24 C <sub>4</sub> 148.79 C <sub>5</sub> 135.79
Sb(Ph) <sub>4</sub> (MCO)		C <sub>1</sub> 127.87 C <sub>2</sub> 111.54 C <sub>3</sub> 159.99 C <sub>4</sub> 46.60 C <sub>5</sub> 43.02 C <sub>6</sub> 66.53 C <sub>7</sub> 68.97
Sb(Ph) <sub>4</sub> (TCO) <i>trans-anti</i>		C <sub>1</sub> 110.92 C <sub>2</sub> 131.63 C <sub>3</sub> 190.01
Sb(Ph) <sub>4</sub> (TCO) <i>trans-syn</i>		C <sub>1</sub> 116.92 C <sub>2</sub> 136.38 C <sub>3</sub> 184.98

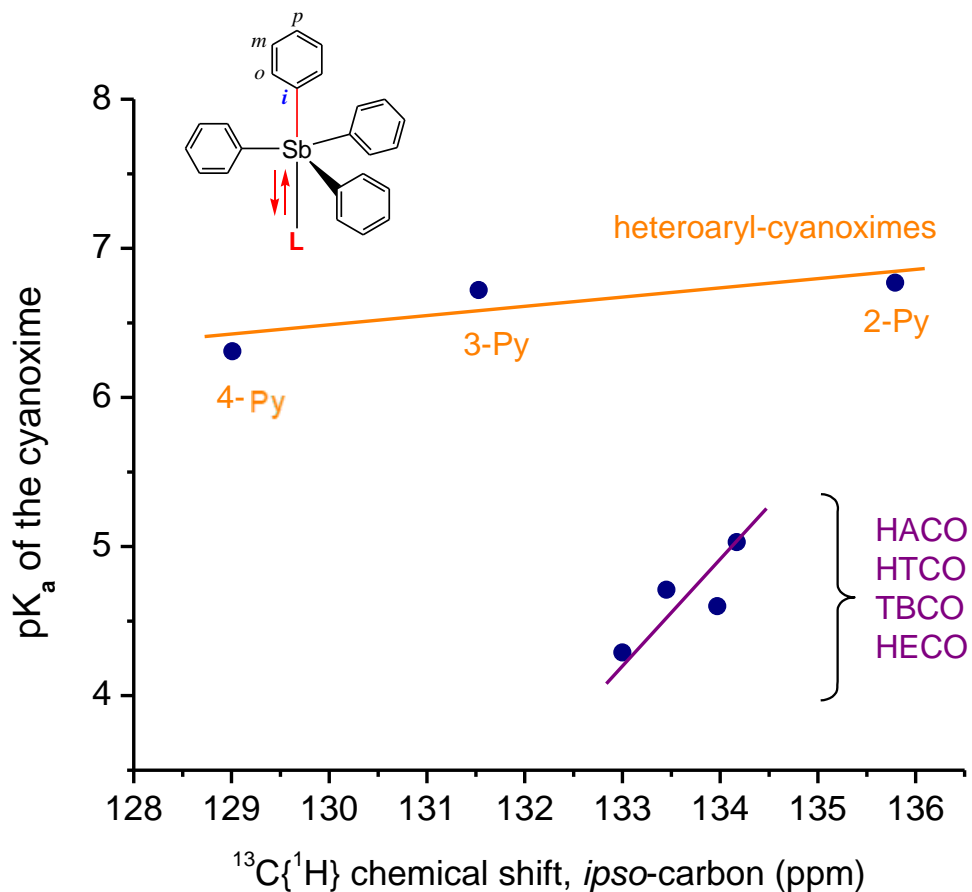


**Figure 50.** Observed correlations between acidity of the free cyanoxime HL and chemical shift of the *ipso* carbon in NMR spectra of organoantimony(V) cyanoximates.

### V.5. UV-Visible Spectroscopy

All obtained organoantimony(V) cyanoximates represent colorless compounds with the exception of Sb(Ph)<sub>4</sub>(TCO) and Sb(Ph)<sub>4</sub>(TDCO). Those exceptions are yellow colored, because the color of the thio-cyanoxime ligands. In the UV-visible spectra bands of  $\pi \rightarrow \pi^*$  transitions of the phenyl groups in all studied compounds at ~270 nm dominate the spectrum and there are no bands in the visible range of the spectrum. As we established earlier by the X-ray analysis, the cyanoxime ligands are bound to the Sb-atom in a monodentate manner. Compounds are soluble in a variety of solvents and form molecular solutions with no electrical conductivity. With a

research goal of performing biological activity studies in mind, it was important to assess the compounds' integrity in solutions formed.

The method of UV-visible spectroscopy is a good tool for such this task, as anionic cyanoximes possess color. Therefore, there is a distinctive gain of color upon deprotonation of a protonated cyanoxime ligand, HL (L = ACO<sup>-</sup>, ECO<sup>-</sup>, 2PCO<sup>-</sup>, 3PCO<sup>-</sup>, 4PCO<sup>-</sup>, and MCO<sup>-</sup>) expressed in Figure 10. If our newly prepared Sb(Ph)<sub>4</sub>L compounds would undergo a solvolytic reaction or dissociate in solutions, then a color will appear shown as in Figure 51. The yellow, orange, or pink color of the cyanoximes anions originates from n → π\* transition that is sensitive to the nature of solvent.<sup>118</sup>

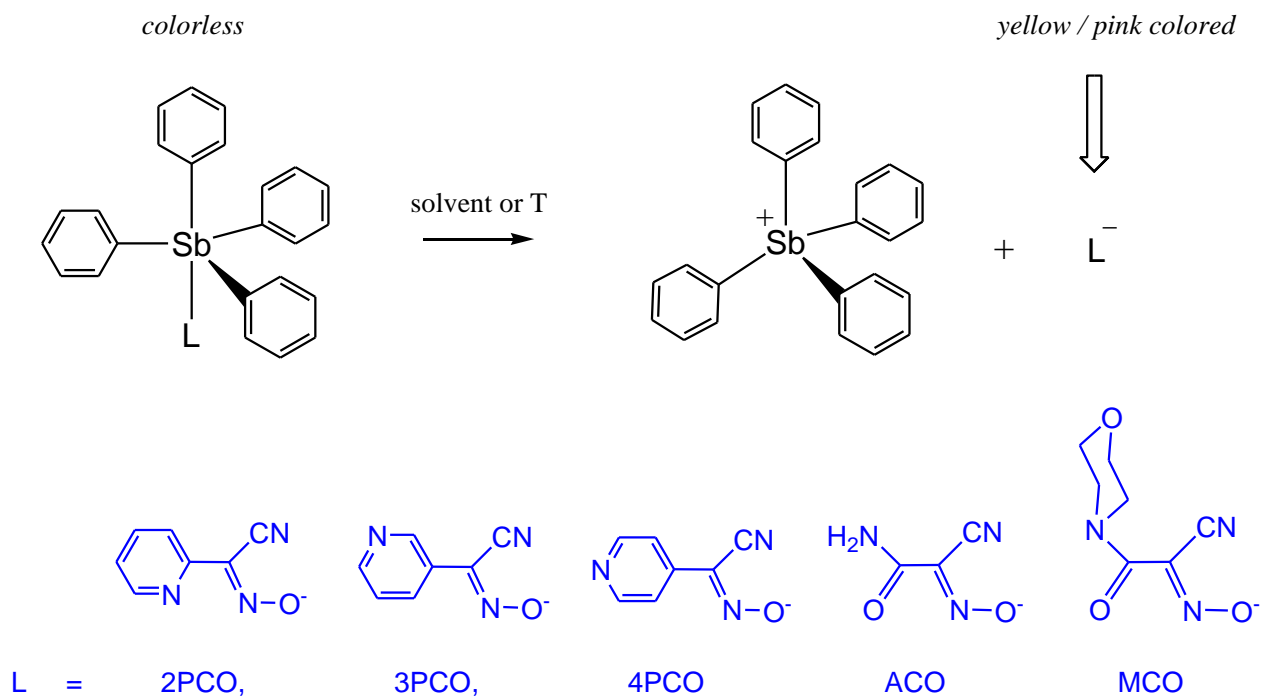


**Figure 51.** Representation of the color gain of solutions of organoantimony(V) cyanoximates in the case of the compounds covalent integrity breaking down.

We performed recordings of the UV-visible spectra of colorless organoantimony(V) cyanoximates in DMSO at room temperature, increasing up to 90°C in 10° intervals. Results evidenced the absence of appreciable ionization of cyanoximes in solutions even at elevated temperatures (Figure 52 and 53). Therefore, all observed in biological studies effects can be associated with the molecular structure of the parent compound  $\text{Sb}(\text{Ph})_4\text{L}$  (L = studied cyanoximes anion) and not to separate  $\text{Sb}(\text{Ph})_4^+$  and  $\text{L}^-$  ions. Of course, there are metabolic processes using biochemical interactions with degradation of our  $\text{Sb}(\text{Ph})_4\text{L}$  in microorganisms, but these investigations were out of the scope of current work.

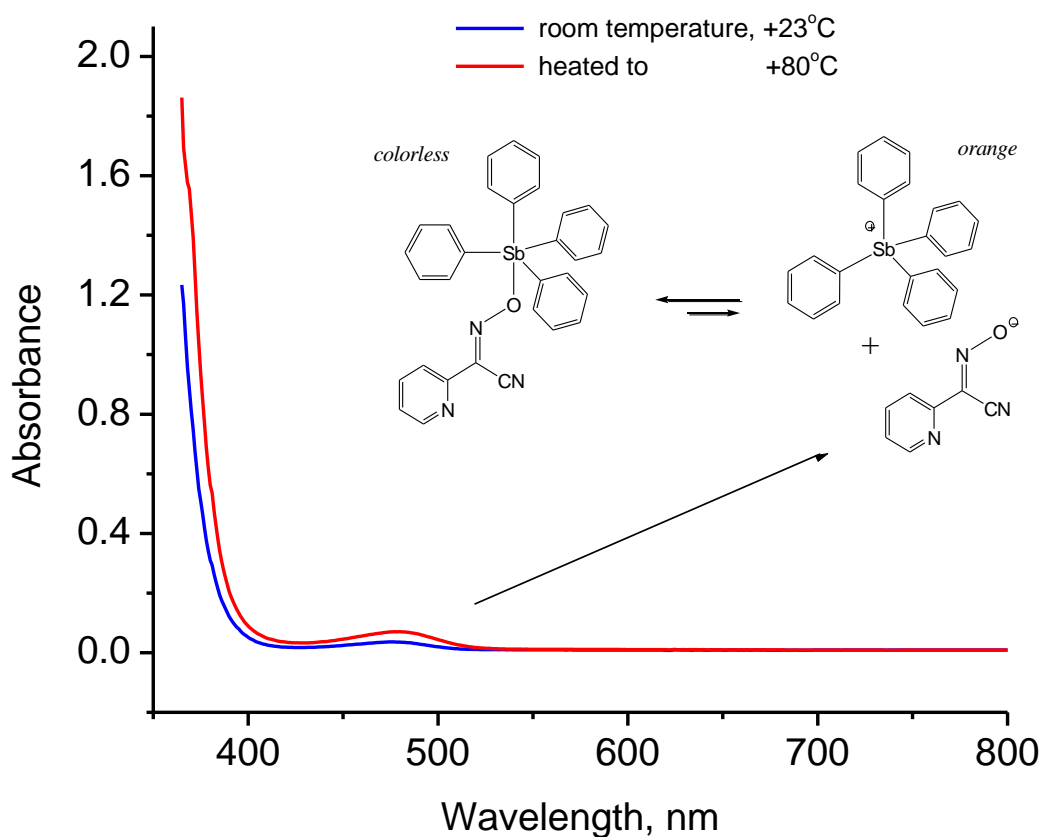


**Figure 52.** An overlay of fragments of the UV-visible spectra of SbPh<sub>4</sub>(2PCO) in DMSO at different temperatures, representing reversible equilibrium of covalent to ionic bonding of Sb(V) complex.

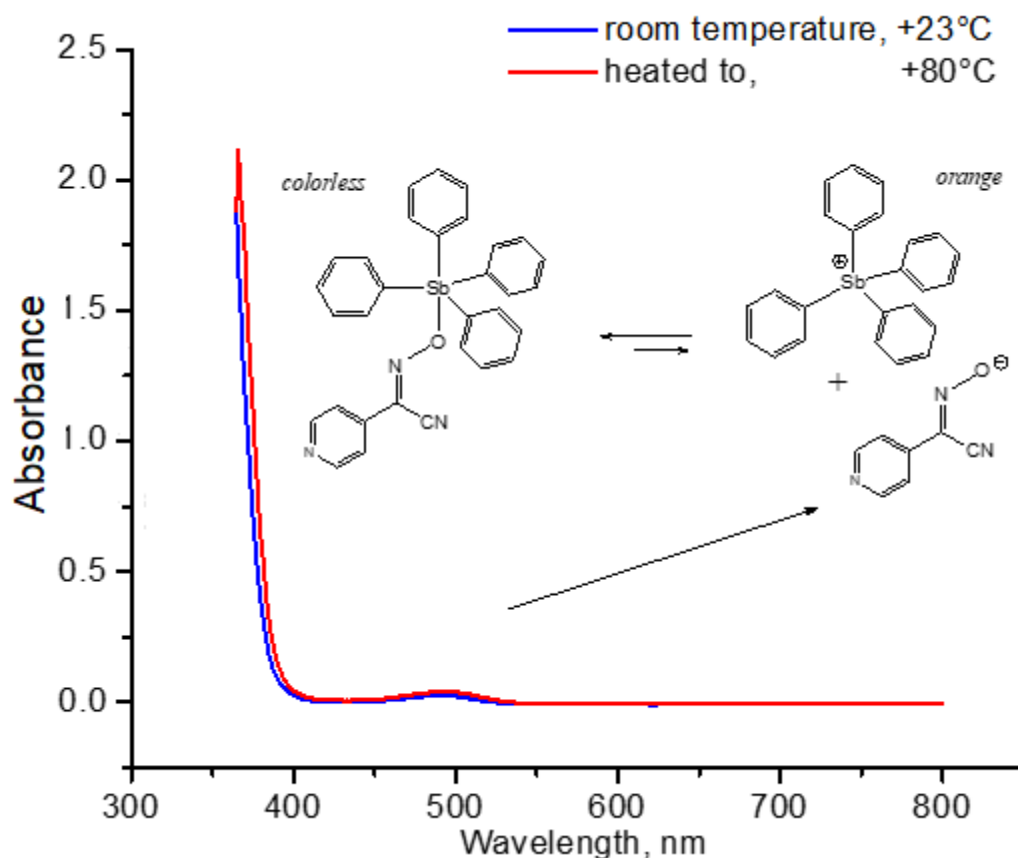


**Figure 53.** An overlay of fragments of the UV-visible spectra of SbPh<sub>4</sub>(4PCO) in propionitrile at different temperatures, representing reversible equilibrium of covalent to ionic bonding of Sb(V) complex.

## V.6. Antimicrobial Studies

These assays were performed by Prof. Marianna Patrauchan and her research group, except the preparation of soaked 100% disks, which was prepared by me. The compounds selected for each assay are explained below in each sub-chapter of results. Minimal inhibition concentration (MIC) samples were dissolved DMSO solutions of the compounds selected prior

to testing. The results for the two sets of inhibition zone measurements and single set of minimal inhibition concentration (MIC) assays are described below.

**V.6.1. First set of inhibition measurements on solid media.** Initial compounds selected for susceptibility tests were:  $\text{Sb(Ph)}_4(\text{ACO})$ ,  $\text{Sb(Ph)}_4(\text{ECO})$  monomer,  $\text{Sb(Ph)}_4(\text{TCO})$ , and  $\text{Sb(Ph)}_4(\text{TDCO})$ . These compounds were tested against gram-negative strains *Escherichia coli* strain S17 and *Pseudomonas aeruginosa* strain PAO1, alongside gram-positive Methicillin-resistant *Staphylococcus aureus* strain NRS70. In this initial test, zone inhibition measurements for  $\text{Sb(Ph)}_4(\text{TDCO})$  were omitted as the PBS buffer was contaminated, results for this compounds were completed in the following round of testing. Figures 54-56 represent the first triplicate set of inhibition zone measurements for antimicrobial activity determination. In the case of  $\text{Sb(Ph)}_4(\text{ACO})$ , it showed a trend against all strains of increased clearance zone inhibition as  $\text{Sb(V)}$  cyanoximate concentration increased (Figure 54). This can be said for the  $\text{Sb(Ph)}_4(\text{ECO})$  monomer for *S. aureus* and *E. coli*, but did not keep that trend against *P. aeruginosa*. Finally,  $\text{Sb(Ph)}_4(\text{TCO})$  demonstrated the decent inhibition against *S. aureus*, but no inhibition at all against *P. aeruginosa* and *E. coli*. Full worksheets including statistical analysis of the first round of susceptibility tests can be found in Appendix D-1 to D-3.

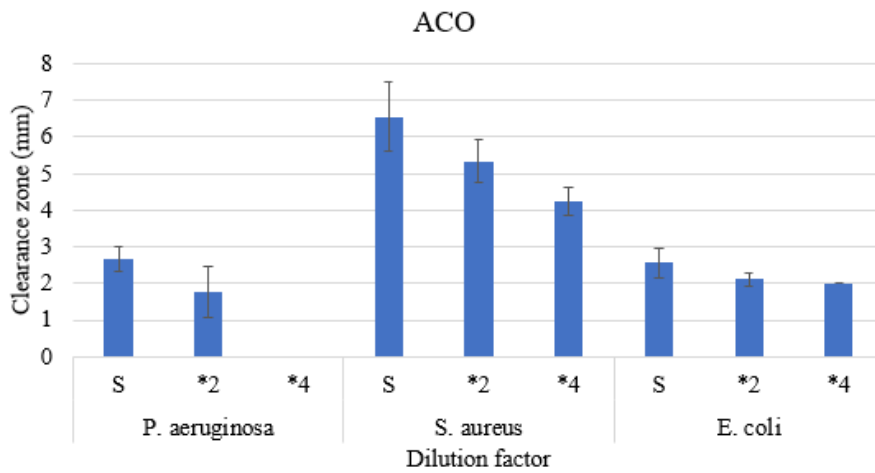


**Figure 54.** Round 1 of Inhibition zone measurements of  $\text{Sb(Ph)}_4(\text{ACO})$  against microbes.

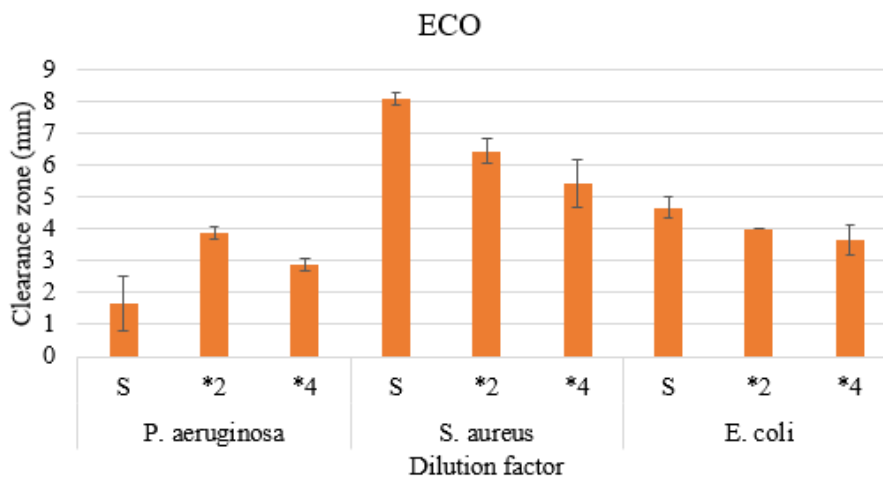


**Figure 55.** Round 1 of Inhibition zone measurements of  $\text{Sb(Ph)}_4(\text{ECO})$  against microbes.



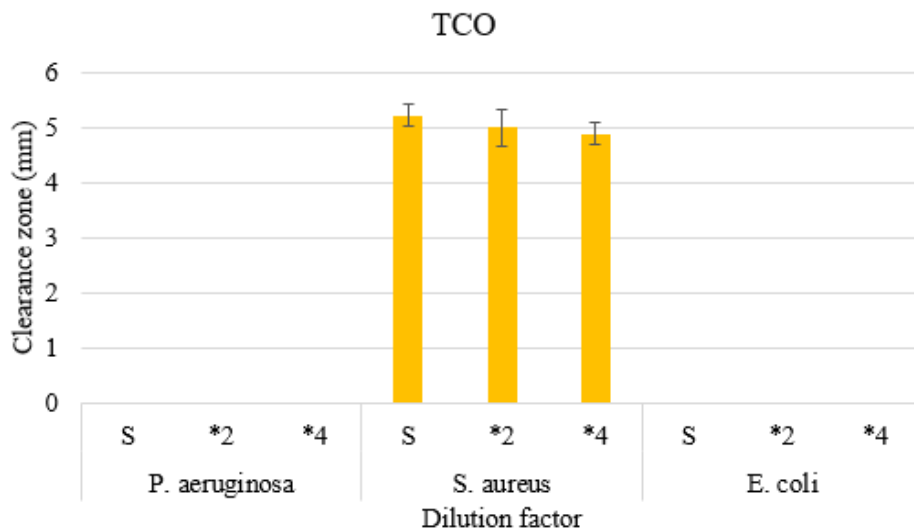


**Figure 56.** Round 1 of inhibition zone measurements of  $\text{Sb}(\text{Ph})_4(\text{TCO})$  against microbes.

**V.6.2. Second set of inhibition measurements.** The second round of susceptibility tests added a new compound, a control  $\text{Sb}(\text{Ph})\text{Br}$  (labeled as CC# in Figure 57), and restarted measurements with  $\text{Sb}(\text{Ph})_4(\text{TDCO})$  due to previous contamination of PBS in the experiment. Each were run in triplicate at three different concentrations. The measurements can be found in Figure 57. Essentially the same outcome occurred for  $\text{Sb}(\text{Ph})_4(\text{ACO})$ ,  $\text{Sb}(\text{Ph})_4(\text{ECO})$ , and  $\text{Sb}(\text{Ph})_4(\text{TCO})$  as the first round of tests. For  $\text{Sb}(\text{Ph})_4\text{Br}$  there was no inhibition against *P. aeruginosa*, and some inhibition against *E. coli*. An interesting outcome is the inhibition zone of  $\text{Sb}(\text{Ph})_4\text{Br}$  with respect to *S. aureus*. A possible reason for this outcome could be due to an ionic halogen exposure to gram-positive bacteria which has less intrinsic defenses as gram-positive bacteria lack a second cell membrane. A similar result with the first round, both of the thioamide cyanoximates,  $\text{Sb}(\text{Ph})_4(\text{TCO})$  and  $\text{Sb}(\text{Ph})_4(\text{TDCO})$ , only had antimicrobial effect against the gram-positive *S. aureus*. The result of zone inhibition being present in only the gram-positive *S. aureus* might show that there an instrinsic antimicrobial resistance against thioamide-

containing organoantimony cyanoximates, though more testing needs to be conducted. Raw data and statistical analysis of this data can be found in under Appendix D-4

**V.6.3. Initial broth dilution MIC tests.** Initial compounds selected for antimicrobial MIC tests were:  $\text{Sb(Ph)}_4(\text{MCO})$ ,  $\text{H(MCO)}$ ,  $\text{H(ECO)}$ , and  $\text{Na}[\text{H(ACO)}_2]$ . The goal of this testing was to determine if free cyanoximes had any effect on inhibition cell growth of the same strains tested in the inhibition zone measurements, as well as testing out an organoantimony(V) cyanoximate. As these compounds were dissolved in DMSO, it must be reiterated that the organic solvent has inhibition effects already once concentrations reach above 5% (Appendix D-1). This inhibition concentration with DMSO would require 200  $\mu\text{g/mL}$  for *P. aeruginosa* and 250  $\mu\text{g/mL}$  for both *E. coli* and *S. aureus*.

Results of the antimicrobial MIC assays are shown in Figure 58 and 59. It is evident in MIC at both the 6 and 24 hours marks that  $\text{Sb(Ph)}_4(\text{MCO})$  had inhibition of cell growth before the DMSO inhibition level at 5%.  $\text{Sb(Ph)}_4(\text{MCO})$  had a definite antimicrobial effect on *E. coli* and *S. aureus* at 200  $\mu\text{g/mL}$  concentration. Compared with *P. aeruginosa*, some inhibition was seen once concentration was increased. Switching over to the free cyanoximes, the inhibition of cells was clearly due to DMSO concentration increasing as the interval from switching to a concentration of zero to 100  $\mu\text{g/mL}$  demonstrated negligible decrease of OD600, therefore an indirect method to quantify microbe concentration. What is a significant factor to free cyanoximes not contributing towards antimicrobial activity is at 6 hours for *P. aeruginosa* for all protonated ligands is the *increase* of concentration from zero to 100  $\mu\text{g/mL}$  causing an increase of microbe concentration. Free cyanoximes tested had no effect against the strain PAO1 of *P. aeruginosa*. As for the other strains, the increasing free cyanoxime concentration had little to no effect on inhibition of microbe growth.

## V.7. Antifungal Studies

These assays were performed by Dr. Karen Wozinak and her research group. Sample preparation was exactly the same as MIC and susceptibility assays for antimicrobial studies. Inhibition zone measurements were completed in two parts and both will be discussed, along with reconstituted MIC assays.

**V.7.1. Kirby-Bauer disk assays.** Initial antifungal studies tested a control (blank cotton disk),  $\text{Sb(Ph)}_4(\text{ECO})$ ,  $\text{Sb(Ph)}_4(\text{ACO})$ ,  $\text{Sb(Ph)}_4(\text{TCO})$ , and  $\text{Sb(Ph)}_4(\text{TDCO})$  against two strains of fungi: *Cryptococcus neoformans* and *Candida albicans*. Disks were prepared at three different concentrations and run in triplicate. Antifungal disk assays can be seen in Figure 60. A general trend with  $\text{Sb(Ph)}_4(\text{ACO})$ ,  $\text{Sb(Ph)}_4(\text{ECO})$ ,  $\text{Sb(Ph)}_4(\text{TDCO})$  against *Cryptococcus neoformans* is that increasing concentration has a positive effect of increasing size of inhibition zone, though for  $\text{Sb(Ph)}_4(\text{TDCO})$ , the zone of inhibition was lower at all concentrations when compared to  $\text{Sb(Ph)}_4(\text{TCO})$  which had an opposite trend than the previous three compounds. With regard to *Candida albicans* against our compounds, it appeared that  $\text{Sb(Ph)}_4(\text{ECO})$  had some form of antifungal activity, but all other compounds were not promising in that field.

**V.7.2. MIC antifungal activity assay.** MIC assays were conducted to show a comparative study of free cyanoximes with an organoantimony(V) cyanoximate against the same fungi strains as disk assays. Results of initial MIC assay in singlet can be seen in Figure 61. Any MICs at 100  $\mu\text{g/mL}$  signified no inhibitory effects. This was the maximum concentration that the lab could identify with their equipment. Considering the results of each free cyanoxime, it is a clear statement that free

cyanoximes have no antifungal activity. On the other hand, when the  $\text{MCO}^-$  cyanoxime anion was coordinated to organoantimony(V) a clear showing of inhibition was recorded. A second run of tests was performed with essentially the same results as the initial MIC assay, except a lower MIC in the case of *Cryptococcus neoformans* (Figure 62). Regardless, if one thing is evident, further studies must be conducted to solidify the practicality of using organoantimony (V) cyanoximates for antifungal treatment.

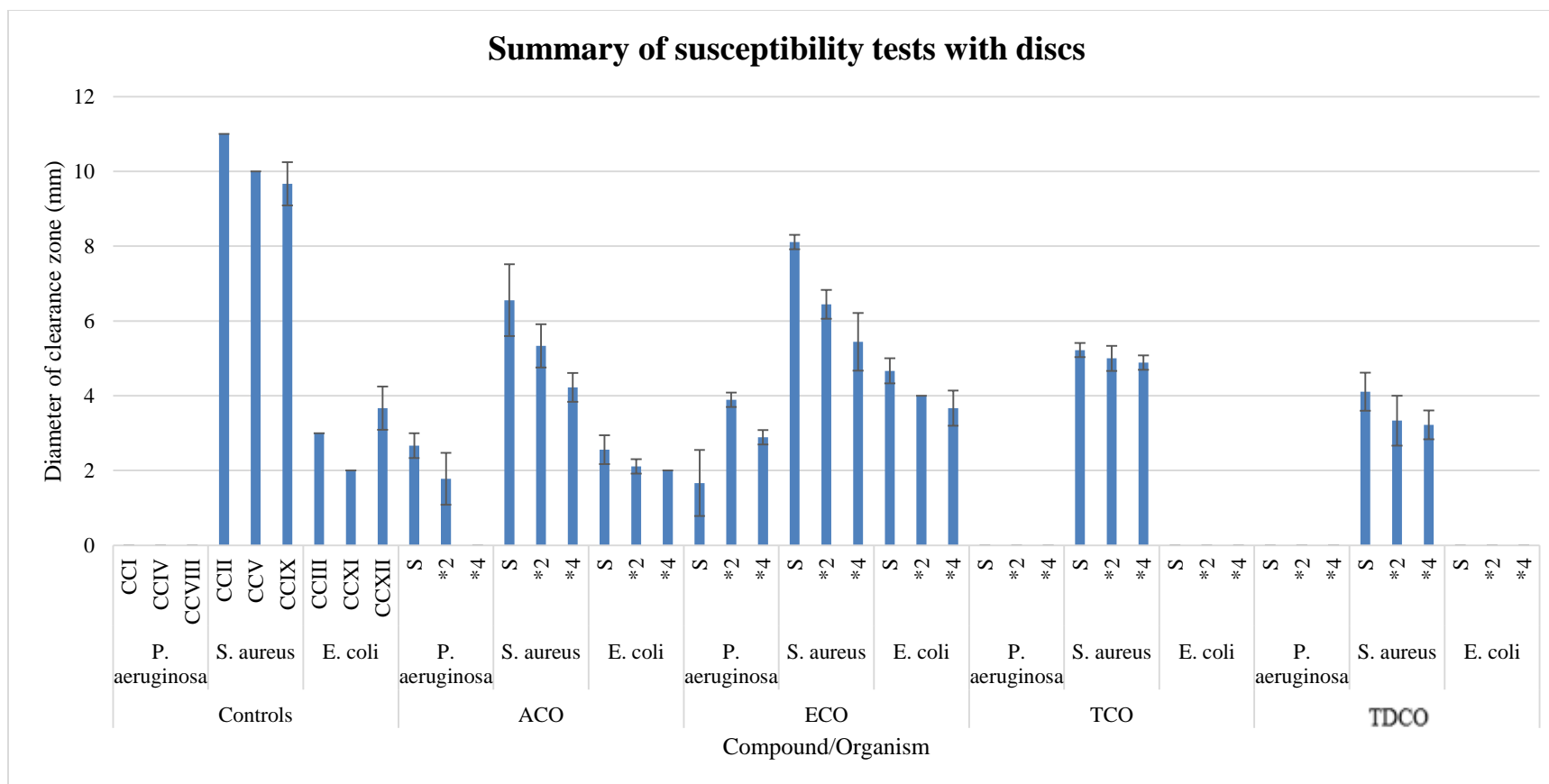


**Figure 57.** Round 2 of inhibition zone measurements of  $\text{Sb}(\text{Ph})_4\text{Br}$ ,  $\text{Sb}(\text{Ph})_4(\text{ECO})$ ,  $\text{Sb}(\text{Ph})_4(\text{TCO})$ , and  $\text{Sb}(\text{Ph})_4(\text{TDCO})$  against microbes.

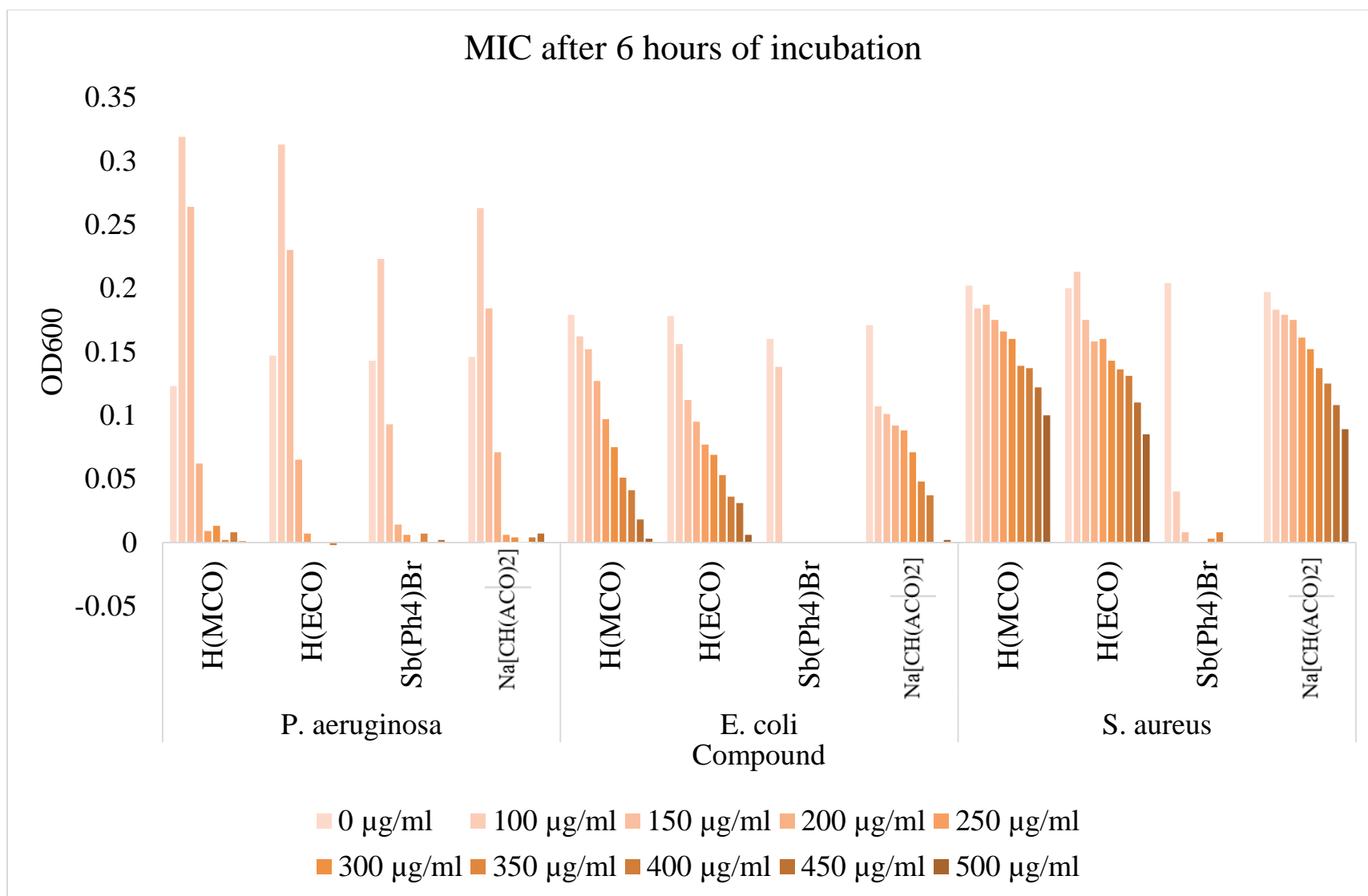


**Figure 58.** Antimicrobial MIC determination after six hours of inoculation with antimicrobial tests.

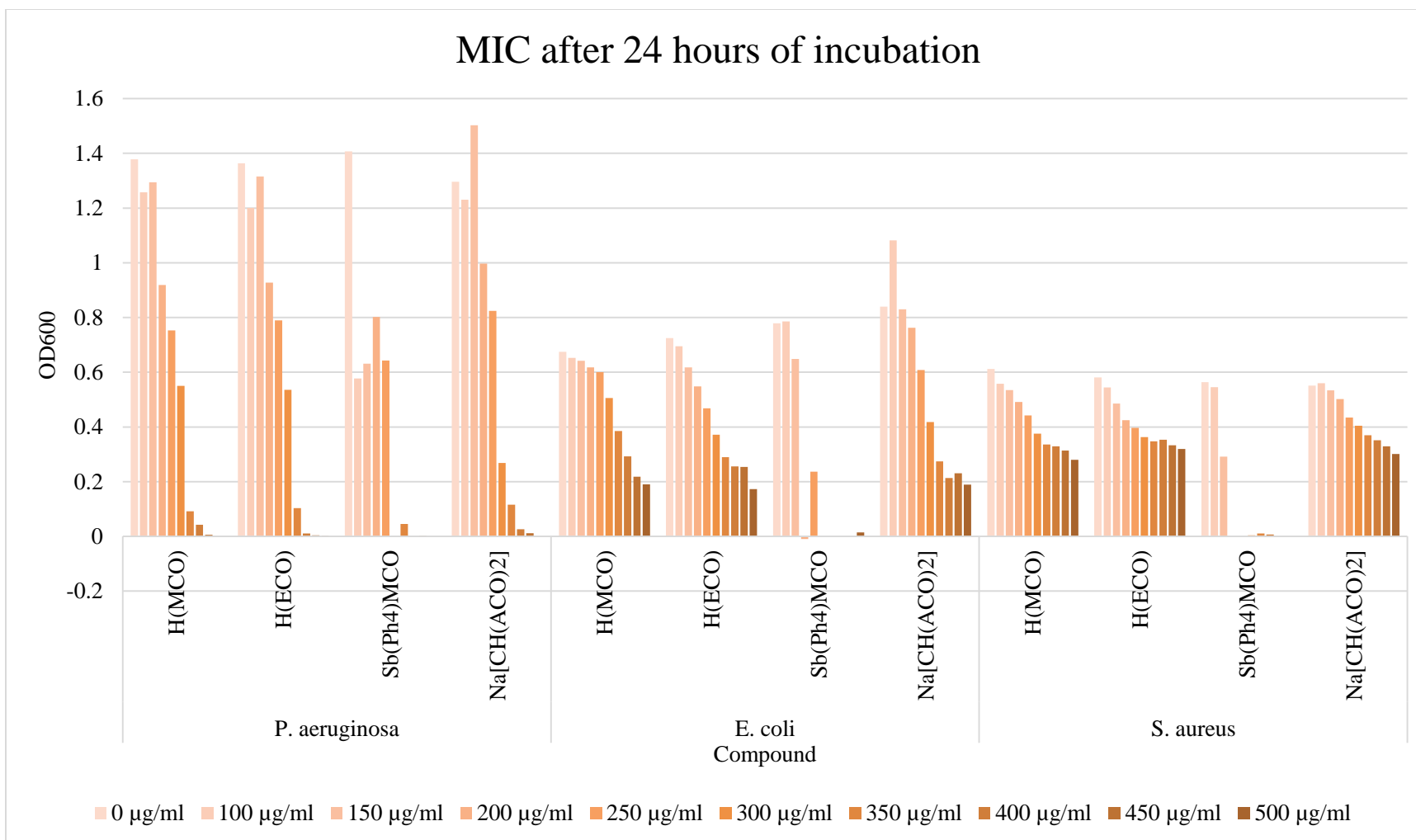


**Figure 59.** Results of initial antimicrobial MIC determination after 24 hours of inoculation with antimicrobial test

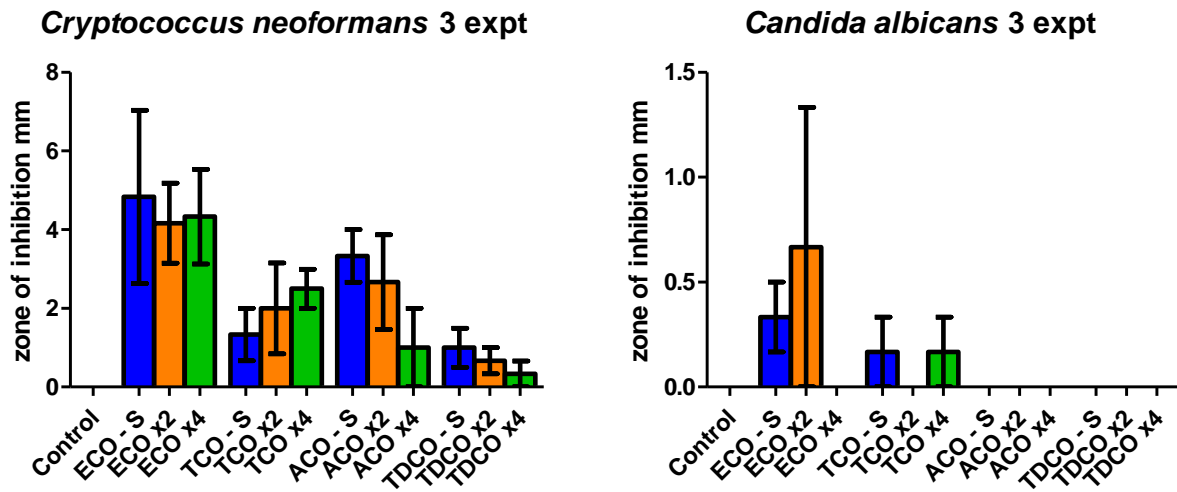


Figure 60. Results of initial disk assays for antifungal activity studies.

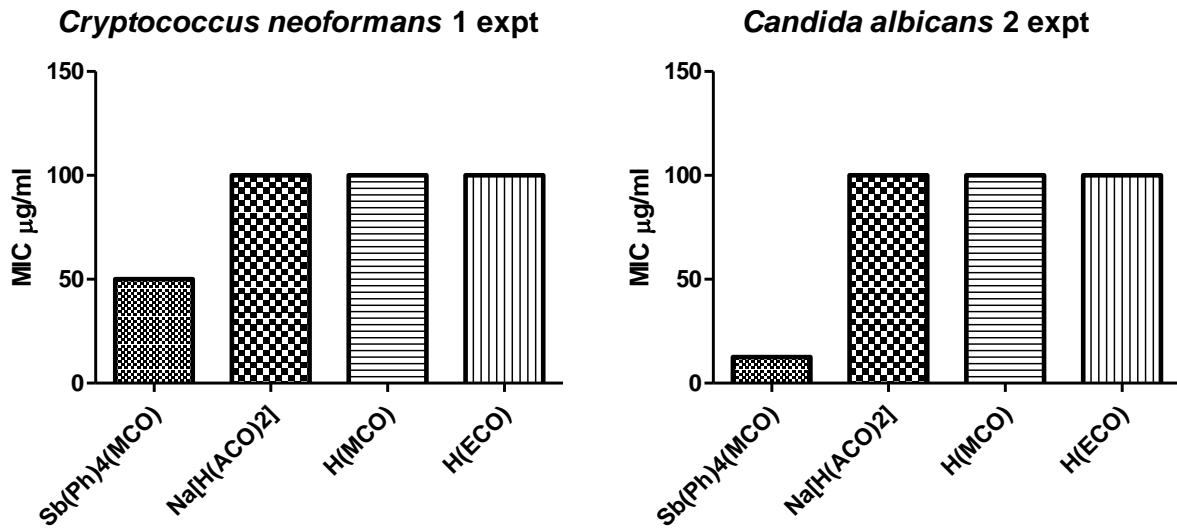
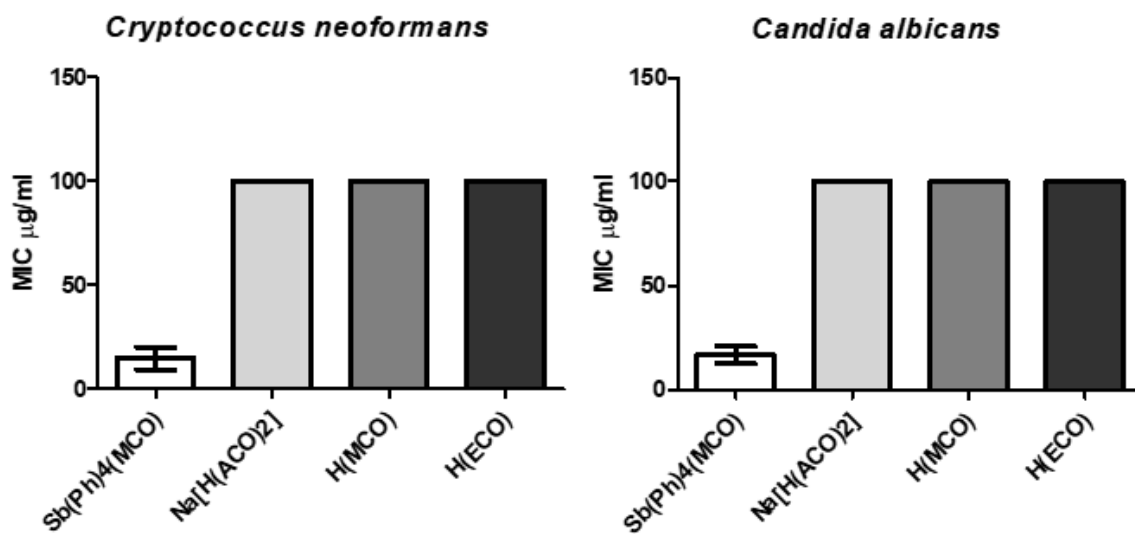


Figure 61. Results of initial MIC assays for antifungal activity studies.





**Figure 62.** Second round of MIC assays for antifungal activity studies.

## VI. CONCLUSIONS AND SUMMARY

This research project has been carried out within the last three years. As the result of conducted investigation all outlined goals at the beginning of this thesis were accomplished. More specific outcomes are presented as *chemical* and *biological* results and listed below.

### Chemical part:

- Several protonated HL cyanoximes, their Ag(I) (for MCO<sup>-</sup>) and Tl(I) (for TCO<sup>-</sup>, TDCO<sup>-</sup> ligands) derivatives have been synthesized and characterized for the purpose of preparation of new organoantimony(V) cyanoximate-containing compounds.
- Synthesized organoantimony(V) cyanoximates were characterized by elemental analysis, TG/DSC analysis, FT-IR, <sup>13</sup>C{<sup>1</sup>H} NMR and, in some cases, variable temperature UV-visible spectroscopy.
- Eight new crystal structures of organoantimony(V) cyanoximates were determined and one previously described in our group compound re-examined second time at low temperature to improve quality of its data. Eight complexes represent mononuclear molecular organometallic compounds and one is a linear μ-oxo dimer with *trans*-positioned cyanoxime moieties (case with ECO<sup>-</sup> ligand).
- Two polymorphs were observed in the Sb(Ph)<sub>4</sub>(TCO) system and their origin relates to the crystallization method. Three structures out of nine contain multiple crystallographically independent molecules in the asymmetric unit (ASU): two in structures of Sb(Ph)<sub>4</sub>(ECO) and Sb(Ph)<sub>4</sub>(MCO) and *eight* in the structure of second polymorph of Sb(Ph)<sub>4</sub>(TCO).
- In all nine organoantimony(V) cyanoximates central atom is in pentavalent state and has distorted trigonal bipyramid environment comprising of four carbon atoms of the phenyl groups and one oxygen atom of the cyanoxime anion bound to a Sb(V) center in a monodentate manner.
- All synthesized compounds are well soluble in common organic solvents and poorly soluble in water and aqueous buffers. All solutions in organic solvents are stable over time and demonstrate negligible dissociation due to ionization at elevated temperatures above 60°C.

### Biological part:

- Two kinds of antimicrobial activity tests were carried out for selected new organoantimony(V) cyanoximates: 1) based on paper disks with solid compounds on solid media determination of zone of inhibition, and 2) determination of the minimal inhibitory concentration (MIC) in solutions of compounds.

- Five Sb(V) cyanoximates: Sb(Ph)<sub>4</sub>(ACO), monomeric Sb(Ph)<sub>4</sub>(ECO), Sb(Ph)<sub>4</sub>(MCO), Sb(Ph)<sub>4</sub>(TCO), and Sb(Ph)<sub>4</sub>(TDCO) were selected at the beginning of antimicrobial and antifungal studies via paper disk susceptibility and MIC assays. The rationale for choices were: a) ACO<sup>-</sup>, ECO<sup>-</sup> and MCO<sup>-</sup> cyanoxime anions possess some water solubility and are rich on oxygen donor atoms; b) TCO<sup>-</sup> and TDCO<sup>-</sup> are thioamides. Therefore, there is a chance of making structure-activity-relationship (SAR) comparing analogous *oxo*- and *thio*- cyanoximes. The control compound was the initial Sb(Ph)<sub>4</sub>Br compound without cyanoximes. Also, pure ligands such as H(MCO), H(ECO) and Na{H(ACO)}<sub>2</sub> without Sb-atoms were used as a second set of controls.
- Antimicrobial paper disk studies indicated that Sb(Ph)<sub>4</sub>(ACO), Sb(Ph)<sub>4</sub>(ECO), have ***significant antimicrobial effect*** against all three employed strains: two gram-negative *Escherichia coli* strain S17 and *Pseudomonas aeruginosa* strain PAO1, alongside a single gram-positive Methicillin-resistant *Staphylococcus aureus* strain NRS70.
- Sb(Ph)<sub>4</sub>(TCO) and Sb(Ph)<sub>4</sub>(TDCO) had ***significant effects*** on the gram- positive Methicillin-resistant *Staphylococcus aureus* strain NRS70, but essentially *no antimicrobial activity* for gram-negative strains used, which we found to be very interesting.
- MIC assay results indicated that free cyanoximes have no antimicrobial effect, but the DMSO solvent used in these assays contributed to the inhibition factor to the MIC assay on cell cultures in solutions.
- Antifungal disk assays were studied with the compounds Sb(Ph)<sub>4</sub>(ACO), Sb(Ph)<sub>4</sub>(ECO), Sb(Ph)<sub>4</sub>(TCO), and Sb(Ph)<sub>4</sub>(TDCO) against the fungi of *Cryptococcus neoformans* and *Candida albicans* strains. Disk assays concluded that Sb(Ph)<sub>4</sub>(ECO) was effective against *Cryptococcus neoformans* and *Candida albicans* in a positive trend. Sb(Ph)<sub>4</sub>(TCO) was the next contributor towards antifungal activity against both strains. Sb(Ph)<sub>4</sub>(ACO) and Sb(Ph)<sub>4</sub>(TDCO) were only effective at inhibition of *Cryptococcus neoformans*, while those compounds did not contribute to any inhibition towards *Candida albicans*.
- Antifungal MIC assays were conducted on the same strains as the disks assays and used the same Sb(V) cyanoximate Sb(Ph)<sub>4</sub>(MCO) along with the free ligands H(MCO), H(ECO), and Na[H(ACO)<sub>2</sub>]. Results indicated that the free, uncomplexed cyanoximes had zero effect on antifungal activity in both replicas of the experiment. On the other hand, Sb(Ph)<sub>4</sub>(MCO) had shown MIC levels ranging from 10 - 50 µg/mL, proving there is ***antifungal activity*** with this organometallic complex.

## VII. FUTURE WORK

The future of using organoantimony(V) cyanoximates as a novel treatment against drug-resistant microbes and fungi is very hopeful. In terms of crystal structures,  $\text{Sb}(\text{Ph})_4(\text{TDCO})$  can be determined. Further antimicrobial and antifungal testing is required to understand how practical Sb(V) cyanoximates are for treatment. Tests would include: a larger variety of ligands both free and Sb(V) coordinated. Testing with the heterocyclic cyanoximes would also be beneficial as expanding the library of biologically active compounds is useful. Progressing with cytotoxicity studies of Sb(V) cyanoximates is in the future, and its result will be detrimental to the development of this promising, new treatment. Given the positive results of certain monodentate ligands in this work, bidentate analogues will be the next step in bringing to life the use as antimicrobials.

## VIII. LITERATURE CITED

- (1) Spellberg, B.: “The antibacterial pipeline: Why is it drying up, and what must be done about it”. In *Antibiotic Resistance: Implications for Global Health and Novel Intervention Strategies – Workshop Summary* The National Academies Press, **2010**.
- (2) CDC. Introduction. *Antibiotic Resistance Threats in the United States, 2019*. Antibiotic Resistance Coordination and Strategy Unit, U.S. Department of Health and Human Services, CDC: Atlanta, GA, 2019; 3.
- (3) Spellberg, B.; Guidos, R.; Gilbert, D.; Bradley, J.; Boucher, H.; Scheld, W.; “ Antibiotic-resistant infections are an epidemic in the United States and Worldwide” In *Resistant Infections*; Miller, D.; Ed.; Greenhaven Press: Farmington Hills, MI, **2009**.
- (4) Allen, A.: “Resistant Infections in Hospitals Kill 90,000 Each Year in the United States.” In *Resistant Infections*; D., M., Ed.; Greenhaven Press: Farmington Hills, MI, **2009**.
- (5) World Health Organization. *Antimicrobial resistance: global report on surveillance 2014*. Geneva: World Health Organization, 2000. ISBN: 978 82 4 156474 8.
- (6) Patrauchan, M. and Salpadoru, T. University of Oklahoma State, Stillwater, OK. Personal communication, 2020.
- (7) Munita, Jose M.; Cesar, A.A. Mechanisms of Antibiotic Resistance. *Microbiology spectrum*. **2016**, 4, 2.
- (8) Wilson DN. Ribosome-targeting antibiotics and mechanisms of bacterial resistance. *Nat Rev Microbiol*. **2014**, 12, 35–48.
- (9) Abraham EP.; Chain E. An enzyme from bacteria able to destroy penicillin. *Nature*. **1940**, 146, 837.
- (10) Schwarz, C.; Froese D.; Zazula, G.; Calmels F.; Debruyne, R.; Golding, G.B.; Poinar, H.N.; Wright, G.D. Antibiotic resistance is ancient. *Nature*. **2011**, 477, 35-48.
- (11) Pagès J.M.; James C.E.; Winterhalter M. The porin and the permeating antibiotic: a selective diffusion barrier in Gram-negative bacteria. *Nat Rev Microbiol*. **2008**, 6, 893–903.

- (12) McMurry L.M.; Petrucci R.E. Jr.; Levy S.B. Active efflux of tetracycline encoded by four genetically different tetracycline resistance determinants in *Escherichia coli*. *Proc Natl. Acad. Sci.* **1980**, *77*, 3974–3977.
- (13) Poole K. Efflux-mediated antimicrobial resistance. *J. Antimicrobial Chemotherapy.* **2005**, *56*, 20– 51.
- (14) Connell S.R.; Tracz D.M.; Nierhaus K.H.; Taylor D.E. Ribosomal protection proteins and their mechanism of tetracycline resistance. *Antimicrob. Agents Chemotherapy.* **2003**, *47*, 3675-3681.
- (15) Projan S.J. Why is big Pharma getting out of antibacterial drug discovery? *Curr Opin Microbiol.* **2003**, *6*, 427–430.
- (16) O’Neill, J. *Antimicrobial Resistance: Tackling a Crisis for the Future Health and Wealth of Nations* [Online]; 2014; pp 1-16. <http://amr-review.org/>, (accessed on May 3<sup>rd</sup>, 2020).
- (17) Alici, E.H.; Gunsel, A.; Bilgicli, A.T.; Jandemir, C.; Mustafa A.; Arabaci, G.; Yarasir, M.N. Comparison of novel tetra-substituted phthalocyanines with their quaternized derivatives: Antioxidant and antibacterial properties. *Synthetic Metals.* **2020**, *260*, 3077-3089.
- (18) Schitter G.; Wrodnigg, T.M. Update on carbohydrate-containing antibacterial agents. *Expert Opinion on Drug Discovery.* **2009**, *4*, 315-356.
- (19) Ford, W.W. The Bacteriological Work of Joseph Lister. *The Scientific Monthly.*, **1928**, *26*, 70–75.
- (20) Kohl, H.H. Antimicrobial activity of N-chloramine compounds. *Journal of Pharmaceutical Sciences.* **1980**, *69*, 1292-1295.
- (21) Nicholas, F.G. *Microbiology of Waterborne Diseases*, second ed; Academic Press: 2014.
- (22) Ghanbar, S.; Kazemian, M.R.; Liu S. New Generation of N-Chloramine/QAC Composite Biocides: Efficient Antimicrobial Agents To Target Antibiotic-Resistant Bacteria in the Presence of Organic Load. *ACS Omega.* **2018**, *3* 9699-9709.
- (23) Sim, W.; Barnard, R.T.; Blaskovich, M.A.T.; Ziora, Z.M. Antimicrobial Silver in Medicinal and Consumer Applications: A Patent Review of the Past Decade (2007-2017). *Antibiotics.* **2018**, *7*, 93.
- (24) Ahonkhai, I.; Pugh, W.J.; Russell, A.D. Sensitivity to antimicrobial agents of some mercury-sensitive and mercury-resistant strains of Gram-negative bacteria. *Current Microbiology.* **1986**, *7*, 183–185.

- (25) Muhammad, M.M.; Muhammad, A.S.; Masood, S.; Sidra, N.; Tayyaba, A.; Muhammad, N.T.; Hafza, M.J.; Muhammad, S.; Saeed, A. (2017) Crystal structure and antimicrobial properties of tetrakis(imidazole)copper(II) triiodide,  $[\text{Cu}(\text{imidazole})_4](\text{I}_3)_2$ . *Inorganic and Nano-Metal Chemistry*. **2017**, 47, 37-40.
- (26) Lefei, J.; Fanghui, L.; Shuting, C.; Chunchun, W.; Huan, W.; Miaoan, Shu.; Caihong, H. Preparation, characterization, antimicrobial and cytotoxicity studies of copper/zinc- loaded montmorillonite. *Journal of animal science and biotechnology*. **2017**, 8.
- (27) Veenstra, D.L.; Saint, S.; Saha, S.; Lumley, T.; Sullivan, S.D. Efficacy of antiseptic-impregnated central venous catheters in preventing catheter-related bloodstream infection - A meta-analysis. *Jama-J. Am. Med. Assoc.* **1999**, 282, 554-560.
- (28) Saint, S.; Elmore, J.G., Sullivan, S.D., Emerson, S.S., Koepsell, T.D. The efficacy of silver alloy-coated urinary catheters in preventing urinary tract infection: A meta-analysis. *Am. J. Med.* **1998**, 105, 236-241.
- (29) Rupp, M.E.; Lisco, S.J.; Lipsett, P.A.; Ped, T.M.; Keating, K.; Civetta, J.M. Effect of a second-generation venous catheter impregnated with chlorhexidine and silver sulfadiazine on central catheter - Related infections - A randomized, controlled trial. *Ann Intern Med.* **2005**, 143, 570-580.
- (30) Eckhardt, S.; Brunetto, P.S.; Gagnon, J.; Priebe, M.; Giese, B.; Fromm, K.M. Nanobio Silver: Its Interactions with Peptides and Bacteria, and Its Uses in Medicine. *Chem. Rev.* **2013**, 113, 4708-4758.
- (31) Kollef, M.H.; Afessa, B.; Anzueto, A.; Veremakis, C.; Kerr, K.M.; Margolis, B.D. Silver-coated endotracheal tubes and incidence of ventilator-associated pneumonia -The NASCENT Randomized Trial. *JAMA-J. Am. Med. Assoc.* **2008**, 300, 805-813.
- (32) Maillard, J.Y.; Hartemann, P. Silver as an antimicrobial: facts and gaps in knowledge. *Crit Rev Microbiol.* **2013**, 39, 373-383
- (33) Randall, C.P.; Gupta, A.; Jackson, N.; Busse, D.; O'Neill, A.J. Silver resistance in Gram-negative bacteria: a dissection of endogenous and exogenous mechanisms. *J. Antimicrobial Chemotherapy.* **2015**, 70, 1037-1046.
- (34) Cabiscol, E.; Piulats, E.; Echave, P.; Herrero, E.; Ros J. Oxidative stress promotes specific protein damage in *Saccharomyces cerevisiae*. *J. Biol. Chem.* **2000**, 275, 27393-27398.
- (35) Holt, K.B.; Bard, A.J. Interaction of silver(I) ions with the respiratory chain of *Escherichia coli*: An electrochemical and scanning electrochemical microscopy study of the antimicrobial mechanism of micromolar Ag. *Biochemistry-US.* **2005**, 44, 13214-13223.
- (36) Sondi, I.; Salopek-Sondi, B. Silver nanoparticles as antimicrobial agent: a case study on *E. coli* as a model for Gram-negative bacteria. *J. Colloid. Interf. Sci.* **2004**, 275, 177-182.

- (37) Cho, K.H.; Park, J.E.; Osaka, T.; Park, S.G. The study of antimicrobial activity and preservative effects of nanosilver ingredient. *Electrochim. Acta.* **2005**, 51, 956-960.
- (38) Cabiscol, E.; Piulats, E.; Echave, P.; Herrero, E.; Ros, J. Oxidative stress promotes specific protein damage in *Saccharomyces cerevisiae*. *J. Biol. Chem.* **2000**, 275, 27393-27398.
- (39) Holt, K.B.; Bard, A.J.; Interaction of silver(I) ions with the respiratory chain of *Escherichia coli*: An electrochemical and scanning electrochemical microscopy study of the antimicrobial mechanism of micromolar Ag. *Biochemistry-US.* **2005**, 44, 13214-23.
- (40) Comstock, M.J. *Platinum, Gold, and Other Metal Chemotherapeutic Agents*. first ed; Lippard S.J. *Chemistry and Biochemistry: American Chemical Society*, ACS Symposium Series; American Chemical Society: Washington DC; 1983; 9-163.
- (41) Cotton, A.F.; Wilkinson, G.; Murillo, C.A.; Bohmann, M. *Advanced Inorganic Chemistry*. sixth ed: John Wiley & Sons, New York; 1999.
- (42) Lippard, S.J.; Jeremy, M.B. *Principles of Bioinorganic Chemistry*. Mill Valley, Calif: University Science Books, 1994.
- (43) Greenwood, N.N.; Earnshaw, A. *Chemistry of the elements*. second ed; Burlington, MA: Butterworth-Heinemann, 1997.
- (44) NNDC; *Nuclear Wallet Cards*, 8th ed. Upton, NY: National Nuclear Data Center, Brookhaven Natl Lab, 2011.
- (45) Cooper, R.G.; Harrison A.P. The exposure to and health effects of antimony. *Indian J. Occup. Environ. Med.* **2009**, 13, 3- 10.
- (46) McCallum, R.I. Occupational exposure to antimony compounds. *J. Environ. Monit.* **2005**, 7, 1245-50.
- (47) Mineral commodity summaries 2020; U.S. Department of the Interior U.S. Geological Survey. U.S. Geological Survey, Reston, VA, 2020.
- (48) Yu-ran L., *Comprehensive handbook of chemical bond energies*. First ed; CRC Press, Boca Raton, FL. 2007.
- (49) Grund, S.C.; Hanusch, K.; Breunig, H. J.; Wolf, H. U. Antimony and Antimony Compounds. *Ullmann's Encyclopedia of Industrial Chemistry.* **2006**.
- (50) Singh, R.V.; Mahajan, K.; Swami, M.; Dawara, L. Microwave Assisted Synthesis, Spectroscopic Characterizations In-Vitro Antibacterial And Antifungal Properties Of Some Antimony And Bismuth Complexes Derived From NnO And NnS Donor Imines. *International Journal of Pharmaceutical Sciences and Research.* **2010**, 33, 141-156.



- (51) Sharma, P.K.; Rehwani, H.; Rai, A.K.; Gupta, R.S.; Singh, Y.P. Antispermatogenic Activity of the Benzothiazoline Ligand and Corresponding Organoantimony(V) Derivative in Male Albino Rats. *Bioinorganic Chemistry & its Applications*. **2006**, 2006, 16895-903.
- (52) Oliveira, L.G.D.; Silva, M.M.; Paula, F.C.S.D.; Pereira-Maia, E.C.; Donnici, C.L.; Simone, C.A.D.; Frézard, F.; Júnior, E.N.D.S.; Demicheli, C. Antimony(V) and Bismuth(V) Complexes of Lapachol: Synthesis, Crystal Structure and Cytotoxic Activity. *Molecules*. **2011**, 16, 10314-10323.
- (53) Haiduc, I. and Silvestru, C. *Organometallics in Cancer Therapy*. first ed; Boca Raton, FL: CRC, 1989.
- (54) Khan, N.U.H.; Sultana, K.; Nadeem, H. Synthesis, Characterization and Antibacterial Activity of New Antimony (III) Complexes of Some Tosyl-Sulfonamide Derivatives. *Middle-East Journal of Scientific Research*. **2013**, 16, 1109-1115.
- (55) Agrawal, R.; Sharma, J.; Nandani, D.; Batra, A.; Singh, Y. Triphenylarsenic(V) and antimony(V) derivatives of multidentate Schiff bases: Synthesis, characterization, and antimicrobial activities. *Journal of Coordination Chemistry*. **2011**, 64, 554-563.
- (56) Silvestru, C.; Silaghi-Dumitrescu, L.; Haiduc, I.; Begley, M. J.; Nunn, M.; Sowerby, D. B. Synthesis of diphenylantimony(III) dialkyldithio- and diaryldithio-phosphinates and -arsinates; Crystal structures of  $\text{Ph}_2\text{SbS}_2\text{MPh}_2$  (M = P or As). *J. Chem. Soc. Dalton Trans*. **1986**, 1031.
- (57) Silvestru, C.; Curtui, M.; Haiduc, I.; Begley, M. J.; Sowerby, D. B. Phenylantimony(III) diorganophosphorodithioates: the crystal structure of diphenylantimony(III) diisopropylphosphorodithioate,  $\text{Ph}_2\text{SbS}_2\text{P}(\text{OiPr})_2$ ; unusual polymerisation through semibonding. *J. Organomet. Chem*. **1992**, 426, 49.
- (58) Silvestru, C.; Haiduc, I.; Tiekink, E.; De Vos, D.; Biesemans, M.; Willem, P.; Gielen, M. Synthesis, structural characterization and in vitro antitumour properties of triorganoantimony(V) disalicylates: Crystal and molecular structures of  $[\text{5-Y-2-(ho)-C}_6\text{H}_3\text{COO}]_2\text{SbMe}_3$  (Y=H, Me, MeO). *Appl. Organomet. Chem*. **1995**, 9, 597-607.
- (59) Silvestru, C.; Socaciu, C.; Bara, A.; Haiduc, I. The first organoantimony(III) compounds possessing antitumor properties: diphenylantimony(III) derivatives of dithiophosphorus ligands. *Anticancer Research*. **1990**, 10, 803-804.
- (60) Domasevitch, K.V.; Gerasimchuck, N.N.; Mokhir, A.A. *Inorg. Chem*. **2000**, 39, 1227-1237.
- (61) Haldar, A.; Sen, P.; Roy, S. Use of Antimony in the Treatment of Leishmaniasis: Current Status and Future Directions. *Molecular biology international*. **2011**.

- (62) Vianna, G. Tratamento da leishmaniose tegumentar por injeções intravenosas de tetrartarato em éetico, 7 Congresso Brasileiro de Medicina Tropical de São Paulo. **1912**, 4,426–428.
- (63) Brahmachari, U.N. Chemotherapy of antimonial compounds in kala-azar infection. Part IV. Further observations on the therapeutic values of urea stibamine. *The Indian Journal of Medical Research*. **1989**, 89, 393–404.
- (64) Brahmachari, U.N. A new form of cutaneous leishmaniasis, dermal leishmanoid. *Indian Medical Gazette*. **1922**, 57, 25–127.
- (65) Brahmachari, U.N. A Treatise on Kala.azar, *J. Bale. Sons Danielsson*. **1928**.
- (66) Kikuth, W.; Schmidt, H. Contribution to the progress of antimony therapy of kala-azar. *Chinese Medical Journal*. **1937**, 52, 425–432.
- (67) Goodwin, L.G. Pentostam (sodium stibogluconate); a 50- year personal reminiscence. *Transactions of the Royal Society of Tropical Medicine and Hygiene*. **1995**, 89, 339–341.
- (68) Shaked-Mishan, P.; Ulrich, N.; Ephros, M.; Zilberstein, D. Novel intracellular SbV reducing activity correlates with antimony susceptibility in *Leishmania donovani*. *J. Biol. Chem.* **2001**, 276, 3971-3976
- (69) Ferreira, C.D.S.; Martins, P.S.; Demicheli, C.; Brochu C.; Ouellette M.; Frezard, F. Thiol-induced reduction of antimony(V) into antimony(III): a comparative study with trypanothione, cysteinyl-glycine, cysteine and glutathione. *BioMetals*. **2003**, 16, 441–446.
- (70) Frezard, F.; Demicheli, C.; Ferreira, C.S.; Costa, M.A.P. Glutathione-induced conversion of pentavalent antimony to trivalent antimony in meglumine antimoniate. *Antimicrobial Agents and Chemotherapy*. **2001**, 45, 913–916.
- (71) Yan, S.; Li, F.; Ding, K.; Sun, H. Reduction of pentavalent antimony by trypanothione and formation of a binary and ternary complex of antimony(III) and trypanothione. *Journal of Biological Inorganic Chemistry*. **2003**, 8, 689–697.
- (72) Mego, J.L. Stimulation of intralysosomal proteolysis by cysteinyl-glycine, a product of the action of  $\gamma$ -glutamyl transpeptidase on glutathione. *Biochimica et Biophysica Acta*. **1985**, 841, 139–144.
- (73) D. Gainey, S. Short, and K. L. McCoy, Intracellular location of cysteine transport activity correlates with productive processing of antigen disulfide. *Journal of Cellular Physiology*. **1996**, 2, 248–254.
- (74) Ge, R.; Sun, H. Bioinorganic Chemistry of Bismuth and Antimony: Target Sites of Metallodrugs. *Accounts of Chemical Research*. **2007**, 40, 267-274.

- (75) Chai, Y.; Yan, S.; Wong, I.L. K.; Chow, L.M.C.; Sun, H. Complexation of antimony (SbV) with guanosine 5'-monophosphate and guanosine 5'-diphospho-d-mannose: Formation of both mono- and bis-adducts. *J. Inorg. Biochem.* **2005**, *99*, 2257- 2263.
- (76) Krauth-Siegel, R.L.; Comini M.A. Redox control in trypanosomatids, parasitic protozoa with trypanothionebased thiol metabolism. *Biochimica et Biophysica Acta.* **2008**, *1780*, 1236–1248.
- (77) Meister, L.; Anderson, M.E. Glutathione. *Annual Review of Biochemistry.* **1983**, *52*, 711–760.
- (78) Webb, J.R.; McMaster, W.R. Molecular cloning and expression of a Leishmania major gene encoding a singlestranded DNA-binding protein containing nine 'CCHC' zinc finger motifs. *Journal of Biological Chemistry.* **1993**, *268*, 13994–14002.
- (79) Leon, O.; Roth, M. Zinc fingers: DNA binding and protein-protein interactions. *Biol. Res.* **2000**, *33*, 21-30
- (80) Demicheli, C.; Frézard, F.; Mangrum, J.B.; Farrell, N.P. Interaction of trivalent antimony with a CCHC zinc finger domain: potential relevance to the mechanism of action of antimonial drugs. *Chem. Commun.* **2008**; *39*, 4828-4830.
- (81) Frézard, F. Pentavalent antimonials: new perspectives for old drugs. *Molecules.* **2009**, *14*, 2317-36.
- (82) Halford, B. An emerging antiviral takes aim at COVID-19. *Chemical & Engineering News*, **2020**, 22-23.
- (83) Paliy G. K., Skopenko V. V.; Gerasimchuk N. N.; Makats E. F.; Domashevskaya O. A.; Rakovskaya R. V. Bis-(Nitrosothiocarbamylcyanmethanide) copper(II) or nickel(II) which exhibit antimicrobial activity. USSR patent, 1405282, **1988**
- (84) Ilkun, O.T.; Archibald, S.J.; Barnes, C.L.; Gerasimchuk, N.; Biagioni, R.; Silchenko, S.; Gerasimchuk, O.A.; Nemykin, V.N. Benz(2-heteroaryl)cyanoximes and their Tl(I) complexes: New Room Temperature Blue Emitters. *The Royal Society of Chemistry, Dalton Trans.* **2008**, 5715–5729.
- (85) Robertson, D.R.; Cannon, J.F.; Gerasimchuk, N.N. Double-Stranded Metal-Organic Networks for One dimensional Mixed Valence Coordination Polymers. *Inorganic Chemistry.* **2005**, *44*, 8326–8342.
- (86) Gerasimchuk, N.N.; Kuzmann, E.; Buki, A.; Vertes, A.; Nagy, L.; Burger, K. "Synthesis, IR-, Mossbauer studies of Eu<sup>3+</sup> complexes formed with cyanoxime anions." *Inorganica Chimica Acta.* **1991**, *188*, 45-50

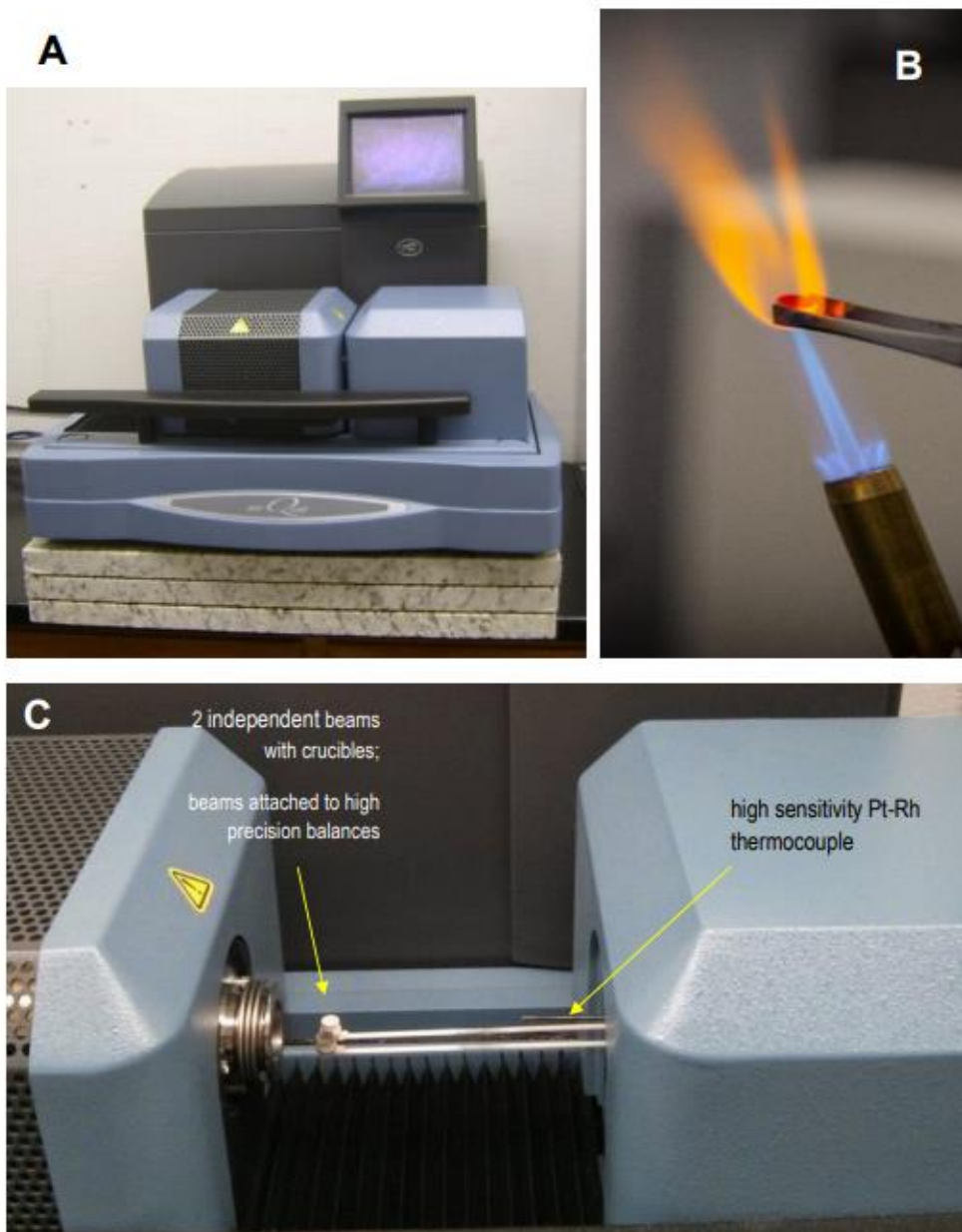
- (87) Gerasimchuk, N.N.; Bowman-James, K. Mixed Donor Ligands. *Encyclopedia of Inorganic Chemistry*. **1994**, 5, 2254 – 2270.
- (88) Cheadle, C.; Gerasimchuk, N.N.; Barnes, C.L.; Tyukhtenko, S.I.; Silchenko, S. The first bis-cyanoxime: Synthesis and properties of a new versatile and accessible polydentate bifunctional building block for coordination and supramolecular chemistry. *Dalton Transaction*. **2013**, 42, 4931-4946.
- (89) Sidman, J.W. Electronic and vibrational states of the nitrite ion. I. electronic states. *Journal of American Chemical Society*, **1957**, 79(11), 2669-2675.
- (90) Gerasimchuk, N. Chemistry and Applications of Cyanoximes and Their Metal Complexes. *Dalton Transactions*. **2019**, 48, 7985–8013.
- (91) Mokhir, A.A.; Domasevich, K.V.; Dalley, N.K.; Kou, X.; Gerasimchuk, N.N.; Gerasimchuk, O.A. Syntheses, crystal structures and coordination compounds of some 2-hetarylcyanoximes. *Inorganica Chimica Acta*, **1999**, 284, 85- 89.
- (92) Ponomareva, V.V.; Dalley, N.K.; Kou, X.; Gerasimchuk, N.N.; Domasevitch, K.V. Synthesis, spectra and crystal structures of complexes of ambidentate C<sub>6</sub>H<sub>5</sub>C(O)C(NO)CN-. *Journal of Chemical Society, Dalton Transaction*. **1996**, 11, 2351-2359.
- (93) Davidson, S. H. 2-Cyano-2-hydroximinoacetamides as plant disease control agents. Patent of the USA #3957847, **1978**. (b) Skopenko, V.V.; Pali, G. K.; Gerasimchuk, N.N.; Makats, E.F.; Domashevskaya, O.A.; Rakovskaya, R.V. Nitrosothiocarbamylcyanmethanid of potassium or sodium which show antimicrobial activity. Patent of the USSR #1405281, 1988. (c) Pali, G.K.; Skopenko, V.V.; Gerasimchuk, N.N.; Makats, E.F.; Domashevskaya, O.A.; Rakovskaya, R.V. Bis-(Nitrosothiocarbamylcyanmethanid) copper(II) or nickel(II) which exhibit antimicrobial activity. Patent of the USSR, #1405282, 1988.
- (94) Skopenko, V. V.; Pali, G. K.; Gerasimchuk, N. N.; Domashevskaya, O. A.; Makats, E. F. Di-(Nitrosothiocarbamylcyanmethanid)-di-(pyridine)-copper which shows bacteriostatic activity towards Staphylococcus Aureus, and method of preparation of the complex. Patent of the USSR, #1487422, 1989.
- (95) Lin, K. Process for making 2-cyano-2-hydroximinoacetamide salts. Patent of the USA #3919284, 1976. (b) Kuhne, A.; Hubele, A. Method for the cultivation of plants employing R-cyano-hydroximinoacetamide derivatives. Patent of the USA #4063921, 1978
- (96) Ciba Geigy A.G. Srodek ochrony Roslin przed dzialaniem agresywnych chemikalii rolniczych. Patent of Poland #127786, 1985. (b) Ciba Geigy AG. Mittel zum Schutz von Kulturpflanzen von aggressiven Herbiziden. Patent of Austria #367268, 1982
- (97) Eddings, D.; Barnes, C.; Durham, P.; Gerasimchuk, N.N.; Domasevich, K.V. *Inorg. Chem.* **2004**, 43, 3894–3909.

- (98) Gerasimchuk, N.; Maher, T.; Durham, P.; Domasevitch, K.; Wilking, J.; Mokhir, A. *Inorg. Chem.* **2007**, 46, 7268–7284.
- (99) Gerasimchuk, N.; Goeden, L.; Durham, P.; Barnes, C. L.; Cannon, J. F.; Silchenko, S.; Hidalgo, 65I. *Inorg. Chim. Acta* **2008**, 361, 1983–2001.
- (100) Paliy, G.K.; Skopenko, V.V.; Gerasimchuk, N.N.; Domashevskaya, O.A.; Makats, E.F.; Rakovskaya, R.V. Patent of the USSR #1405281, 1988.
- (101) Gerasimchuk, N.; A. Gamian, A.; Glover G.; Szponar B. Light Insensitive Silver(I) Cyanoximates As Antimicrobial Agents for Indwelling Medical Devices, *Inorg. Chem.* **2010**, 49, 9863–9874.
- (102) Riddles, C.N.; Whited, M.; Lotlikar, S.R.; Still, K.; Patrauchan, M; Silchenko, S.;Gerasimchuk, N. Synthesis and characterization of two cyanoxime ligands, theirprecursors, and light insensitive antimicrobial silver(I) cyanoximates. *Inorganica Chimica Acta.* **2014**, 11, 94-103.
- (103) Gerasimchuk, N.; Esaulenko, A.N.; Dalley, K.N.;Moore, C. 2-Cyano-2-isonitrosoacetamide and its Ag(I) complexes. Silver(I) cyanoximate as a non-electric gas sensor. *Dalton Transaction*, **2010**, 39, 749-764.
- (104) K. V. Domasevitch , V. V. Skopenko and E. B. Rusanov , *Z. Naturforsch*, **1996**, 51b , 832-837.
- (105) Gerasimchuk, N.; Goeden, L.; Durham, P.; Barnes, C.; Cannon, J.F. Synthesis and Characterization of the First Disubstituted Aryl cyanoximes and their Several Metal Complexes. *Inorganica Chimica Acta.* **2008**, 361, 1983-2001.
- (106) Gerasimchuk, N.N.; Tchernega, A.N., Kapshuk. A.A. Synthesis, IR spectra and structure of complex Tl(I) with carbamoylcyanoxime HONC(CN)C(O)NH<sub>2</sub>. *Russian Journal of Inorganic Chemistry.* **1993**, 38, 1530-1534.
- (107) Lin, M.; Lin, Y.; Lan, C. Minimal Inhibitory Concentration (MIC) Assay for *Acinetobacter baumannii*. *Bio-protocol.* **2014**, 4.
- (108) SHELXTL, Crystallographic Software Package, version 5.1.
- (109) Sheldrick, G. M., **2002**. TWINABS. Bruker-AXS, Madison, Wisconsin, USA.
- (110) Burnett, M.N., & Johnson, C.K., **1996**. OR TEP-III: Oak Ridge Thermal Ellipsoid Plot Program for Crystal Structure Illustration, Oak Ridge National Laboratory Report ORNL-6895.

- (111) Macrae, C.F, Edginton, P.R., McCabe, P., Pidcock, E., van de Streek, J, Bruno, I.J., Taylor, R., Chisholm, J.A., & Wood, P.A. ,**2008**. Mercury CSD 2.0 – New Features for the Visualization and Investigation of Crystal Structures. *Journal of Applied Crystallography*, 41, 466 – 470.
- (112) Marcano, D. Pyridylcyanoximes and Their Metal Complexes M.S. Thesis, Missouri State University, Springfield, MO. 2007.
- (113) Opalade, A. The Synthesis And Characterization Of Ni(II) And Cu(II) Cyanoximates M.S. Thesis, Missouri State University, Springfield, MO. 2016.
- (114) K.V. Domasevitch, Ph.D. dissertation. Synthesis and studies of donor properties of new acido-ligands of the cyanoxime-type. Kiev, **1993**, 170 pp.
- (115) Кочешков, К.А.; Сколдинов, А.П.; Землянский, Н.М. «Методы элементарной органической химии. Сурьма, висмут». **1976**, Наука, 483 стр.
- (116) Gerasimchuk, N.N. Missouri State University, Springfield, MO. Personal communication, 2020.
- (117) Gerasimchuk, N.; Guzei, I.; Sipos, P. Structural Peculiarities of Cyanoximes and their Anions: Co-crystallization of Two Diastereomers and Formation of Acid-salts. *Current Inorganic Chemistry*. **2015**, 5, 38-63.
- (118) Morton, J.; Dennison, R.; Nemykin, V.; Gerasimchuk, N. Planochromism of cyanoxime anions: Computational and mechanistic studies in solid state and solutions. *Inorganica Chimica Acta*. **2020**, 507.

## **APPENDICES**

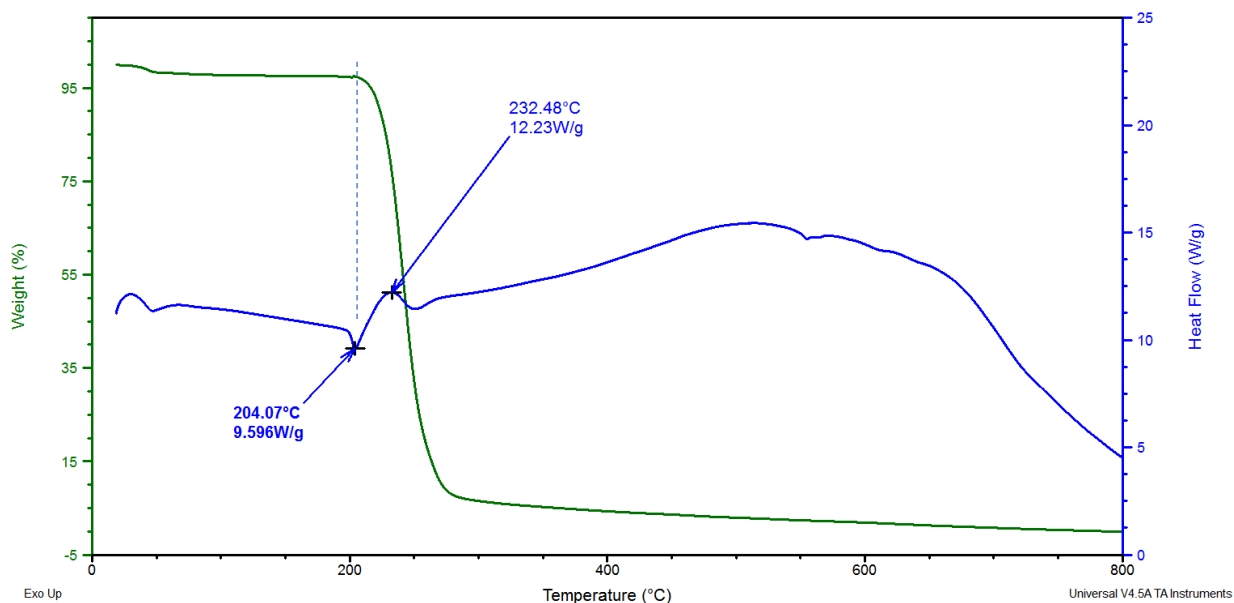
### **Appendix A. Instrumentation of TG/DSC Analysis**



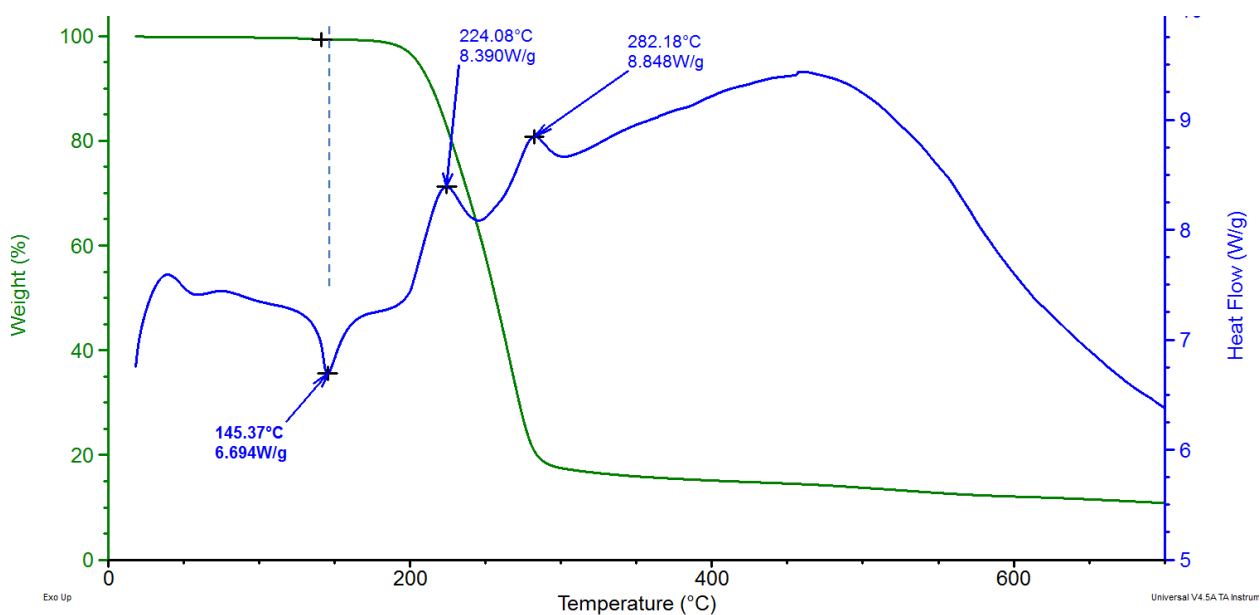
**Appendix A-1.** A – general view of the thermal analyzer showing blow torch used for crucible cleaning and tools; B – cleaning of alumina crucible with flame; C – opened furnace view showing two beams with alumina crucibles for differential analysis.

**Appendix B. Traces of TG/DSC analyses.**

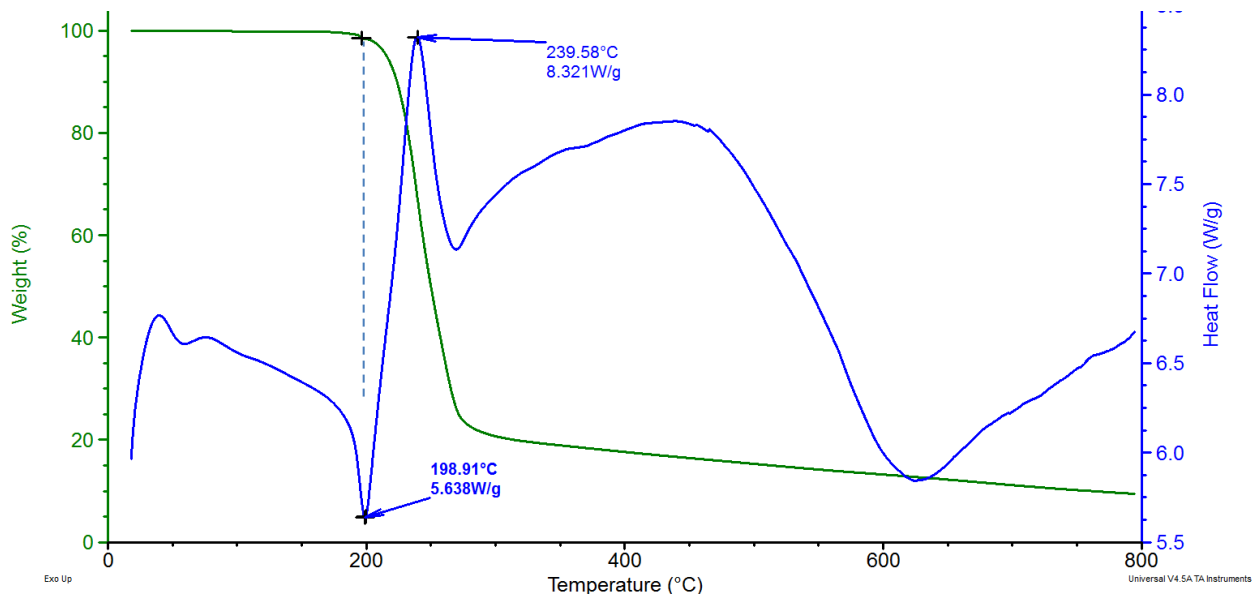




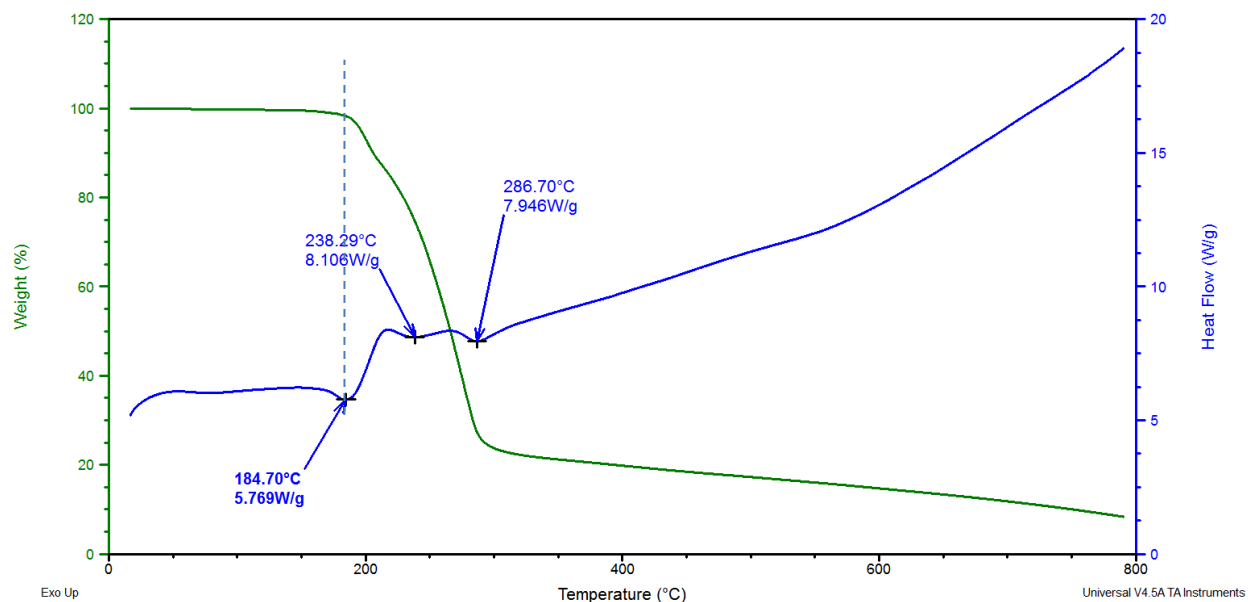
**Appendix B-1.** TG/DSC traces for a sample of  $\text{SbPh}_4(2\text{PCO})$  showing compounds melting with rapidly following decomposition.



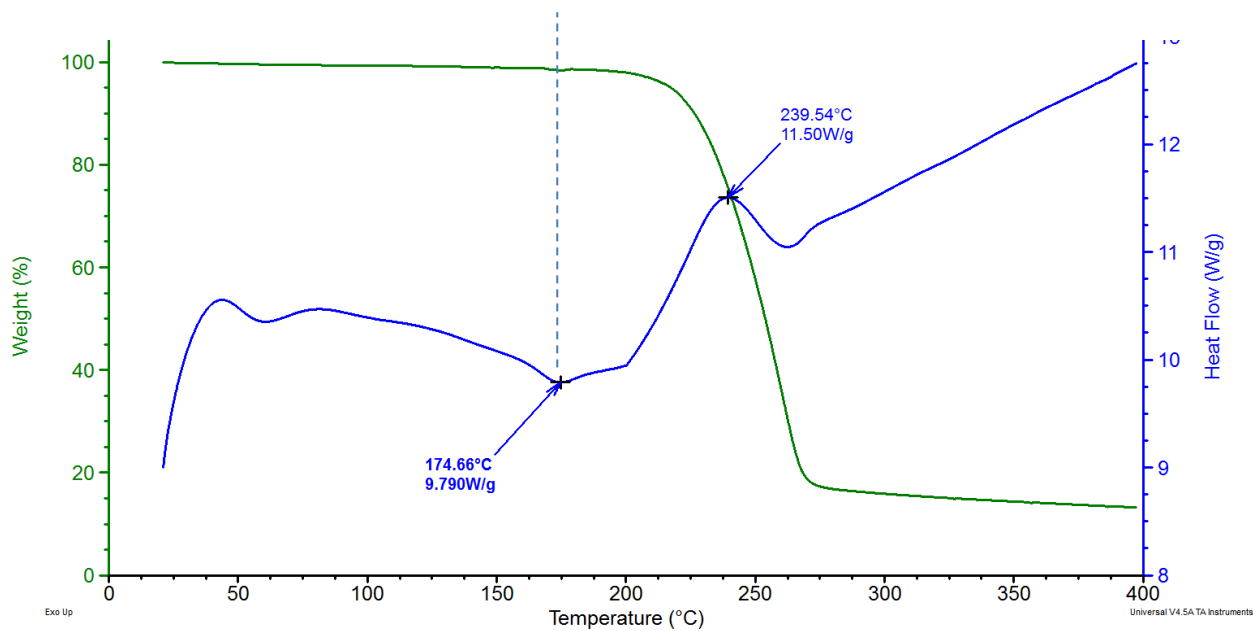
**Appendix B-2.** TG/DSC traces for a sample of  $\text{SbPh}_4(4\text{PCO})$  showing compounds melting followed by decomposition.



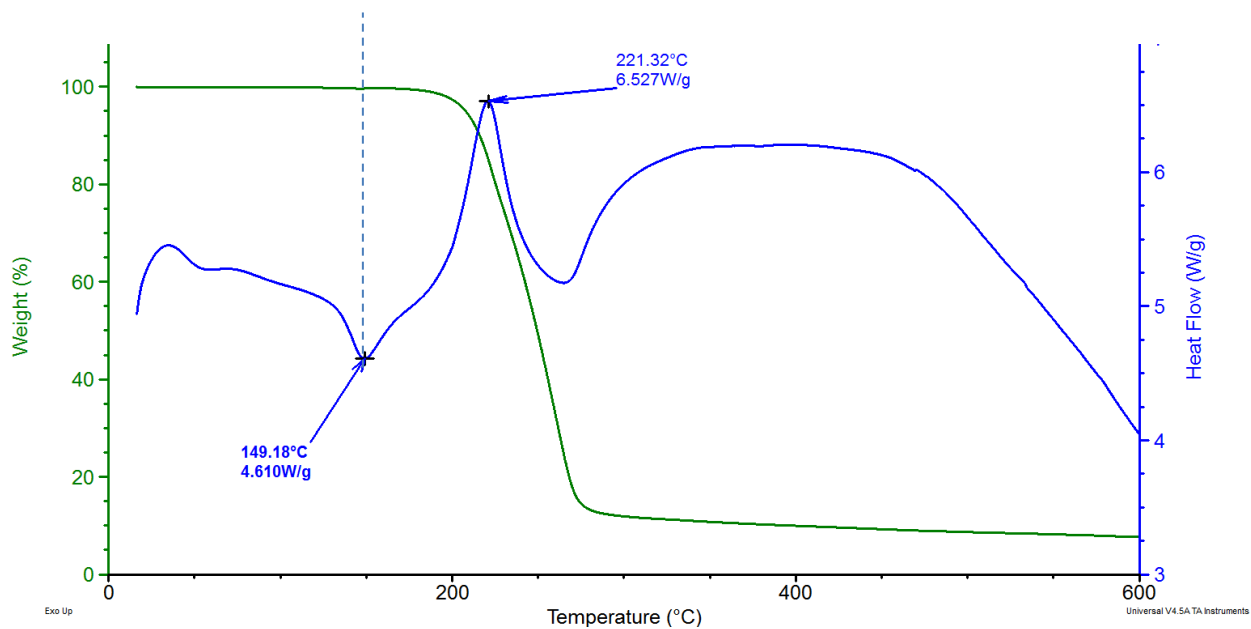
**Appendix B-3.** TG/DSC traces for a sample of SbPh<sub>4</sub>(ACO) showing compounds melting with rapidly following decomposition.



**Appendix B-4.** TG/DSC traces for a sample of SbPh<sub>4</sub>(TCO) showing compounds melting with rapidly following decomposition.



**Appendix B-5.** TG/DSC traces for a sample of SbPh<sub>4</sub>(MCO) (in usable range) showing compounds melting followed by decomposition.



**Appendix B-6.** TG/DSC traces for a sample of SbPh<sub>4</sub>(TDCO) (in usable range) showing compounds melting followed by decomposition.

## Appendix C. Crystal checkCIF Reports for Studied Complexes

Appendix C-1. checkCIF-reports for Sb(Ph)<sub>4</sub>(ACO).

### checkCIF/PLATON (basic structural check)

---

*Structure factors have been supplied for datablock(s) Sb-pH4-ACO*

THIS REPORT IS FOR GUIDANCE ONLY. IF USED AS PART OF A REVIEW PROCEDURE FOR PUBLICATION, IT SHOULD NOT REPLACE THE EXPERTISE OF AN EXPERIENCED CRYSTALLOGRAPHIC REFEREE.

No syntax errors found.

Please wait while processing ....

report

Structure factor report

CIF dictionary

Interpreting this

### Datablock: Sb-Ph4-ACO

---

Bond precision: C-C = 0.0034 Å      Wavelength=0.71073

Cell:            a=14.8336(8) b=9.9060(6)      c=17.3977(10)

                alpha=90      beta=112.713(1) gamma=90

Temperature: 120 K

	Calculated	Reported
Volume	2358.2(2)	2358.2(2)
Space group	P 21/c	P 21/c
Hall group	-P 2ybc	-P 2ybc
Moiety formula	C27 H22 N3 O2 Sb	C27 H22 N3 O2 Sb
Sum formula	C27 H22 N3 O2 Sb	C27 H22 N3 O2 Sb
Mr	542.24	542.22
Dx, g cm <sup>-3</sup>	1.527	1.527
Z	4	4
Mu (mm <sup>-1</sup> )	1.199	1.199
F000	1088.0	1088.0
F000'	1086.02	
h, k, lmax	22, 15, 26	22, 15, 26
Nref	8912	8465
Tmin, Tmax	0.864, 0.901	0.648, 0.953
Tmin'	0.839	

Correction method= # Reported T Limits:

Tmin=0.648 Tmax=0.953 AbsCorr = NUMERICAL

Data completeness= 0.950 Theta(max)= 33.019

R(reflections)= 0.0288(      wR2(reflections)= 0.0726(  
7070)                      8465)

S = 1.172                  Npar= 386

The following ALERTS were generated. Each ALERT has the format  
**test-name\_ALERT\_alert-type\_alert-level.**  
Click on the hyperlinks for more details of the test.

---

**●Alert level B**

[PLAT919](#) ALERT 3 B Reflection # Likely Affected by the Beamstop ... 1  
Check  
[PLAT934](#) ALERT 3 B Number of (Iobs-Icalc)/Sigma(W) > 10 Outliers .. 8  
Check

---

**●Alert level C**

[PLAT094](#) ALERT 2 C Ratio of Maximum / Minimum Residual Density .... 2.71  
Report  
[PLAT420](#) ALERT 2 C D-H Without Acceptor N3 --H2N3 . Please  
Check  
[PLAT971](#) ALERT 2 C Check Calcd Resid. Dens. 2.26A From C5 1.62  
eA-3

---

**●Alert level G**

[PLAT164](#) ALERT 4 G Nr. of Refined C-H H-Atoms in Heavy-Atom Struct. 20  
Note  
[PLAT720](#) ALERT 4 G Number of Unusual/Non-Standard Labels ..... 2  
Note  
[PLAT883](#) ALERT 1 G No Info/Value for \_atom\_sites\_solution\_primary . Please  
Do !  
[PLAT912](#) ALERT 4 G Missing # of FCF Reflections Above STh/L= 0.600 447  
Note  
[PLAT941](#) ALERT 3 G Average HKL Measurement Multiplicity ..... 4.5  
Low  
[PLAT965](#) ALERT 2 G The SHELXL WEIGHT Optimisation has not Converged Please  
Check  
[PLAT978](#) ALERT 2 G Number C-C Bonds with Positive Residual Density. 4  
Info

---

0 **ALERT level A** = Most likely a serious problem - resolve or explain  
2 **ALERT level B** = A potentially serious problem, consider carefully  
3 **ALERT level C** = Check. Ensure it is not caused by an omission or  
oversight  
7 **ALERT level G** = General information/check it is not something unexpected

1 ALERT type 1 CIF construction/syntax error, inconsistent or missing data  
5 ALERT type 2 Indicator that the structure model may be wrong or  
deficient  
3 ALERT type 3 Indicator that the structure quality may be low  
3 ALERT type 4 Improvement, methodology, query or suggestion  
0 ALERT type 5 Informative message, check

---

**PLATON version of 04/06/2020; check.def file version of 02/06/2020**  
**Datablock Sb-Ph4-ACO - ellipsoid plot**

---

**Appendix C-2.** checkCIF-reports for Sb(Ph)<sub>4</sub>(2PCO).

---

## checkCIF/PLATON (basic structural check)

---

*Structure factors have been supplied for datablock(s) Sb-Ph4-2pc*

THIS REPORT IS FOR GUIDANCE ONLY. IF USED AS PART OF A REVIEW PROCEDURE FOR PUBLICATION, IT SHOULD NOT REPLACE THE EXPERTISE OF AN EXPERIENCED CRYSTALLOGRAPHIC REFEREE.

No syntax errors found.

Please wait while processing ....  
report

CIF dictionary  
Interpreting this

Structure factor report

### Datablock: Sb-Ph4-2PCO

---

Bond precision: C-C = 0.0044 Å      Wavelength=0.71073

Cell:            a=12.6027(8) b=14.4415(10)      c=14.6694(10)  
                 alpha=90      beta=104.9644(10) gamma=90

Temperature: 100 K

	Calculated	Reported
Volume	2579.3(3)	2579.3(3)
Space group	P 21/n	P 21/n
Hall group	-P 2yn	-P 2yn
Moiety formula	C31 H24 N3 O Sb	C31 H24 N3 O Sb
Sum formula	C31 H24 N3 O Sb	C31 H24 N3 O Sb
Mr	576.29	576.28
Dx, g cm <sup>-3</sup>	1.484	1.484
Z	4	4
Mu (mm <sup>-1</sup> )	1.098	1.098
F000	1160.0	1160.0
F000'	1158.02	
h, k, lmax	15, 18, 18	15, 18, 18
Nref	5461	5458
Tmin, Tmax	0.846, 0.912	0.872, 0.949
Tmin'	0.829	

Correction method= # Reported T Limits:

Tmin=0.872 Tmax=0.949 AbsCorr = NUMERICAL

Data completeness= 0.999 Theta(max)= 26.710

R(reflections)= 0.0329(      wR2(reflections)= 0.0792(  
4414)                              5458)

S = 1.039                      Npar= 421

---

The following ALERTS were generated. Each ALERT has the format

**test-name\_ALERT\_alert-type\_alert-level.**

Click on the hyperlinks for more details of the test.

---

### ● Alert level C

<a href="#">PLAT094 ALERT 2 C</a>	Ratio of Maximum / Minimum Residual Density ....	3.47
Report		
<a href="#">PLAT245 ALERT 2 C</a>	U(iso) H7                    Smaller than U(eq) C7                    by	0.013
Ang**2		
<a href="#">PLAT245 ALERT 2 C</a>	U(iso) H24                    Smaller than U(eq) C24                    by	0.012
Ang**2		
<a href="#">PLAT350 ALERT 3 C</a>	Short C-H (X0.96,N1.08A) C22                    - H22                    .	0.84
Ang.		
<a href="#">PLAT975 ALERT 2 C</a>	Check Calcd Resid. Dens. 1.06A                    From O1	0.43
eA-3		

---

### ● Alert level G

<a href="#">PLAT164 ALERT 4 G</a>	Nr. of Refined C-H H-Atoms in Heavy-Atom Struct.	24
Note		
<a href="#">PLAT883 ALERT 1 G</a>	No Info/Value for _atom_sites_solution_primary .	Please
Do !		
<a href="#">PLAT912 ALERT 4 G</a>	Missing # of FCF Reflections Above STh/L= 0.600	3
Note		
<a href="#">PLAT965 ALERT 2 G</a>	The SHELXL WEIGHT Optimisation has not Converged	Please
Check		
<a href="#">PLAT978 ALERT 2 G</a>	Number C-C Bonds with Positive Residual Density.	7
Info		

---

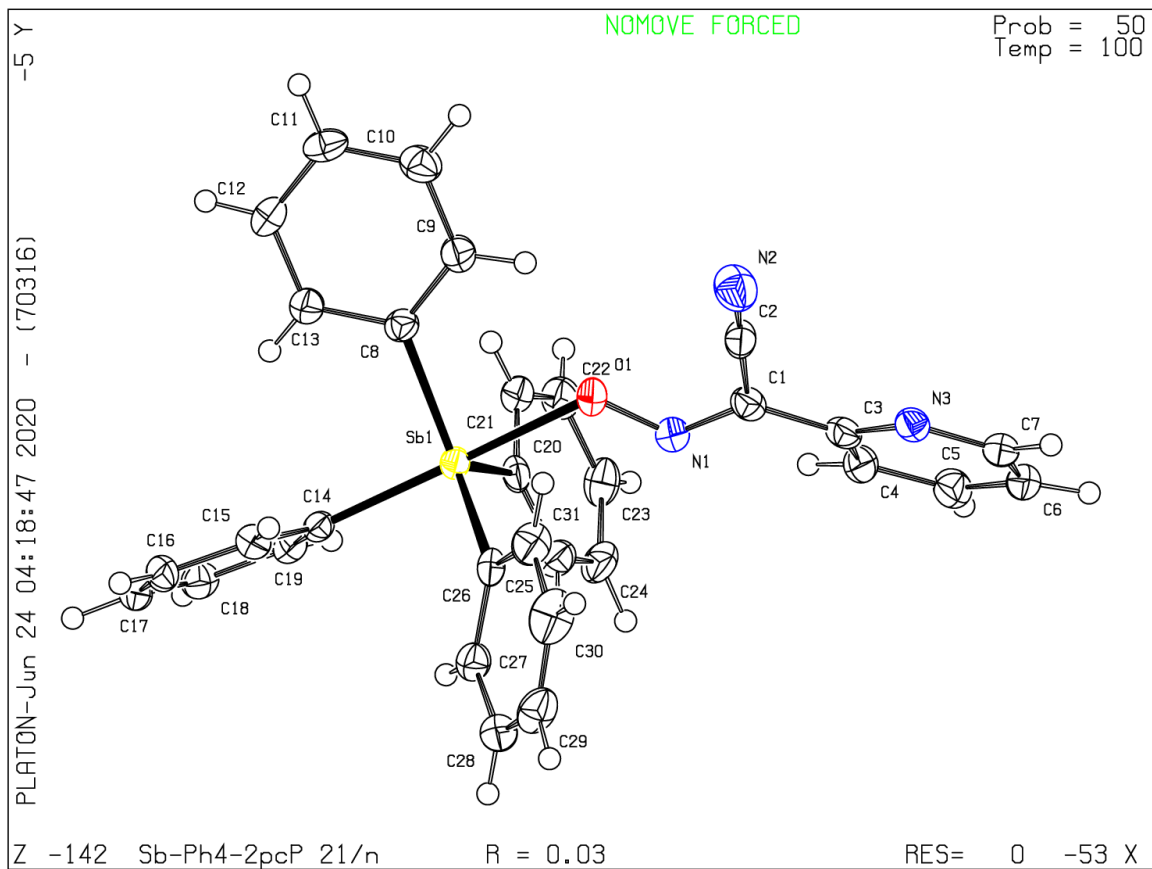
0 **ALERT level A** = Most likely a serious problem - resolve or explain  
0 **ALERT level B** = A potentially serious problem, consider carefully  
5 **ALERT level C** = Check. Ensure it is not caused by an omission or oversight  
5 **ALERT level G** = General information/check it is not something unexpected

1 ALERT type 1 CIF construction/syntax error, inconsistent or missing data  
6 ALERT type 2 Indicator that the structure model may be wrong or deficient  
1 ALERT type 3 Indicator that the structure quality may be low  
2 ALERT type 4 Improvement, methodology, query or suggestion  
0 ALERT type 5 Informative message, check

---

**PLATON version of 04/06/2020; check.def file version of 02/06/2020**

**Datablock Sb-Ph4-2PCO - ellipsoid plot**



[Download CIF editor \(publCIF\) from the IUCr](#)  
[Download CIF editor \(enCIFer\) from the CCDC](#)  
[Test a new CIF entry](#)



Appendix C-3. checkCIF-reports for Sb(Ph)<sub>4</sub>(3PCO).

---

**Structure factors have been supplied for datablock(s) Sb-Ph4-3PCO**

THIS REPORT IS FOR GUIDANCE ONLY. IF USED AS PART OF A REVIEW PROCEDURE FOR PUBLICATION, IT SHOULD NOT REPLACE THE EXPERTISE OF AN EXPERIENCED CRYSTALLOGRAPHIC REFEREE.

No syntax errors found.

Please wait while processing ....  
[report](#)

[CIF dictionary](#)  
[Interpreting this](#)

Structure factor report

## Datablock: Sb-Ph4-3PCO

---

Bond precision: C-C = 0.0036 A                      Wavelength=0.71073

Cell:            a=10.0228(4)    b=10.4598(4)    c=13.8258(5)  
                 alpha=69.324(1) beta=72.086(1) gamma=83.971(1)

Temperature: 296 K

	Calculated	Reported
Volume	1290.34(9)	1290.34(9)
Space group	P -1	P -1
Hall group	-P 1	-P 1
Moiety formula	C31 H24 N3 O Sb	C31 H24 N3 O Sb
Sum formula	C31 H24 N3 O Sb	C31 H24 N3 O Sb
Mr	576.29	576.28
Dx, g cm-3	1.483	1.483
Z	2	2
Mu (mm-1)	1.098	1.098
F000	580.0	580.0
F000'	579.01	
h, k, lmax	13, 13, 18	13, 13, 18
Nref	6224	6218
Tmin, Tmax	0.822, 0.897	0.697, 0.747
Tmin'	0.798	

Correction method= # Reported T Limits:

Tmin=0.697 Tmax=0.747 AbsCorr = MULTI-SCAN

Data completeness= 0.999 Theta(max)= 27.999

R(reflections)= 0.0242(         wR2(reflections)= 0.0585(  
5636)                                    6218)

S = 1.055                      Npar= 421

---

The following ALERTS were generated. Each ALERT has the format

**test-name\_ALERT\_alert-type\_alert-level.**

Click on the hyperlinks for more details of the test.

---

● Alert level C

<u>PLAT230 ALERT 2 C</u>	Hirshfeld Test Diff for	C11	--C12	.	6.5
	s.u.				
<u>PLAT241 ALERT 2 C</u>	High 'MainMol' Ueq as Compared to Neighbors of				C5
	Check				
<u>PLAT242 ALERT 2 C</u>	Low 'MainMol' Ueq as Compared to Neighbors of				C3
	Check				
<u>PLAT350 ALERT 3 C</u>	Short C-H (X0.96,N1.08A)	C4	- H4	.	0.83
	Ang.				

**And 2 other PLAT350 Alerts**

<u>PLAT350 ALERT 3 C</u>	Short C-H (X0.96,N1.08A)	C12	- H12	.	0.84
	Ang.				
<u>PLAT350 ALERT 3 C</u>	Short C-H (X0.96,N1.08A)	C19	- H19	.	0.84
	Ang.				
<u>PLAT911 ALERT 3 C</u>	Missing FCF Refl Between Thmin & STh/L=			0.600	2
	Report				

---

● **Alert level G**

<u>PLAT154 ALERT 1 G</u>	The s.u.'s on the Cell Angles are Equal ..(Note)				0.001
	Degree				
<u>PLAT164 ALERT 4 G</u>	Nr. of Refined C-H H-Atoms in Heavy-Atom Struct.				24
	Note				
<u>PLAT230 ALERT 2 G</u>	Hirshfeld Test Diff for	C1	--C2	.	6.2
	s.u.				
<u>PLAT232 ALERT 2 G</u>	Hirshfeld Test Diff (M-X)	Sb1	--O1	.	6.1
	s.u.				
<u>PLAT883 ALERT 1 G</u>	No Info/Value for _atom_sites_solution_primary			.	Please
	Do !				
<u>PLAT912 ALERT 4 G</u>	Missing # of FCF Reflections Above STh/L=			0.600	4
	Note				
<u>PLAT933 ALERT 2 G</u>	Number of OMIT Records in Embedded .res File ...				4
	Note				
<u>PLAT941 ALERT 3 G</u>	Average HKL Measurement Multiplicity .....				2.9
	Low				
<u>PLAT965 ALERT 2 G</u>	The SHELXL WEIGHT Optimisation has not Converged				Please
	Check				
<u>PLAT978 ALERT 2 G</u>	Number C-C Bonds with Positive Residual Density.				12
	Info				

---

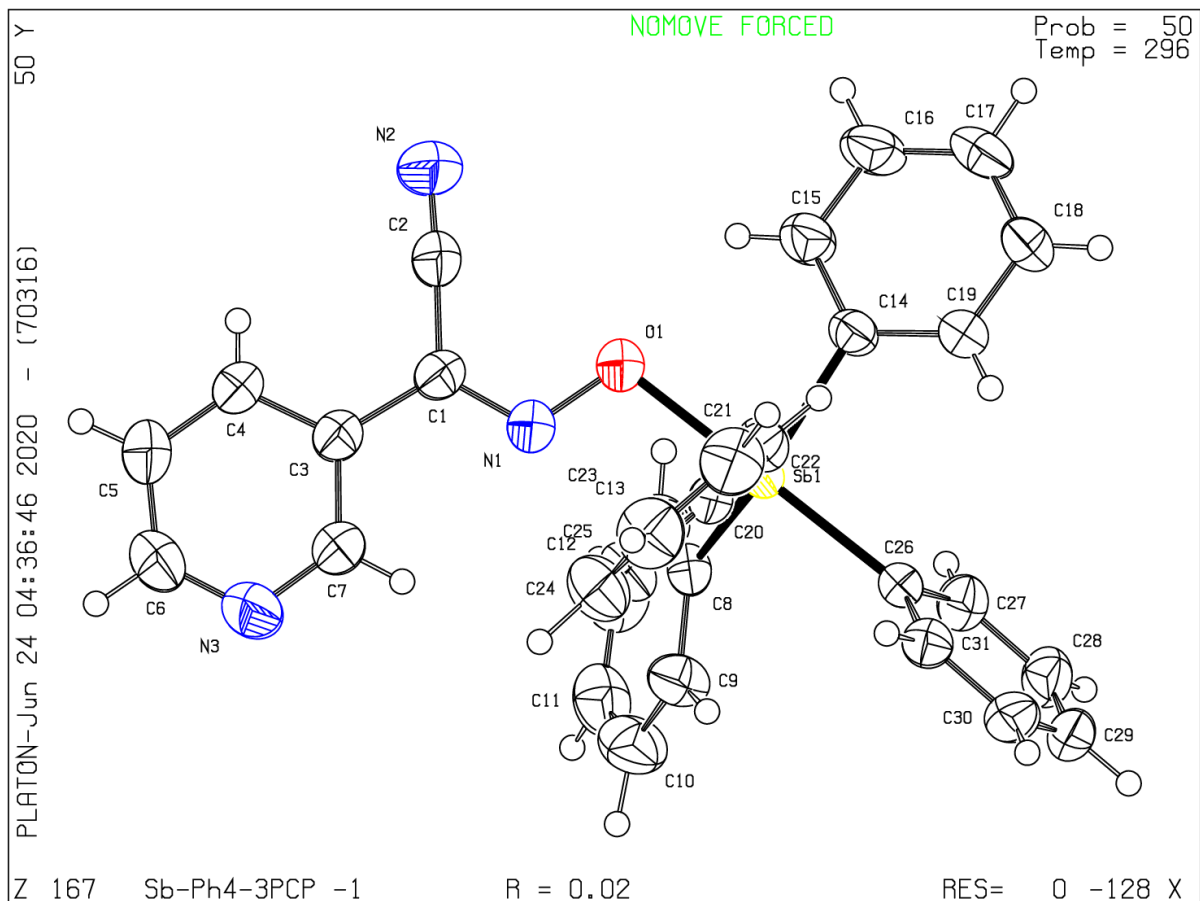
0 **ALERT level A** = Most likely a serious problem - resolve or explain  
0 **ALERT level B** = A potentially serious problem, consider carefully  
7 **ALERT level C** = Check. Ensure it is not caused by an omission or oversight  
10 **ALERT level G** = General information/check it is not something unexpected

2 ALERT type 1 CIF construction/syntax error, inconsistent or missing data  
8 ALERT type 2 Indicator that the structure model may be wrong or deficient  
5 ALERT type 3 Indicator that the structure quality may be low  
2 ALERT type 4 Improvement, methodology, query or suggestion  
0 ALERT type 5 Informative message, check

---

**PLATON version of 04/06/2020; check.def file version of 02/06/2020**

## Datablock Sb-Ph4-3PCO - ellipsoid plot



[Download CIF editor \(publCIF\) from the IUCr](#)  
[Download CIF editor \(enCIFer\) from the CCDC](#)  
[Test a new CIF entry](#)

## checkCIF/PLATON (basic structural check)

---

*Structure factors have been supplied for datablock(s) Sb-Ph4-4PCO*

THIS REPORT IS FOR GUIDANCE ONLY. IF USED AS PART OF A REVIEW PROCEDURE FOR PUBLICATION, IT SHOULD NOT REPLACE THE EXPERTISE OF AN EXPERIENCED CRYSTALLOGRAPHIC REFEREE.

No syntax errors found.

Please wait while processing ....  
report

CIF dictionary  
Interpreting this

### Structure factor report

## Datablock: Sb-Ph4-4PCO

---

Bond precision: C-C = 0.0031 A                      Wavelength=0.71073

Cell:            a=15.3352(10) b=9.7848(6)        c=19.6576(9)  
                 alpha=90            beta=119.272(4) gamma=90

Temperature: 120 K

	Calculated	Reported
Volume	2573.0(3)	2573.0(3)
Space group	P 21/c	P 21/c
Hall group	-P 2ybc	-P 2ybc
Moiety formula	C31 H24 N3 O Sb	C31 H24 N3 O Sb
Sum formula	C31 H24 N3 O Sb	C31 H24 N3 O Sb
Mr	576.29	576.28
Dx, g cm <sup>-3</sup>	1.488	1.428
Z	4	4
Mu (mm <sup>-1</sup> )	1.101	1.099
F000	1160.0	1068.0
F000'	1158.02	
h, k, lmax	23, 15, 30	22, 14, 29
Nref	9749	9309
Tmin, Tmax	0.730, 0.803	0.683, 0.880
Tmin'	0.514	

Correction method= # Reported T Limits:

Tmin=0.683 Tmax=0.880 AbsCorr = NUMERICAL

Data completeness= 0.955 Theta(max)= 33.082

R(reflections)= 0.0286(        wR2(reflections)= 0.0678(  
7879)                            9309)

S = 1.098                      Npar= 417

---

The following ALERTS were generated. Each ALERT has the format

**test-name\_ALERT\_alert-type\_alert-level.**

Click on the hyperlinks for more details of the test.

---

**● Alert level C**

DENSD01 ALERT 1 C The ratio of the submitted crystal density and that  
calculated from the formula is outside the range 0.99 <> 1.01  
Crystal density given = 1.428  
Calculated crystal density = 1.488  
PLAT046 ALERT 1 C Reported Z, MW and D(calc) are Inconsistent .... 1.488  
Check  
PLAT068 ALERT 1 C Reported F000 Differs from Calcd (or Missing)... Please  
Check  
PLAT094 ALERT 2 C Ratio of Maximum / Minimum Residual Density .... 2.99  
Report  
PLAT971 ALERT 2 C Check Calcd Resid. Dens. 1.12A From C21 1.73  
eA-3

---

**● Alert level G**

PLAT128 ALERT 4 G Alternate Setting for Input Space Group P21/c P21/n  
Note  
PLAT164 ALERT 4 G Nr. of Refined C-H H-Atoms in Heavy-Atom Struct. 23  
Note  
PLAT232 ALERT 2 G Hirshfeld Test Diff (M-X) Sb1 --O1 . 5.3  
s.u.  
PLAT883 ALERT 1 G No Info/Value for \_atom\_sites\_solution\_primary . Please  
Do !  
PLAT912 ALERT 4 G Missing # of FCF Reflections Above STh/L= 0.600 400  
Note  
PLAT933 ALERT 2 G Number of OMIT Records in Embedded .res File ... 10  
Note  
PLAT941 ALERT 3 G Average HKL Measurement Multiplicity ..... 4.5  
Low  
PLAT965 ALERT 2 G The SHELXL WEIGHT Optimisation has not Converged Please  
Check  
PLAT978 ALERT 2 G Number C-C Bonds with Positive Residual Density. 15  
Info

---

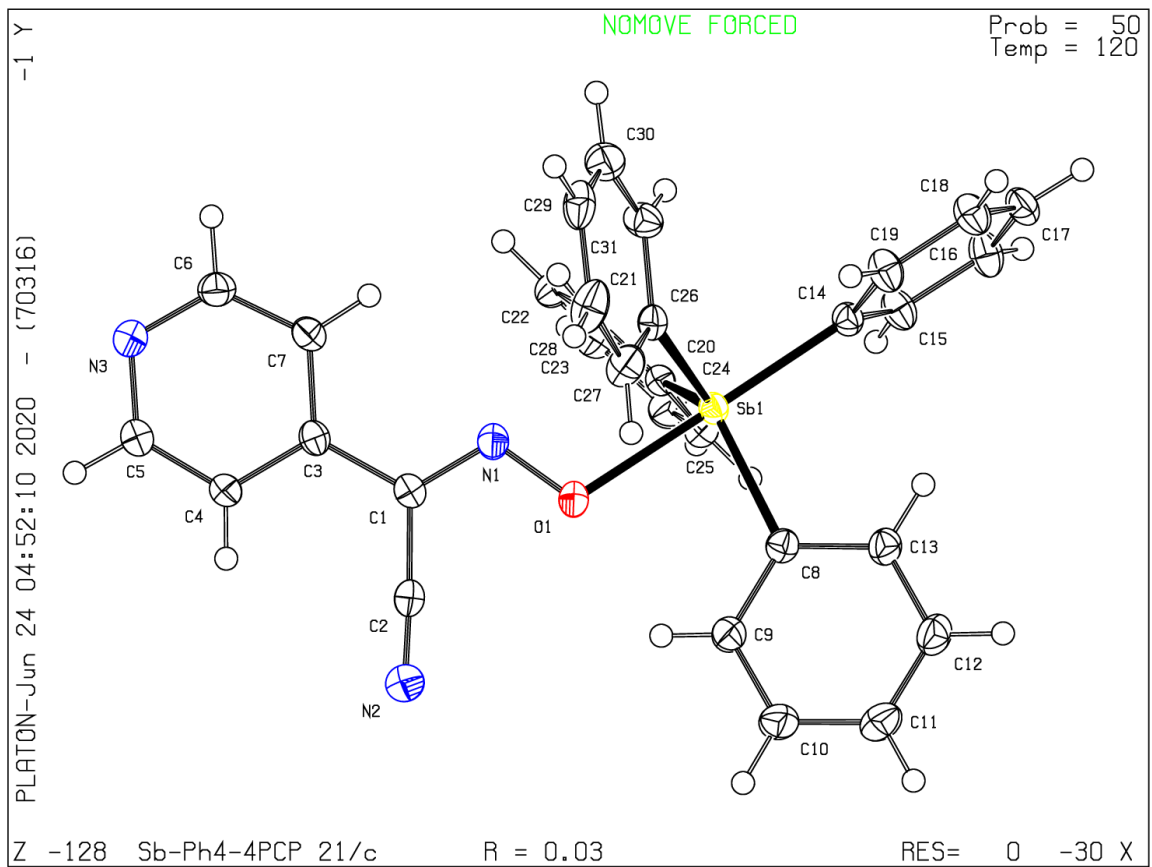
0 **ALERT level A** = Most likely a serious problem - resolve or explain  
0 **ALERT level B** = A potentially serious problem, consider carefully  
5 **ALERT level C** = Check. Ensure it is not caused by an omission or  
oversight  
9 **ALERT level G** = General information/check it is not something unexpected

4 ALERT type 1 CIF construction/syntax error, inconsistent or missing data  
6 ALERT type 2 Indicator that the structure model may be wrong or  
deficient  
1 ALERT type 3 Indicator that the structure quality may be low  
3 ALERT type 4 Improvement, methodology, query or suggestion  
0 ALERT type 5 Informative message, check

---

**PLATON version of 04/06/2020; check.def file version of 02/06/2020**

**Datablock Sb-Ph4-4PCO - ellipsoid plot**



[Download CIF editor \(publCIF\) from the IUCr](#)  
[Download CIF editor \(enCIFer\) from the CCDC](#)  
[Test a new CIF entry](#)

## checkCIF/PLATON (basic structural check)

---

### *Structure factors have been supplied for datablock(s) Sb-Ph4-ECI-oxo-dimer*

No syntax errors found.

Please wait while processing ....  
report

CIF dictionary

Interpreting this

### Structure factor report

## Datablock: Sb-Ph4-ECO-oxo-dimer

---

Bond precision: C-C = 0.0024 Å      Wavelength=0.71073  
Cell:            a=9.1828(9)      b=10.0829(10)      c=13.4714(16)  
                  alpha=111.957(1) beta=103.200(2) gamma=95.405(1)  
Temperature: 120 K

	Calculated	Reported
Volume	1103.8(2)	1103.8(2)
Space group	P -1	P -1
Hall group	-P 1	-P 1
Moiety formula	C46 H40 N4 O7 Sb2	C46 H40 N4 O7 Sb2
Sum formula	C46 H40 N4 O7 Sb2	C46 H40 N4 O7 Sb2
Mr	1004.34	1004.32
Dx, g cm <sup>-3</sup>	1.511	1.511
Z	1	1
Mu (mm <sup>-1</sup> )	1.277	1.277
F000	502.0	502.0
F000'	501.02	
h, k, lmax	13, 14, 19	13, 14, 19
Nref	6741	6688
Tmin, Tmax	0.712, 0.795	0.824, 1.000
Tmin'	0.282	

Correction method= # Reported T Limits:  
Tmin=0.824 Tmax=1.000 AbsCorr = NUMERICAL

Data completeness= 0.992 Theta(max)= 30.508

R(reflections)= 0.0188(      wR2(reflections)= 0.0447(  
6300)                              6688)

S = 1.079                      Npar= 348

---

The following ALERTS were generated. Each ALERT has the format  
**test-name\_ALERT\_alert-type\_alert-level.**  
Click on the hyperlinks for more details of the test.

---

● **Alert level C**

PLAT094 ALERT 2 C Ratio of Maximum / Minimum Residual Density .... 2.52  
Report

---

● **Alert level G**

PLAT063 ALERT 4 G Crystal Size Possibly too Large for Beam Size .. 0.98  
mm  
PLAT164 ALERT 4 G Nr. of Refined C-H H-Atoms in Heavy-Atom Struct. 20  
Note  
PLAT720 ALERT 4 G Number of Unusual/Non-Standard Labels ..... 1  
Note  
PLAT883 ALERT 1 G No Info/Value for \_atom\_sites\_solution\_primary . Please  
Do !  
PLAT912 ALERT 4 G Missing # of FCF Reflections Above STh/L= 0.600 52  
Note  
PLAT941 ALERT 3 G Average HKL Measurement Multiplicity ..... 2.6  
Low  
PLAT965 ALERT 2 G The SHELXL WEIGHT Optimisation has not Converged Please  
Check  
PLAT978 ALERT 2 G Number C-C Bonds with Positive Residual Density. 16  
Info

---

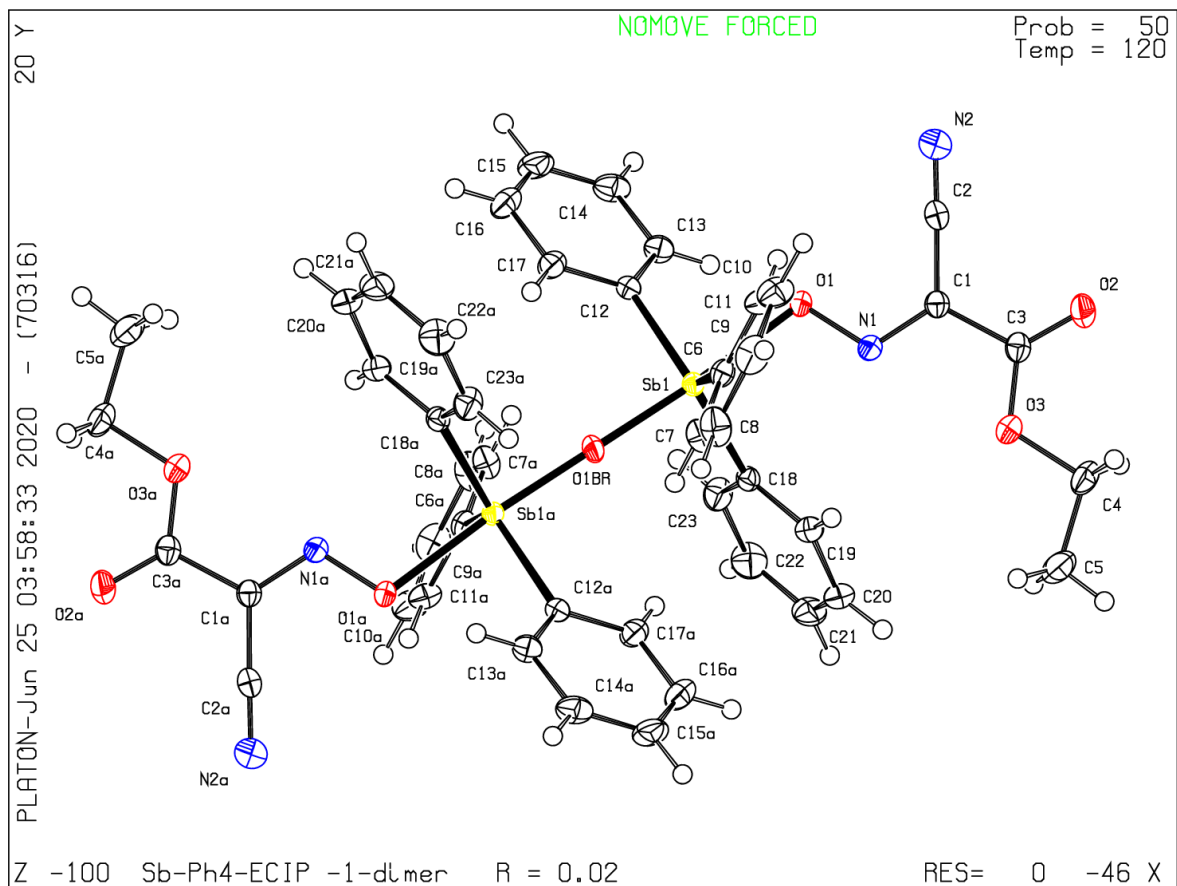
0 **ALERT level A** = Most likely a serious problem - resolve or explain  
0 **ALERT level B** = A potentially serious problem, consider carefully  
1 **ALERT level C** = Check. Ensure it is not caused by an omission or  
oversight  
8 **ALERT level G** = General information/check it is not something unexpected

1 ALERT type 1 CIF construction/syntax error, inconsistent or missing data  
3 ALERT type 2 Indicator that the structure model may be wrong or  
deficient  
1 ALERT type 3 Indicator that the structure quality may be low  
4 ALERT type 4 Improvement, methodology, query or suggestion  
0 ALERT type 5 Informative message, check

---

**PLATON version of 04/06/2020; check.def file version of 02/06/2020**  
**Datablock Sb-Ph4-ECO-oxo-dimer - ellipsoid plot**





[Download CIF editor \(pubCIF\) from the IUCr](#)  
[Download CIF editor \(enCIFer\) from the CCDC](#)  
[Test a new CIF entry](#)

## checkCIF/PLATON (basic structural check)

---

### *Structure factors have been supplied for datablock(s) Sb-Ph4-ECO-monomer*

No syntax errors found.

Please wait while processing ....  
report

CIF dictionary

Interpreting this

### Structure factor report

## Datablock: Sb-Ph4-ECO-monomer

---

Bond precision: C-C = 0.0080 Å      Wavelength=0.71073

Cell:            a=9.7871 (6) b=14.9208 (9)    c=17.6984 (11)  
                  alpha=90    beta=94.613 (1) gamma=90

Temperature: 120 K

	Calculated	Reported
Volume	2576.2 (3)	2576.1 (3)
Space group	P n	P n
Hall group	P -2yac	P -2yac
Moiety formula	C29 H25 N2 O3 Sb	C29 H25 N2 O3 Sb
Sum formula	C29 H25 N2 O3 Sb	C29 H25 N2 O3 Sb
Mr	571.27	571.26
Dx, g cm <sup>-3</sup>	1.473	1.473
Z	4	4
Mu (mm <sup>-1</sup> )	1.103	1.103
F000	1152.0	1152.0
F000'	1150.07	
h, k, lmax	15, 22, 27	14, 22, 26
Nref	19496 [ 9759]	9092
Tmin, Tmax	0.815, 0.849	0.653, 0.747
Tmin'	0.791	

Correction method= # Reported T Limits:

Tmin=0.653 Tmax=0.747 AbsCorr = MULTI-SCAN

Data completeness=

0.93/0.47

Theta(max)= 33.076

R(reflections)= 0.0351(      wR2(reflections)= 0.0774(  
8454)                            9092)

S = 1.193

Npar= 654

---

The following ALERTS were generated. Each ALERT has the format

**test-name ALERT alert-type alert-level.**

Click on the hyperlinks for more details of the test.

---

● **Alert level C**

STRVA01 ALERT 4 C Flack test results are ambiguous.  
 From the CIF: `_refine_ls_abs_structure_Flack` 0.530  
 From the CIF: `_refine_ls_abs_structure_Flack_su` 0.040

PLAT220 ALERT 2 C NonSolvent Resd 1 C Ueq(max) / Ueq(min) Range Ratio 3.2

PLAT220 ALERT 2 C NonSolvent Resd 2 C Ueq(max) / Ueq(min) Range Ratio 3.3

PLAT222 ALERT 3 C NonSolvent Resd 1 H Uiso(max)/Uiso(min) Range Ratio 6.6

PLAT342 ALERT 3 C Low Bond Precision on C-C Bonds ..... 0.00802 Ang.

PLAT907 ALERT 2 C Flack x > 0.5, Structure Needs to be Inverted? . Check 0.53

PLAT914 ALERT 3 C No Bijvoet Pairs in FCF for Non-centro Structure Check Please

PLAT971 ALERT 2 C Check Calcd Resid. Dens. 0.85A From Sb1B eA-3 1.73

**And 2 other PLAT971 Alerts**

PLAT971 ALERT 2 C Check Calcd Resid. Dens. 1.30A From C18B eA-3 1.51

PLAT971 ALERT 2 C Check Calcd Resid. Dens. 0.64A From Sb1A eA-3 1.51

PLAT977 ALERT 2 C Check Negative Difference Density on H13A eA-3 -0.41

**And 2 other PLAT977 Alerts**

PLAT977 ALERT 2 C Check Negative Difference Density on H16B eA-3 -0.32

PLAT977 ALERT 2 C Check Negative Difference Density on H26A eA-3 -0.35

---

**Alert level G**

PLAT083 ALERT 2 G SHELXL Second Parameter in WGHT Unusually Large Why ? 5.57

PLAT164 ALERT 4 G Nr. of Refined C-H H-Atoms in Heavy-Atom Struct. Note 5

PLAT720 ALERT 4 G Number of Unusual/Non-Standard Labels ..... Note 10

PLAT883 ALERT 1 G No Info/Value for `_atom_sites_solution_primary` . Do ! Please

PLAT912 ALERT 4 G Missing # of FCF Reflections Above STh/L= 0.600 Note 656

PLAT933 ALERT 2 G Number of OMIT Records in Embedded .res File ... Note 5

PLAT941 ALERT 3 G Average HKL Measurement Multiplicity ..... Low 1.0

PLAT961 ALERT 5 G Dataset Contains no Negative Intensities ..... Check Please

PLAT978 ALERT 2 G Number C-C Bonds with Positive Residual Density. Info 0

PLAT992 ALERT 5 G Repd & Actual `_reflns_number_gt` Values Differ by Check 8

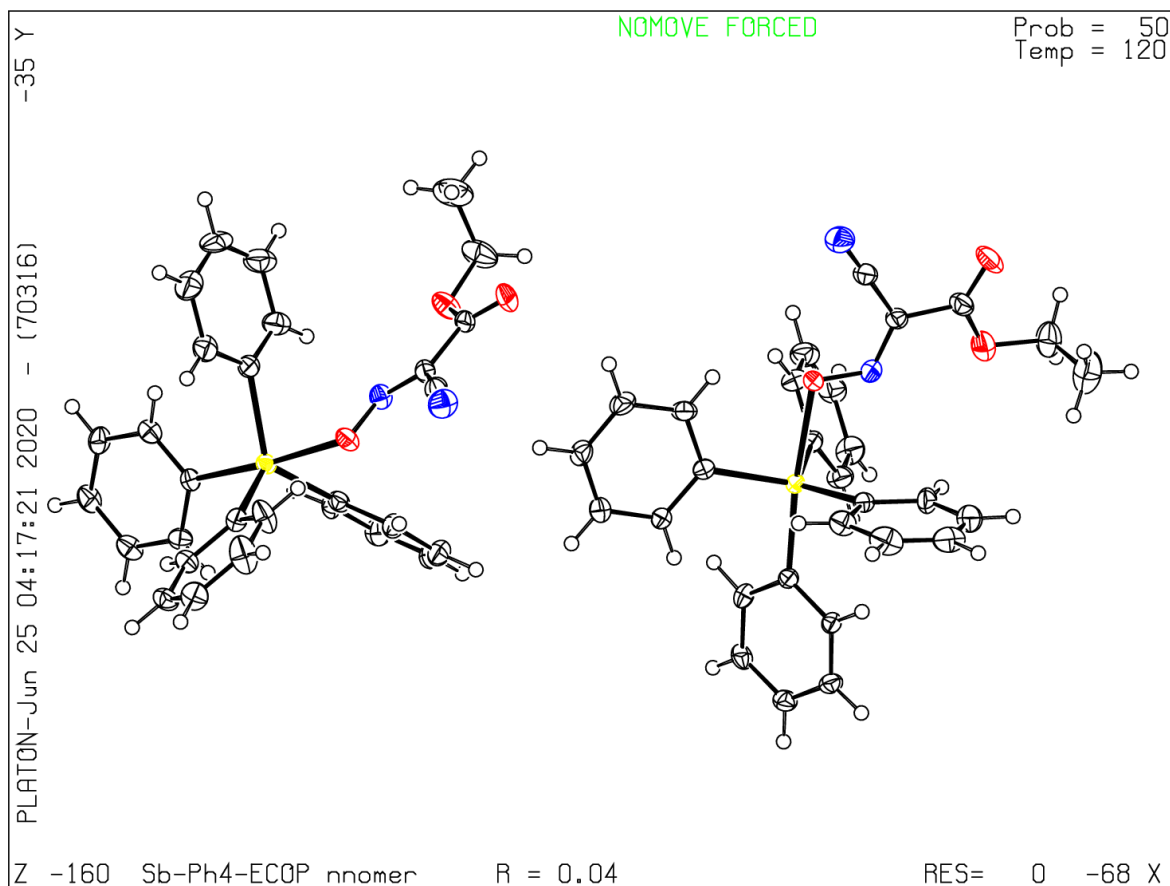
---

0 **ALERT level A** = Most likely a serious problem - resolve or explain  
 0 **ALERT level B** = A potentially serious problem, consider carefully  
 13 **ALERT level C** = Check. Ensure it is not caused by an omission or oversight  
 10 **ALERT level G** = General information/check it is not something unexpected

1 ALERT type 1 CIF construction/syntax error, inconsistent or missing data  
 12 ALERT type 2 Indicator that the structure model may be wrong or deficient  
 4 ALERT type 3 Indicator that the structure quality may be low  
 4 ALERT type 4 Improvement, methodology, query or suggestion  
 2 ALERT type 5 Informative message, check

---

**PLATON version of 04/06/2020; check.def file version of 02/06/2020**  
**Datablock Sb-Ph4-ECO-monomer - ellipsoid plot**



[Download CIF editor \(publCIF\) from the IUCr](#)  
[Download CIF editor \(enCIFer\) from the CCDC](#)  
[Test a new CIF entry](#)

## checkCIF/PLATON (basic structural check)

---

### *Structure factors have been supplied for datablock(s) Sb-Ph4-MCO*

No syntax errors found.

Please wait while processing ....  
[report](#)

[CIF dictionary](#)

[Interpreting this](#)

### Structure factor report

## Datablock: Sb-Ph4-MCO

---

Bond precision: C-C = 0.0065 Å      Wavelength=0.71073

Cell:            a=17.6451(4) b=10.8777(3)    c=28.3876(7)  
                  alpha=90        beta=94.836(1) gamma=90

Temperature: 100 K

	Calculated	Reported
Volume	5429.3(2)	5429.3(2)
Space group	P 21/c	P 21/c
Hall group	-P 2ybc	-P 2ybc
Moiety formula	C31 H28 N3 O3 Sb	C31 H28 N3 O3 Sb
Sum formula	C31 H28 N3 O3 Sb	C31 H28 N3 O3 Sb
Mr	612.32	612.31
Dx, g cm <sup>-3</sup>	1.498	1.498
Z	8	8
Mu (mm <sup>-1</sup> )	1.054	1.054
F000	2480.0	2480.0
F000'	2476.19	
h, k, lmax	22, 13, 35	22, 13, 35
Nref	11273	11251
Tmin, Tmax	0.863, 0.881	0.689, 0.745
Tmin'	0.863	

Correction method= # Reported T Limits:

Tmin=0.689 Tmax=0.745 AbsCorr = MULTI-SCAN

Data completeness= 0.998 Theta(max)= 26.516

R(reflections)= 0.0447(      wR2(reflections)= 0.1109(  
9235)                            11251)

S = 1.114                    Npar= 750

---

The following ALERTS were generated. Each ALERT has the format

**test-name\_ALERT\_alert-type\_alert-level.**

Click on the hyperlinks for more details of the test.

---

● **Alert level C**

<u>PLAT094 ALERT 2 C</u>	Ratio of Maximum / Minimum Residual Density ....			3.19
Report				
<u>PLAT222 ALERT 3 C</u>	NonSolvent Resd 2 H Uiso(max)/Uiso(min) Range			7.7
Ratio				
<u>PLAT245 ALERT 2 C</u>	U(iso) H28A	Smaller than U(eq) C28A	by	0.017
Ang**2				
<b>And 3 other PLAT245 Alerts</b>				
<u>PLAT245 ALERT 2 C</u>	U(iso) H13B	Smaller than U(eq) C13B	by	0.012
Ang**2				
<u>PLAT245 ALERT 2 C</u>	U(iso) H21B	Smaller than U(eq) C21B	by	0.014
Ang**2				
<u>PLAT245 ALERT 2 C</u>	U(iso) H30B	Smaller than U(eq) C30B	by	0.012
Ang**2				
<u>PLAT906 ALERT 3 C</u>	Large K Value in the Analysis of Variance .....			4.570
Check				
<u>PLAT911 ALERT 3 C</u>	Missing FCF Refl Between Thmin & STh/L=	0.600		9
Report				
<u>PLAT971 ALERT 2 C</u>	Check Calcd Resid. Dens.	1.05A	From C26B	1.94
eA-3				
<u>PLAT971 ALERT 2 C</u>	Check Calcd Resid. Dens.	1.18A	From Sb1A	1.65
eA-3				
<u>PLAT975 ALERT 2 C</u>	Check Calcd Resid. Dens.	0.81A	From O1A	0.57
eA-3				

---

### ● Alert level G

<u>PLAT083 ALERT 2 G</u>	SHELXL Second Parameter in WGHT Unusually Large			14.34
Why ?				
<u>PLAT164 ALERT 4 G</u>	Nr. of Refined C-H H-Atoms in Heavy-Atom Struct.			16
Note				
<u>PLAT232 ALERT 2 G</u>	Hirshfeld Test Diff (M-X) Sb1A	--O1A	.	5.3
s.u.				
<u>PLAT398 ALERT 2 G</u>	Deviating C-O-C Angle From 120 for O3B			109.9
Degree				
<u>PLAT720 ALERT 4 G</u>	Number of Unusual/Non-Standard Labels .....			16
Note				
<u>PLAT883 ALERT 1 G</u>	No Info/Value for _atom_sites_solution_primary .			Please
Do !				
<u>PLAT912 ALERT 4 G</u>	Missing # of FCF Reflections Above STh/L=	0.600		15
Note				
<u>PLAT933 ALERT 2 G</u>	Number of OMIT Records in Embedded .res File ...			10
Note				
<u>PLAT965 ALERT 2 G</u>	The SHELXL WEIGHT Optimisation has not Converged			Please
Check				
<u>PLAT978 ALERT 2 G</u>	Number C-C Bonds with Positive Residual Density.			2
Info				

- 
- 0 **ALERT level A** = Most likely a serious problem - resolve or explain
  - 0 **ALERT level B** = A potentially serious problem, consider carefully
  - 11 **ALERT level C** = Check. Ensure it is not caused by an omission or oversight
  - 10 **ALERT level G** = General information/check it is not something unexpected
  - 1 **ALERT type 1** CIF construction/syntax error, inconsistent or missing data

14 ALERT type 2 Indicator that the structure model may be wrong or deficient

3 ALERT type 3 Indicator that the structure quality may be low

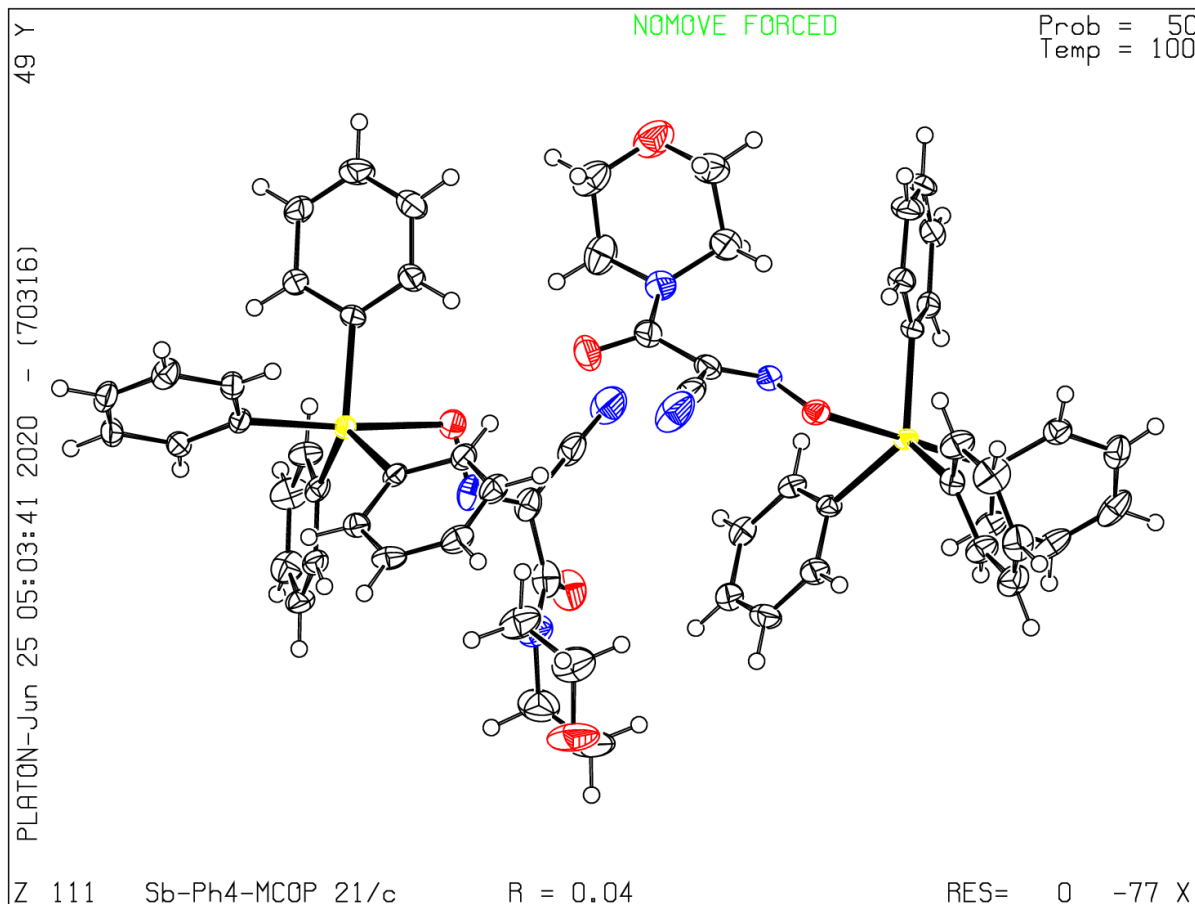
3 ALERT type 4 Improvement, methodology, query or suggestion

0 ALERT type 5 Informative message, check

---

**PLATON version of 04/06/2020; check.def file version of 02/06/2020**

## **Datablock Sb-Ph4-MCO - ellipsoid plot**



---

[Download CIF editor \(pubCIF\) from the IUCr](#)

[Download CIF editor \(enCIFer\) from the CCDC](#)

[Test a new CIF entry](#)

**Appendix C-8.** checkCIF-reports for Sb(Ph)<sub>4</sub>(TCO) polymorph 1.

# checkCIF/PLATON (basic structural check)

---

## *Structure factors have been supplied for datablock(s) done\_Sb-Ph4-TCO-polymorph-1*

No syntax errors found.  
Please wait while processing ....  
[report](#)

[CIF dictionary](#)  
[Interpreting this](#)

### Structure factor report

## Datablock: Sb-Ph4-TCO-polymorph-1

---

Bond precision: C-C = 0.0045 Å      Wavelength=0.71073

Cell:            a=14.6709(7) b=9.8468(5)      c=18.3414(9)  
                  alpha=90      beta=111.994(1) gamma=90

Temperature: 120 K

	Calculated	Reported
Volume	2456.8(2)	2456.8(2)
Space group	P 21/c	P 21/c
Hall group	-P 2ybc	-P 2ybc
Moiety formula	C27 H21 N3 O S Sb	C27 H21 N3 O S Sb
Sum formula	C27 H21 N3 O S Sb	C27 H21 N3 O S Sb
Mr	557.29	557.28
Dx, g cm <sup>-3</sup>	1.507	1.507
Z	4	4
Mu (mm <sup>-1</sup> )	1.232	1.232
F000	1116.0	1116.0
F000'	1114.48	
h, k, lmax	18, 12, 23	18, 12, 23
Nref	5478	5476
Tmin, Tmax	0.814, 0.840	0.894, 0.931
Tmin'	0.814	

Correction method= # Reported T Limits:

Tmin=0.894 Tmax=0.931 AbsCorr = NUMERICAL

Data completeness= 1.000 Theta(max)= 27.202

R(reflections)= 0.0308(      wR2(reflections)= 0.0764(  
4595)                              5476)

S = 1.033                      Npar= 391

---

The following ALERTS were generated. Each ALERT has the format

**test-name\_ALERT\_alert-type\_alert-level.**

Click on the hyperlinks for more details of the test.

---

● **Alert level C**



PLAT094	ALERT 2 C	Ratio of Maximum / Minimum Residual Density ....	2.03
Report			
PLAT420	ALERT 2 C	D-H Without Acceptor N3 --H3B .	Please
Check			
PLAT973	ALERT 2 C	Check Calcd Positive Resid. Density on Sb1	1.03
eA-3			
PLAT975	ALERT 2 C	Check Calcd Resid. Dens. 0.84A From C8	0.68
eA-3			

---

● **Alert level G**

PLAT007	ALERT 5 G	Number of Unrefined Donor-H Atoms .....	4
Report			
PLAT164	ALERT 4 G	Nr. of Refined C-H H-Atoms in Heavy-Atom Struct.	14
Note			
PLAT171	ALERT 4 G	The CIF-Embedded .res File Contains EADP Records	6
Report			
PLAT301	ALERT 3 G	Main Residue Disorder .....(Resd 1 )	24%
Note			
PLAT343	ALERT 2 G	Unusual sp? Angle Range in Main Residue for	C8
Check			
PLAT432	ALERT 2 G	Short Inter X...Y Contact C18 ..N2A	2.93
Ang.			
			$1-x, -1/2+y, 1/2-z = 2\_645$
Check			
PLAT720	ALERT 4 G	Number of Unusual/Non-Standard Labels .....	2
Note			
PLAT883	ALERT 1 G	No Info/Value for _atom_sites_solution_primary .	Please
Do !			
PLAT910	ALERT 3 G	Missing # of FCF Reflection(s) Below Theta(Min).	1
Note			
PLAT912	ALERT 4 G	Missing # of FCF Reflections Above STh/L= 0.600	2
Note			
PLAT933	ALERT 2 G	Number of OMIT Records in Embedded .res File ...	1
Note			
PLAT978	ALERT 2 G	Number C-C Bonds with Positive Residual Density.	2
Info			

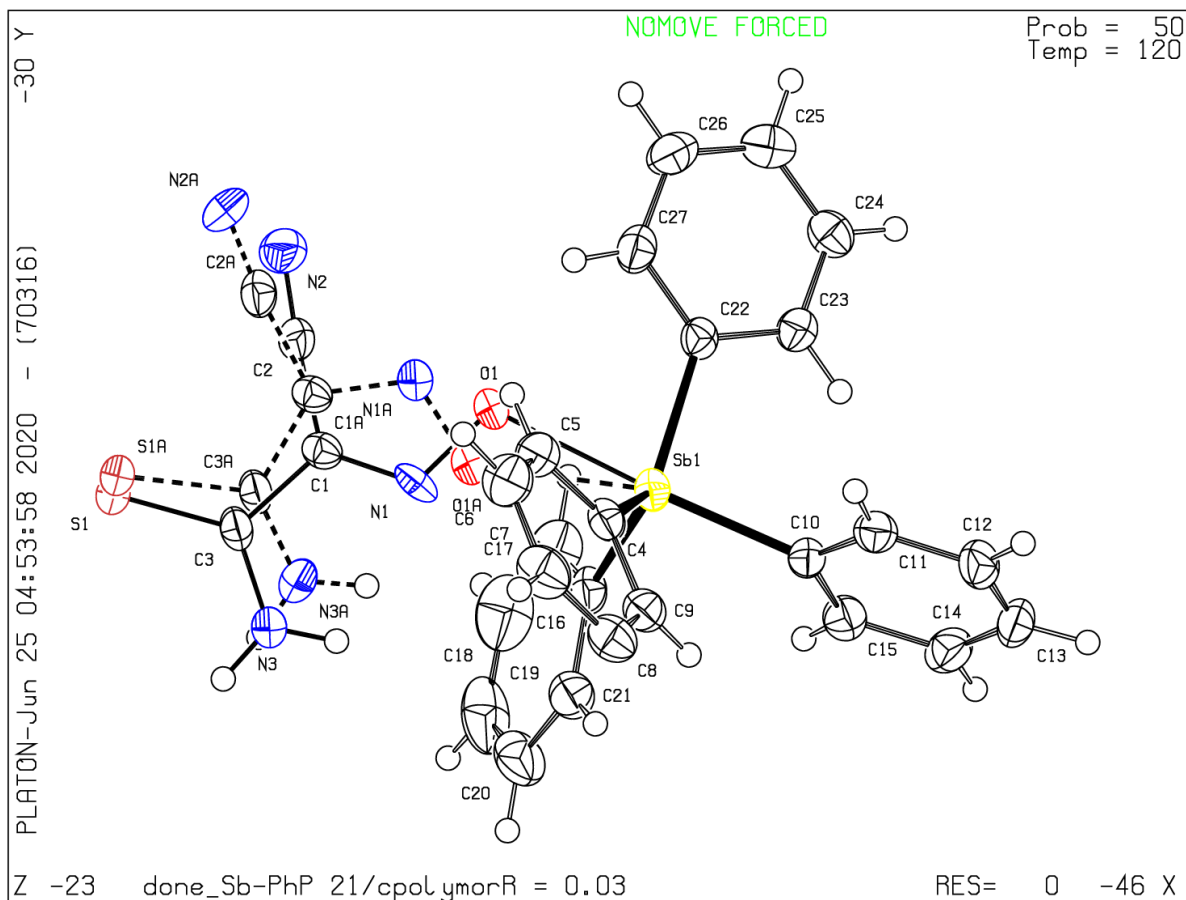
---

0 **ALERT level A** = Most likely a serious problem - resolve or explain  
0 **ALERT level B** = A potentially serious problem, consider carefully  
4 **ALERT level C** = Check. Ensure it is not caused by an omission or oversight  
12 **ALERT level G** = General information/check it is not something unexpected

1 ALERT type 1 CIF construction/syntax error, inconsistent or missing data  
8 ALERT type 2 Indicator that the structure model may be wrong or deficient  
2 ALERT type 3 Indicator that the structure quality may be low  
4 ALERT type 4 Improvement, methodology, query or suggestion  
1 ALERT type 5 Informative message, check

---

**PLATON version of 04/06/2020; check.def file version of 02/06/2020**  
**Datablock Sb-Ph4-TCO-polymorph-1 - ellipsoid plot**



[Download CIF editor \(publCIF\) from the IUCr](#)  
[Download CIF editor \(enCIFer\) from the CCDC](#)  
[Test a new CIF entry](#)



Click on the hyperlinks for more details of the test.

---

**Alert level A**

PLAT213 ALERT 2 A Atom C24D                    has ADP max/min Ratio .....            5.3  
prolat  
PLAT213 ALERT 2 A Atom C18F                    has ADP max/min Ratio .....            5.9  
oblate  
PLAT971 ALERT 2 A Check Calcd Resid. Dens. 1.59A    From N1D                                    5.81  
eA-3

**And 7 other PLAT971 Alerts**

PLAT971 ALERT 2 A Check Calcd Resid. Dens. 1.56A    From C21B                                    5.72  
eA-3  
  
PLAT971 ALERT 2 A Check Calcd Resid. Dens. 1.61A    From C17Q                                    5.42  
eA-3  
  
PLAT971 ALERT 2 A Check Calcd Resid. Dens. 1.56A    From N1C                                    5.25  
eA-3  
  
PLAT971 ALERT 2 A Check Calcd Resid. Dens. 1.49A    From C11E                                    5.21  
eA-3  
  
PLAT971 ALERT 2 A Check Calcd Resid. Dens. 1.51A    From N1F                                    5.12  
eA-3  
  
PLAT971 ALERT 2 A Check Calcd Resid. Dens. 1.58A    From C17A                                    4.91  
eA-3  
  
PLAT971 ALERT 2 A Check Calcd Resid. Dens. 1.53A    From C11H                                    4.84  
eA-3

---

**Alert level B**

PLAT097 ALERT 2 B Large Reported Max. (Positive) Residual Density            5.68  
eA-3  
PLAT971 ALERT 2 B Check Calcd Resid. Dens. 1.66A    From C13E                                    2.89  
eA-3

**And 3 other PLAT971 Alerts**

PLAT971 ALERT 2 B Check Calcd Resid. Dens. 1.80A    From C19A                                    2.88  
eA-3  
  
PLAT971 ALERT 2 B Check Calcd Resid. Dens. 1.79A    From C19Q                                    2.73  
eA-3  
  
PLAT971 ALERT 2 B Check Calcd Resid. Dens. 1.80A    From C25D                                    2.54  
eA-3

---

**Alert level C**

DIFMX02 ALERT 1 C The maximum difference density is > 0.1\*ZMAX\*0.75  
The relevant atom site should be identified.  
PLAT094 ALERT 2 C Ratio of Maximum / Minimum Residual Density ....            2.76  
Report

<u>PLAT213 ALERT 2 C</u>	Atom C6C	has ADP max/min Ratio .....	3.4
prolat			
<u>PLAT234 ALERT 4 C</u>	Large Hirshfeld Difference C19B	--C20B .	0.18
Ang.			
<u>PLAT234 ALERT 4 C</u>	Large Hirshfeld Difference C6C	--C7C .	0.17
Ang.			
<u>PLAT342 ALERT 3 C</u>	Low Bond Precision on C-C Bonds .....		0.01521
Ang.			
<u>PLAT911 ALERT 3 C</u>	Missing FCF Refl Between Thmin & STh/L=	0.600	14
Report			
<u>PLAT971 ALERT 2 C</u>	Check Calcd Resid. Dens.	1.76A From C13H	2.39
eA-3			

**And 8 other PLAT971 Alerts**

<u>PLAT971 ALERT 2 C</u>	Check Calcd Resid. Dens.	1.78A From C19B	2.27
eA-3			
<u>PLAT971 ALERT 2 C</u>	Check Calcd Resid. Dens.	1.67A From C19F	2.15
eA-3			
<u>PLAT971 ALERT 2 C</u>	Check Calcd Resid. Dens.	1.66A From C7C	2.04
eA-3			
<u>PLAT971 ALERT 2 C</u>	Check Calcd Resid. Dens.	1.95A From C2A	1.72
eA-3			
<u>PLAT971 ALERT 2 C</u>	Check Calcd Resid. Dens.	1.93A From C2E	1.70
eA-3			
<u>PLAT971 ALERT 2 C</u>	Check Calcd Resid. Dens.	1.82A From C2H	1.69
eA-3			
<u>PLAT971 ALERT 2 C</u>	Check Calcd Resid. Dens.	1.80A From C2Q	1.68
eA-3			
<u>PLAT971 ALERT 2 C</u>	Check Calcd Resid. Dens.	1.93A From C2F	1.54
eA-3			
<u>PLAT972 ALERT 2 C</u>	Check Calcd Resid. Dens.	0.60A From Sb1B	-1.96
eA-3			

**And 8 other PLAT972 Alerts**

<u>PLAT972 ALERT 2 C</u>	Check Calcd Resid. Dens.	0.74A From Sb1C	-1.85
eA-3			
<u>PLAT972 ALERT 2 C</u>	Check Calcd Resid. Dens.	0.72A From Sb1D	-1.83
eA-3			
<u>PLAT972 ALERT 2 C</u>	Check Calcd Resid. Dens.	0.75A From Sb1Q	-1.71
eA-3			
<u>PLAT972 ALERT 2 C</u>	Check Calcd Resid. Dens.	0.78A From Sb1F	-1.67
eA-3			

<u>PLAT972 ALERT 2 C</u>	Check Calcd Resid. Dens.	0.61A	From Sb1E	-1.58
eA-3				
<u>PLAT972 ALERT 2 C</u>	Check Calcd Resid. Dens.	0.61A	From Sb1F	-1.55
eA-3				
<u>PLAT972 ALERT 2 C</u>	Check Calcd Resid. Dens.	0.78A	From Sb1C	-1.53
eA-3				
<u>PLAT972 ALERT 2 C</u>	Check Calcd Resid. Dens.	0.77A	From Sb1B	-1.51
eA-3				
<u>PLAT977 ALERT 2 C</u>	Check Negative Difference Density on H9H			-0.31
eA-3				
<u>PLAT977 ALERT 2 C</u>	Check Negative Difference Density on H23E			-0.35
eA-3				

---

**Alert level G**

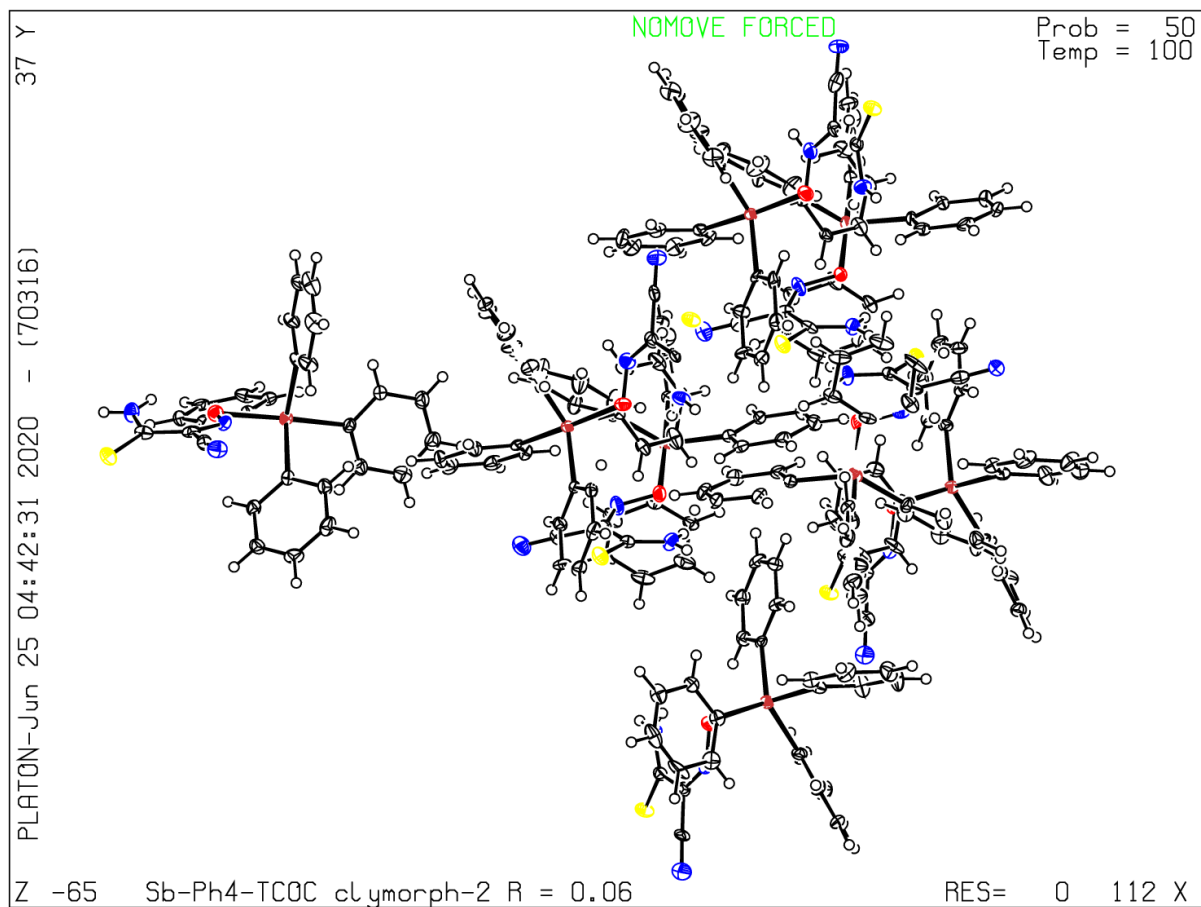
<u>FORMU01 ALERT 1 G</u>	There is a discrepancy between the atom counts in the _chemical_formula_sum and _chemical_formula_moiety. This is usually due to the moiety formula being in the wrong format. Atom count from _chemical_formula_sum: C216 H176 N24 O8 S8 Sb8 Atom count from _chemical_formula_moiety:C27 H22 N3 O1 S1 Sb1			
<u>PLAT007 ALERT 5 G</u>	Number of Unrefined Donor-H Atoms .....			16
Report				
<u>PLAT045 ALERT 1 G</u>	Calculated and Reported Z Differ by a Factor ...			8.00
Check				
<u>PLAT083 ALERT 2 G</u>	SHELXL Second Parameter in WGHT Unusually Large			137.89
Why ?				
<u>PLAT720 ALERT 4 G</u>	Number of Unusual/Non-Standard Labels .....			16
Note				
<u>PLAT883 ALERT 1 G</u>	No Info/Value for _atom_sites_solution_primary .			Please
Do !				
<u>PLAT912 ALERT 4 G</u>	Missing # of FCF Reflections Above STh/L= 0.600			1520
Note				
<u>PLAT933 ALERT 2 G</u>	Number of OMIT Records in Embedded .res File ...			15
Note				
<u>PLAT965 ALERT 2 G</u>	The SHELXL WEIGHT Optimisation has not Converged			Please
Check				
<u>PLAT978 ALERT 2 G</u>	Number C-C Bonds with Positive Residual Density.			0
Info				
<u>PLAT992 ALERT 5 G</u>	Repd & Actual _reflns_number_gt Values Differ by			2
Check				

- 
- 10 **ALERT level A** = Most likely a serious problem - resolve or explain
  - 5 **ALERT level B** = A potentially serious problem, consider carefully
  - 27 **ALERT level C** = Check. Ensure it is not caused by an omission or oversight
  - 11 **ALERT level G** = General information/check it is not something unexpected
- 
- 4 ALERT type 1 CIF construction/syntax error, inconsistent or missing data
  - 41 ALERT type 2 Indicator that the structure model may be wrong or deficient
  - 2 ALERT type 3 Indicator that the structure quality may be low
  - 4 ALERT type 4 Improvement, methodology, query or suggestion
  - 2 ALERT type 5 Informative message, check

---

PLATON version of 04/06/2020; check.def file version of 02/06/2020

## Datablock Sb-Ph4-TCO\_polymorph-2 - ellipsoid plot



---

[Download CIF editor \(pubCIF\) from the IUCr](#)

[Download CIF editor \(enCIFer\) from the CCDC](#)

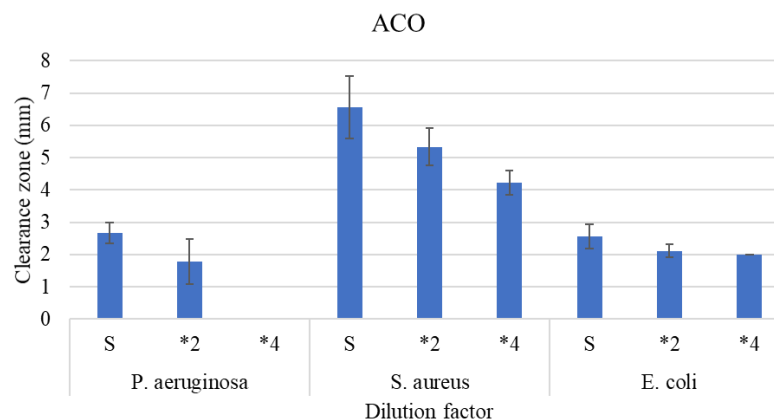
[Test a new CIF entry](#)

## Appendix D. Biological Activity Studies Data.

### ACO

Organism	Dilution	A	B	C	Disc average
A1	S	4	2	3	3
	*2	2	3	2	2.333333
	*4	0	0	0	0
A2	S	3	3	2	2.666667
	*2	1	1	1	1
	*4	0	0	0	0
A3	S	3	2	2	2.333333
	*2	2	2	2	2
	*4	0	0	0	0
B1	S	6	6	6	6
	*2	5	5	5	5
	*4	4	4	4	4
B2	S	6	6	6	6
	*2	6	6	6	6
	*4	4	4	4	4
B3	S	8	8	7	7.666667
	*2	5	5	5	5
	*4	5	4	5	4.666667
C1	S	3	2	2	2.333333
	*2	2	2	2	2
	*4	2	2	2	2
C2	S	3	2	2	2.333333
	*2	2	2	2	2
	*4	2	2	2	2
C3	S	3	3	3	3
	*2	2	3	2	2.333333
	*4	2	2	2	2

Organism		Dilution factor	Average	SD
A	<i>P. aeruginosa</i>	S	2.666667	0.333333
		*2	1.777778	0.693889
		*4	0	0
B	<i>S. aureus</i>	S	6.555556	0.96225
		*2	5.333333	0.57735
		*4	4.222222	0.3849
C	<i>E. coli</i>	S	2.555556	0.3849
		*2	2.111111	0.19245
		*4	2	0



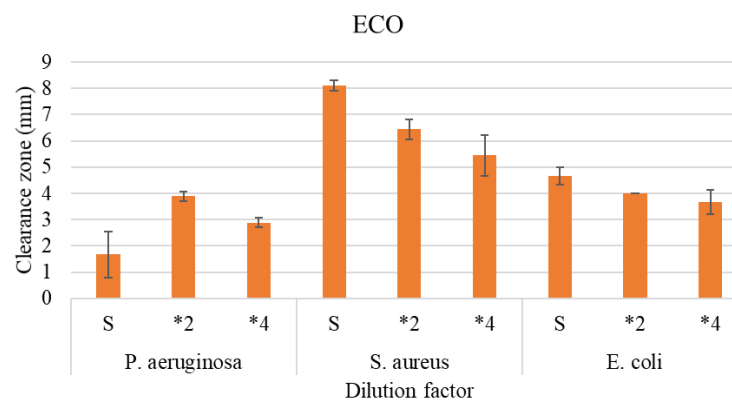
**Appendix D-1.** Raw data and statistical analysis of Sb(Ph)<sub>4</sub>(ACO) in the first round of inhibition zone measurements.



## ECO

Organism	Dilution	A	B	C	Disc average
A1	S	2	2	2	2
	*2	4	4	4	4
	*4	3	3	3	3
A2	S	1	0	1	0.666667
	*2	4	3	4	3.666667
	*4	2	3	3	2.666667
A3	S	2	3	2	2.333333
	*2	4	4	4	4
	*4	3	3	3	3
B1	S	8	8	8	8
	*2	7	7	6	6.666667
	*4	5	5	5	5
B2	S	8	9	8	8.333333
	*2	6	7	7	6.666667
	*4	7	6	6	6.333333
B3	S	8	8	8	8
	*2	6	6	6	6
	*4	5	5	5	5
C1	S	5	5	5	5
	*2	4	4	4	4
	*4	4	4	4	4
C2	S	5	5	4	4.666667
	*2	4	4	4	4
	*4	3	3	4	3.333333
C3	S	5	4	4	4.333333
	*2	4	4	4	4
	*4	?	?	?	

Organism		Dilution factor	Average	SD
A	<i>P. aeruginosa</i>	S	1.666667	0.881917
		*2	3.888889	0.19245
		*4	2.888889	0.19245
B	<i>S. aureus</i>	S	8.111111	0.19245
		*2	6.444444	0.3849
		*4	5.444444	0.7698
C	<i>E. coli</i>	S	4.666667	0.333333
		*2	4	0
		*4	3.666667	0.471405

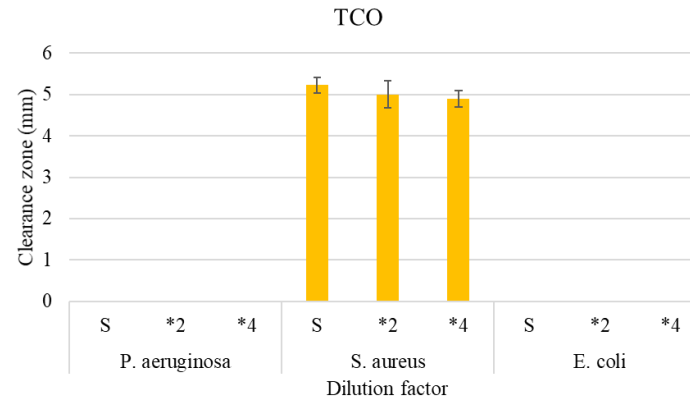


**Appendix D-2.** Raw data and statistical analysis of Sb(Ph)<sub>4</sub>(ECO) in the first round of inhibition zone measurements.

## TCO

Organism	Dilution	A	B	C	Disc average
A1	S	0	0	0	0
	*2	0	0	0	0
	*4	0	0	0	0
A2	S	0	0	0	0
	*2	0	0	0	0
	*4	0	0	0	0
A3	S	0	0	0	0
	*2	0	0	0	0
	*4	0	0	0	0
B1	S	5	5	5	5
	*2	5	5	6	5.333333
	*4	5	5	5	5
B2	S	6	5	5	5.333333
	*2	5	4	5	4.666667
	*4	5	5	5	5
B3	S	5	6	5	5.333333
	*2	5	5	5	5
	*4	5	5	4	4.666667
C1	S	0	0	0	0
	*2	0	0	0	0
	*4	0	0	0	0
C2	S	0	0	0	0
	*2	0	0	0	0
	*4	0	0	0	0
C3	S	0	0	0	0
	*2	0	0	0	0
	*4	0	0	0	0

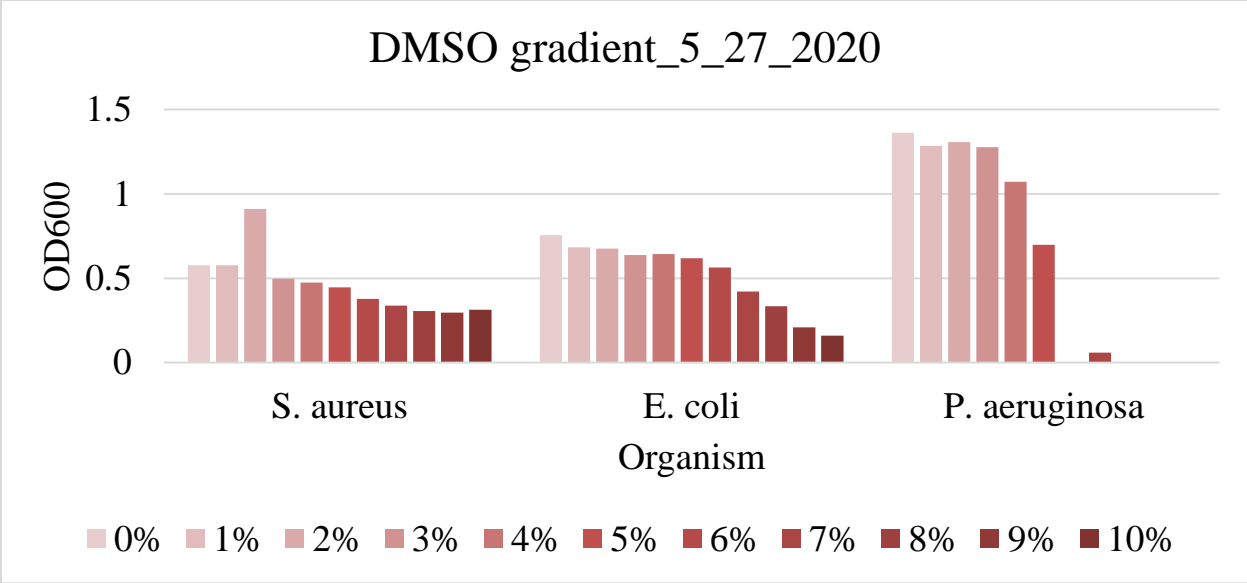
Organism		Dilution factor	Average	SD
A	<i>P. aeruginosa</i>	S	0	0
		*2	0	0
		*4	0	0
B	<i>S. aureus</i>	S	5.222222	0.19245
		*2	5	0.333333
		*4	4.888889	0.19245
C	<i>E. coli</i>	S	0	0
		*2	0	0
		*4	0	0



**Appendix D-3.** Raw data and statistical analysis of Sb(Ph)<sub>4</sub>(TCO) in the first round of inhibition zone measurements.

Compound		Dilution factor	Average	SD
Controls	<i>P. aeruginosa</i>	CCI	0	0
		CCIV	0	0
		CCVIII	0	0
	<i>S. aureus</i>	CCII	11	0
		CCV	10	0
		CCIX	9.666667	0.57735
	<i>E. coli</i>	CCIII	3	0
		CCXI	2	0
		CCXII	3.666667	0.57735
ACO	<i>P. aeruginosa</i>	S	2.666667	0.333333
		*2	1.777778	0.693889
		*4	0	0
	<i>S. aureus</i>	S	6.555556	0.96225
		*2	5.333333	0.57735
		*4	4.222222	0.3849
	<i>E. coli</i>	S	2.555556	0.3849
		*2	2.111111	0.19245
		*4	2	0
ECO	<i>P. aeruginosa</i>	S	1.666667	0.881917
		*2	3.888889	0.19245
		*4	2.888889	0.19245
	<i>S. aureus</i>	S	8.111111	0.19245
		*2	6.444444	0.3849
		*4	5.444444	0.7698
	<i>E. coli</i>	S	4.666667	0.333333
		*2	4	0
		*4	3.666667	0.471405
TCO	<i>P. aeruginosa</i>	S	0	0
		*2	0	0
		*4	0	0
	<i>S. aureus</i>	S	5.222222	0.19245
		*2	5	0.333333
		*4	4.888889	0.19245
	<i>E. coli</i>	S	0	0
		*2	0	0
		*4	0	0
TOCO	<i>P. aeruginosa</i>	S	0	0
		*2	0	0
		*4	0	0
	<i>S. aureus</i>	S	4.111111	0.509175
		*2	3.333333	0.666667
		*4	3.222222	0.3849
	<i>E. coli</i>	S	0	0
		*2	0	0
		*4	0	0

**Appendix D-4.** Statistical analysis of the second round of inhibition zone measurements for antimicrobial testing.



**Appendix D-5.** Effect of DMSO concentration on MIC of studied selected strains.